National Institute of Standards and Technology
Technology Administration, U.S. Department of Commerce

NIST TECHNICAL NOTE 1903

Methodology to Analyze Wind Pressure Data on Components and Cladding of Low-Rise Buildings

Dat Duthinh, Joseph A. Main, and Brian M. Phillips

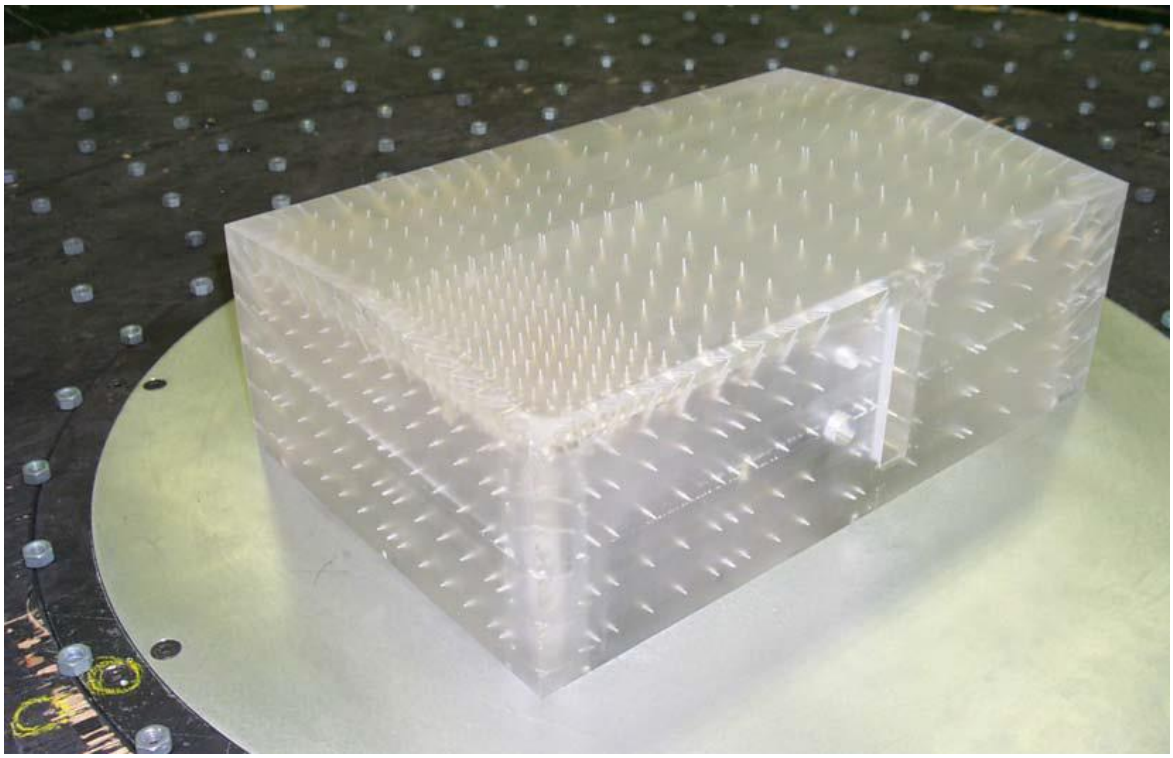

This publication is available free of charge from:
http://dx.doi.org/10.6028/NIST.TN.1903

NIST TECHNICAL NOTE 1903

Methodology to Analyze Wind Pressure Data on Components and Cladding of Low-Rise Buildings

Dat Duthinh*
Joseph A. Main*
Brian M. Phillips**

*Engineering Laboratory
National Institute of Standards and Technology
Gaithersburg, MD 20899-7311

**Department of Civil and Environmental Engineering
University of Maryland, College Park, MD

This publication is available free of charge from:
http://dx.doi.org/10.6028/NIST.TN.1903

December 2015

U.S. Department of Commerce
Penny Pritzker, Secretary

National Institute of Standards and Technology
Willie May, Under Secretary of Commerce for Standards and Technology and Director

Disclaimers

(1) The policy of the National Institute of Standards and Technology is to use the International System of Units in its technical communications. In this document however, works of authors outside NIST are cited which describe measurements in certain non-SI units. Thus, it is more practical to include the non-SI unit measurements from these references.

(2) Certain trade names or company products or procedures may be mentioned in the text to specify adequately the experimental procedure or equipment used. In no case does such identification imply recommendation or endorsement by the National Institute of Standards and Technology, nor does it imply that the products or procedures are the best available for the purpose.

Cover photo

University of Western Ontario Boundary Layer Wind Tunnel model perforated with holes for pressure measurements. The results of tests of this model and others, commissioned by NIST, are analyzed in this report. Photo by T. Ho, D. Surry & D. Morrish, BLWT-SS20-2003, May 2003.

Acknowledgment

The authors are grateful to Drs. Emil Simiu and Marc Levitan of NIST for their insightful advice and thorough review.

National Institute of Standards and Technology Technical Note 1903
Natl. Inst. Stand. Technol. Tech. Note 1903, 55 pages (December 2015)
CODEN: NTNOEF

This publication is available free of charge from:
http://dx.doi.org/10.6028/NIST.TN.1903

Abstract

This note establishes a method to analyze wind pressure data on cladding and components of low-rise buildings using the National Institute of Standards and Technology-University of Western Ontario (NIST-UWO) database. The aerodynamic pressures induced on a structure by the wind field are random both in time and space. For design purposes, the pressure on any given area *A* is a function of *A*, and is defined as the aerodynamic force acting on area *A* divided by *A*. That aerodynamic force is obtained by summing up the product of pressure time series measured in wind tunnel tests at adjoining pressure taps by their respective tributary areas. The area *A* is the sum of those tributary areas. These operations are carried out for all sums of tributary areas that make up rectangles with aspect ratio not exceeding four. The peak of the resulting area-averaged time series is extrapolated to a realistic storm duration by the Sadek-Simiu method. The envelope of peaks over all wind directions is compared with current specifications from the American Society of Civil Engineers, ASCE 7-10. Results for two low-rise buildings for one terrain condition indicate serious underestimation by these specifications of the negative pressures (suction) on gable roofs, by factors ranging from 1.3 to 2.5, and of both positive and negative pressures on walls, by factors ranging from 1.5 to 2.0 and 1.2 to 2.4, respectively. More definitive conclusions will require analysis of more data from the NIST-UWO and other databases using the proposed or equivalent methodology. Future research includes the analysis of additional low-rise building configurations and the estimation of peak pressures by alternative methods.

Keywords: ASCE 7-10; components and cladding; gable roofs; low-rise buildings; NIST-UWO database; walls; wind pressure; wind tunnel.

DOI: dx.doi.org/10.6028/NIST.TN.1903

Contents

Disclaimers, cover photo, acknowledgment …… i

Abstract …… ii

Contents…… iii

List of figures ……. iv

List of tables……..…… vi

Introduction ……... 1

Background…… …… 1

Methodology……. 2

Duration ratio…… 6

Results ……...7

Aspect ratio…….. 11

Uncertainty ……..……. 17

Conclusion …… 17

References……..…18

Appendix A: UWO Bldg 7 roof 3……. 20

Appendix B: UWO Bldg 7 roof 2……. 27

Appendix C: Building 7 Wall 1……..32

Appendix D: Building 7 Wall 4…… 35

Appendix E: Bldg 15 Roof 3……. 38

Appendix F: Bldg 15 Roof 2…… 44

Appendix G: Bldg 15 Wall 1……. 50

Appendix H: Bldg 15 Wall 4……. 53

List of Figures

Fig. 1 ASCE roof and wall zones for wind loads……... 2
Fig. 2a, b Definition of tributary areas or cells for taps on a particular face ...…..…… 3
Fig. 3 Cell area combinations …… 4
Fig. 4 Partial cell areas……5
Fig. 5a, b Combination of areas with different tap density.. ……..……5
Fig. 6a, b, c Bldg 7 roof 3 ASCE zone 1 interior (1 ft^2 = 0.0929 m^2)…….……8
Fig. 7a, b, c Bldg 7 roof 3 ASCE zone 2 lower edge (1 ft^2 = 0.0929 m^2)…….. 9
Fig. 8a, b Bldg 7 roof 3 ASCE zone 3 lower corner (1 ft^2 = 0.0929 m^2)……12
Fig. 9a, b Building 7 Wall 1 ASCE zone 5 left edge (1 ft^2 = 0.0929 m^2)……...……13
Fig. 10a, b Building 7 Wall 1 ASCE zone 4 interior (1 ft^2 = 0.0929 m^2)..……14

Appendix A: UWO Bldg 7 roof 3
Fig. A1a, b Bldg 7 roof 3 ASCE zone 3 lower corner (1 ft^2 = 0.0929 m^2) ……..20
Fig. A2a, b, c Bldg 7 roof 3 ASCE zone 2 side edge (1 ft^2 = 0.0929 m^2) ……21
Fig. A3a, b, c Bldg 7 roof 3 ASCE zone 2 upper edge (1 ft^2 = 0.0929 m^2) …… 22
Fig. A4a, b Bldg 7 roof 3 ASCE zone 2 lower edge (1 ft^2 = 0.0929 m^2) …… 24
Fig. A5a, b Bldg 7 roof 3 ASCE zone 1 interior (1 ft^2 = 0.0929 m^2)…… ..25

Appendix B: UWO Bldg 7 roof 2
Fig. B1a, b UWO Bldg 7 roof 2 ASCE zone 2 side edge (1 ft^2 = 0.0929 m^2)……27
Fig. B2a, b UWO Bldg 7 roof 2 ASCE zone 2 top edge (1 ft^2 = 0.0929 m^2) ……28
Fig. B3a, b UWO Bldg 7 roof 2 ASCE zone 2 bottom edge (1 ft^2 = 0.0929 m^2) ……..29
Fig. B4a, b UWO Bldg 7 roof 2 ASCE zone 1 interior (1 ft^2 = 0.0929 m^2) ……..30
Fig. B5a, b UWO Bldg 7 roof 2 ASCE zone 3 corners (1 ft^2 = 0.0929 m^2) …….…….31

Appendix C: Building 7 Wall 1
Fig. C1a, b Building 7 Wall 1 ASCE interior (1 ft^2 = 0.0929 m^2) ……32
Fig. C2a, b Building 7 Wall 1 ASCE right edge (1 ft^2 = 0.0929 m^2)……33
Fig. C3a, b Building 7 Wall 1 ASCE left edge (1 ft^2 = 0.0929 m^2)……..34

Appendix D: Building 7 Wall 4
Fig. D1a, b Building 7 Wall 4 ASCE interior (1 ft^2 = 0.0929 m^2) ……35
Fig. D2a, b Building 7 Wall 4 ASCE left edge (1 ft^2 = 0.0929 m^2) ……..36
Fig. D3a, b Building 7 Wall 4 ASCE right edge (1 ft^2 = 0.0929 m^2) ……37

Appendix E: Bldg 15 Roof 3
Fig. E1a, b Bldg 15 Roof 3 ASCE interior (1 ft^2 = 0.0929 m^2) ……38
Fig. E2a, b Bldg 15 Roof 3 ASCE lower edge (1 ft^2 = 0.0929 m^2) ……39
Fig. E3a, b Bldg 15 Roof 3 ASCE upper edge (1 ft^2 = 0.0929 m^2) ……..40
Fig. E4a, b Bldg 15 Roof 3 ASCE right edge (1 ft^2 = 0.0929 m^2) ……41
Fig. E5a, b Bldg 15 Roof 3 ASCE lower corner (1 ft^2 = 0.0929 m^2) ……42
Fig. E6a, b Bldg 15 Roof 3 ASCE upper corner (1 ft^2 = 0.0929 m^2) ……43

Appendix F: Bldg 15 Roof 2
Fig. F1a, b Bldg 15 Roof 2 ASCE interior (1 ft^2 = 0.0929 m^2) ……44
Fig. F2a, b Bldg 15 Roof 2 lower edge (1 ft^2 = 0.0929 m^2) ……..45
Fig. F3a, b Bldg 15 Roof 2 upper edge (1 ft^2 = 0.0929 m^2) ……46
Fig. F4a, b Bldg 15 Roof 2 side edge (1 ft^2 = 0.0929 m^2) ……47
Fig. F5a, b Bldg 15 Roof 2 lower corner (1 ft^2 = 0.0929 m^2) ……48
Fig. F6a, b Bldg 15 Roof 2 upper corner (1 ft^2 = 0.0929 m^2) ……49

Appendix G: Bldg 15 Wall 1
Fig. G1a, b Bldg 15 Wall 1 Interior (1 ft^2 = 0.0929 m^2) ……50
Fig. G2a, b Bldg 15 Wall 1 left edge (1 ft^2 = 0.0929 m^2)……...51
Fig. G3a, b Bldg 15 Wall 1 right edge (1 ft^2 = 0.0929 m^2) ……52

Appendix H: Bldg 15 Wall 4
Fig. H1a, b Bldg 15 Wall 4 Interior (1 ft^2 = 0.0929 m^2) ……53
Fig. H2a, b Bldg 15 Wall 4 left edge (1 ft^2 = 0.0929 m^2)…….…..54
Fig. H3a, b Bldg 15 Wall 4 right edge (1 ft^2 = 0.0929 m^2) ……..……..55

List of Tables

Table 1 Results for Building 7 ……...15

Table 2 Results for Building 15…… 16

Introduction

Current ASCE 7-10 (American Society of Civil Engineers 2010) specifications of wind pressures on low-rise buildings are based on data that are thirty to forty years old. Advances in computer technology allow simultaneous recording of many more pressure taps (on the order of hundreds) than was possible a few decades ago. Furthermore, wind tunnel test measurements have become publicly available for considerably more building geometries. The most well-referenced publicly available sources of data are the National Institute of Standards and Technology (NIST 2004) database, which covers tests conducted at the University of Western Ontario (UWO, Ho et al. 2003, 2003, 2005), and the Tokyo Polytechnic Institute (TPU, Tamura 2012) database.

The main purpose of this study is to establish a clear and reproducible methodology for using a general wind tunnel test database, namely the NIST-UWO database, to calculate peaks of wind pressure over different size areas of building surfaces. The methodology is an essential component to updating wind pressure coefficients for the design of components and cladding, considering the deficiencies in current wind load specifications. A similar effort has been carried out with the TPU database (Gierson et al. 2015) with methodology based on the unique features of that database.

Background

Current ASCE 7-10 wind load provisions on components and cladding of low-rise buildings are largely based on the work of Stathopoulos (1979), supplemented by Meecham (1988) for hip roofs, and updated by Stathopoulos et al. (1999). Wind pressure on building enclosures continues to be an active area of research.

Gavanski et al. (2013 a, b) tested 1:50 scale models of houses with gable or hip roofs and concluded that roof slope and upstream terrain had the most significant effect on wind loads acting on roof sheathing, and that ASCE 7-10 standards substantially underestimated wind pressures, more so for gable roofs than hip roofs. Pressure coefficients were averaged over the area of sheathing panels 4 ft × 8 ft (1.2 m × 2.4 m) and the Best Linear Unbiased Estimator (BLUE, Lieblein 1974) method was used to determine the peak pressure coefficients. Vickery et al. (2013) analyzed the same data and found that, for gable roof zone 1 (interior, Fig. 1), ASCE 7-10 provisions were "woefully inadequate" for effective areas less than 50 ft^2 (5 m^2), but could be reduced for areas greater than 100 ft^2 (10 m^2); for zone 2 (edges), ASCE 7-10 provisions underestimated roof pressure for areas less than 100 ft^2 (10 m^2), but were adequate for larger areas. For zone 3 (corners), Vickery et al. (2013) suggested that the ASCE 7-10 minimum area of 10 ft^2 (1 m^2) was too large because of the large pressure gradients at roof corners.

Gavanski and Uematsu (2014) analyzed wind pressure on walls of low-rise buildings and concluded that zoning for positive pressure is unnecessary as pressure was approximately uniform over the entire wall surface. For roof slopes less than 14°, positive wall pressures increased slightly as the roof slope decreased. For negative pressures, larger suctions were observed at the wall edges than in the interior, as expected, and the width of these higher suction zones increased with roof slope and eave height. ASCE 7-10 provisions underestimated positive pressures for almost all effective areas by a factor of 1.2 to 1.5. A similar tendency was found

for negative pressures, though not for all building geometries. In fact, for several geometries, ASCE 7-10 provisions overestimated wall pressures on large effective areas.

Under the sponsorship of the NIST, the University of Western Ontario (UWO) conducted wind tunnel tests on thirty seven different buildings of one basic type: rectangular in plan; gable roofs with various slopes and no overhang; and open country and suburban terrain conditions (Ho et al. 2003, 2003, 2005). The roof slope ranged from ¼:12 (1.2°) to 6:12 (26.6°), the building width from 30 ft (9.14 m) to 160 ft (48.80 m), the building length from 45 ft (13.70 m) to 200 ft (61.0 m), and the eave height from 12 ft (3.66 m) to 40 ft (12.20 m). These test results underpinned the Database-Assisted Design (DAD) method for Main Wind Force Resisting Systems (Main and Fritz 2006, Habte, Chowdhury and Park 2015) and were used in the current study.

Methodology

Herein, the methodology is developed around the NIST-UWO database, and results for two buildings are presented in the appendices, with illustrations excerpted in the main text for explanation purposes.

1. Within NIST-UWO wind tunnel database, select the building, roof or wall zones to study. Zones currently defined in ASCE 7-10 (Fig. 1) are investigated. For wind loads, ASCE 7-10 divides a gable roof, with slope not exceeding 7°, into four corner zones (zone 3) of side *a*, four edge zones (zone 2) of width *a* running along the edges, excluding the corners, and an interior zone (zone 1), which is the rest of the gable. *a* is defined as 10 % of the least horizontal dimension of the building, or 0.4 *h*, whichever is smaller, but not less than either 4 % of the least horizontal dimension or 3 ft (0.9 m). *h* is the eave height (or the mean roof height when the roof slope exceeds 10°). For walls, two edge zones (zone 5) of width *a* are defined, and the rest of the wall is called zone 4.

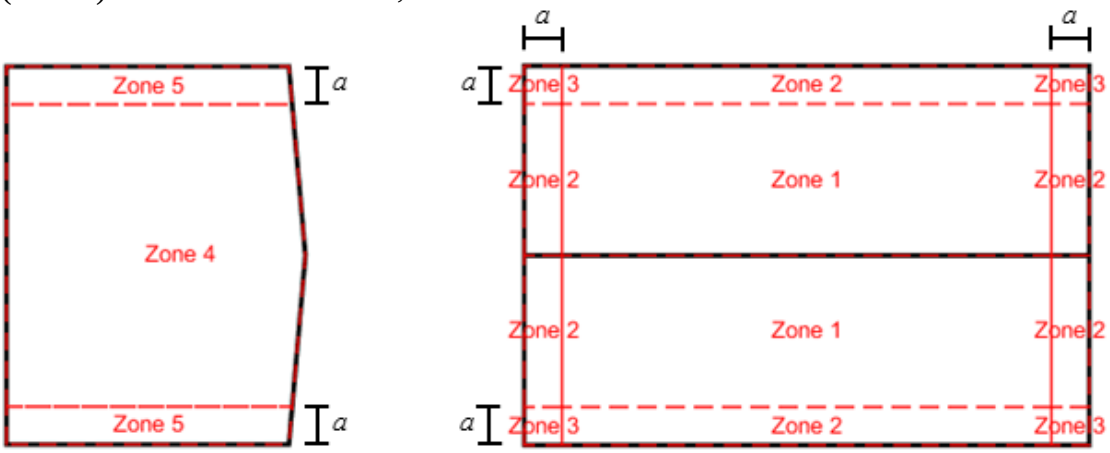

Fig. 1 ASCE roof and wall zones for wind loads
(adapted from ASCE 7-10 Figs. 30.4-1 and 30.4-2A by M. Gierson)

2. The aerodynamic pressures induced on a structure by the wind field are random both in time and space. The randomness in space means that, at any given time, the pressures

differ from point to point, that is, the spatial coherence of the pressures at any two points decreases as the distance between those points increases. For design purposes the pressure on any given area *A* is, therefore, a function of *A*, and is defined as the aerodynamic force acting on area *A* divided by *A*. That aerodynamic force is obtained by summing up the product of pressure time series measured in wind tunnel tests at adjoining pressure taps by their respective tributary areas or cells. Cell boundaries are straight lines equidistant to adjacent taps, but taps are at the center of cells only in a regular grid (Fig. 2). The area *A* is the sum of those tributary areas. These operations were carried out for all sums of tributary areas that make up rectangles.

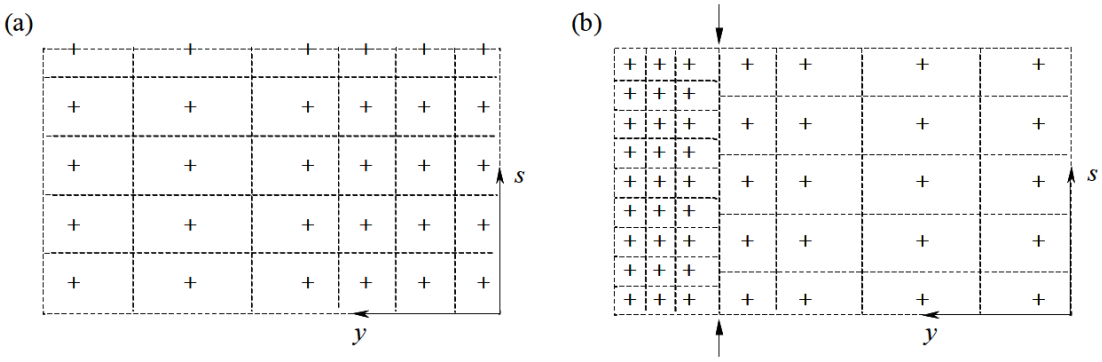

Fig. 2 Definition of tributary areas or cells for taps on a particular face: a) simple tap array; b) more complicated tap array with varying tap density (from Main and Fritz 2006)

The summation of tributary areas is simplest when the grid of taps is regular, and that is explained in Fig. 3. Special consideration must be given to the study zone edges and corners, which generally do not coincide with cell boundaries; and to places where grids of different densities merge (indicated by arrows in Fig. 2b). These situations are explained in Figs. 4 and 5.

Figure 3 illustrates a case where the zone of interest only includes six cells. The area summation procedure starts with the step denoted by Aa, which consists of the selection of one cell on the upper left corner. This is the first rectangle where the number of cells is the same in both coordinate directions, denoted by *s* and *y*. The next step, denoted by Aa2, consists of adding a cell in the *y* direction downward. With this step the lower boundary of the zone is reached; therefore no additional cell can be added in direction *y*. To the cell selected in step Aa is added one cell in direction *s*, rightward, in step Aa3,1. In a next step, denoted by Aa3,2, an additional cell is added, again in direction *s*, rightward. Thus two additional rectangles have been created in step Aa3. With step Aa3,2 the rightmost boundary of the zone has been reached, so further expansion in the direction *s* is not possible. Next, step Ab consists of adding to the cell selected in step Aa via expansion in both directions *y* downward and *s* rightward. Thus a rectangle consisting of four cells is created. Expansion in the direction *y* downward is attempted in step Ab2, but is not possible. Step Ab3 consists of expanding in the *s* direction rightward, which results in a six-cell rectangle. All possibilities of expansion from the single cell selected in step Aa being exhausted, one proceeds to the next initial cell (step Ba). The procedure is repeated until all possible initial cells have been used. Figure 3 shows six rectangles formed by one cell, seven rectangles formed by two cells, two rectangles formed by

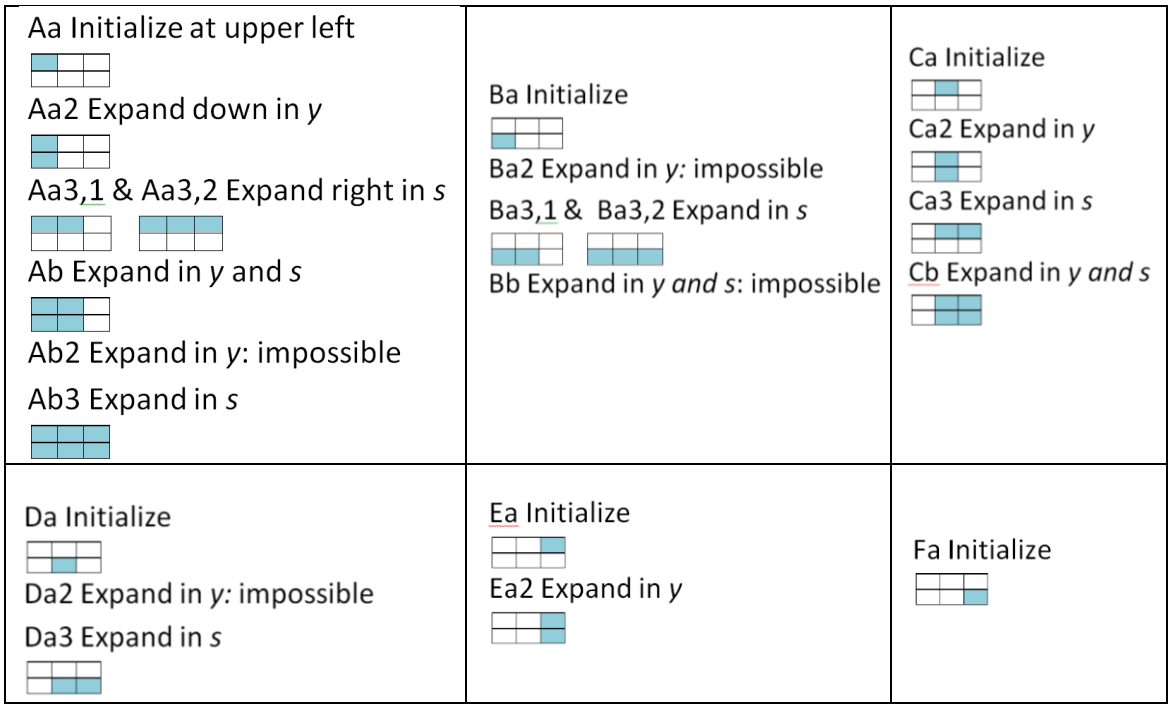

Fig. 3 Cell area combinations

three cells, two rectangles formed by four cells, and one rectangle formed by six cells, for a total of eighteen rectangles.

To limit the number of combinations of a_i, the aspect ratio of the rectangles formed by the aggregation of cells is limited not to exceed 4. This aspect ratio covers many practical units of components and cladding, and allows consideration of long, narrow zones along the edges of roofs and walls. This choice also covers all "effective wind areas used to evaluate *(GC_p)*", whose width, according to the Commentary of ASCE 7-10, "need not be taken as less than one-third of the length of the area. This increase in effective wind area has the effect of reducing the average wind pressure acting on the component." How the aspect ratio of rectangular areas affect the peak area-averaged pressure will be discussed further in the results section.

Partial cells may be necessary and are accounted for at the edges and the corners of the study zone being considered. In Figs. 4 and 5 the black lines represent the cell boundaries. In Fig. 4, a corner of the zone being studied is colored and includes one full cell and three partial cells. The pressures in the partial cell areas are the same as in the three full cells from which the partial cells are formed. The partial areas are considered when calculating weighted average pressures.

If the zone being studied overlaps areas of different tap density, the coarser density is used overall, and full and partial cell areas in the high density region are combined as needed. Figure 5a shows a portion of a study zone, with two grid densities. To conform with the coarser grid, the two rows of three cells each at the bottom of the figure are transformed into two rectangles each (Fig. 5b).

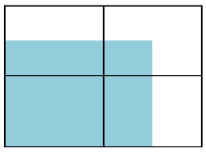

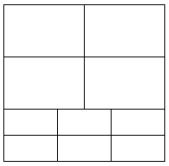

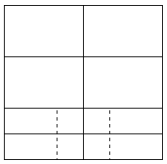

Fig. 4 Partial cell areas Fig. 5a, b Combination of areas with different tap density

3. Database-Assisted Design (DAD) software (Main and Fritz 2006) was supplemented by software developed as part of this project to calculate the time series of wind pressure coefficients C_{p3600} on area $A = \sum a_i$ for each specified wind direction. The time series is the area-weighted average of pressure coefficients C_{pi} calculated from wind pressures p_i measured by taps with their tributary areas a_i that overlap with the zone being studied. Typically, there are many combinations of a_i for the same value of A. As the peak of the sum is less than the sum of the peaks of several time series, the peak pressure decreases as the area increases. In physical terms, the spatial correlation of pressure peaks as measured by the taps decreases as the area increases, resulting in lower peak pressures over larger areas. p_i, C_{pi}, and C_{p3600} are functions of time and wind direction.

$$C_{pi} = \frac{p_i - p_0}{½\,\rho\, V_{3600}^2}; \qquad C_{p3600} = \frac{\sum(a_i\, C_{pi})}{\sum a_i}$$

p_0 = static pressure at reference height (roof eave);
V_{3600} = mean hourly wind speed at reference height;
ρ = air density.

4. For each area combination $A = \sum a_i$, use Rice's zero up-crossing method adapted to non-Gaussian time series (Sadek and Simiu 2002, Main 2011) to calculate minima and maxima *over time* of C_p for a 60-minute (full scale) windstorm. The Sadek-Simiu method uses the Gamma distribution and a normal distribution to estimate the peaks corresponding, respectively, to the upper and lower tails of the time series' histograms. The peak distribution is represented by the Extreme Value Type I (Gumbel) distribution, and the values selected correspond to the mean of this distribution applied to the upper and lower tails. The extension of test results to a longer time than the test duration converted to full scale is discussed in more detail in the next section.

   The selection of peaks (in absolute value) of minima (negative pressure or suction) and maxima (positive pressure inward) of C_p for each area combination $A = \sum a_i$ results in two vectors of minima and maxima versus A for each wind direction. The gust effect factor G accounts for the variability of the pressure coefficient due to the randomness of the aerodynamic response and is introduced implicitly when the averaging process and the peak selection process are applied (Simiu, 2011). The peak pressures are functions of wind direction.

5. Repeat for all wind directions tested. This results in two matrices of minima and maxima of GC_p for various areas and wind directions. From these two matrices, select two vectors of peaks *over all wind directions* of minima and maxima of GC_p vs. A.

6. Renormalize results to 3-s wind gust speed V_3 as in ASCE 7-10 using the Durst (1960) curve.

$$GC_p \equiv GC_{p3} = GC_{p3600}\left(\frac{V_{3600}}{V_3}\right)^2 = GC_{p3600}\left(\frac{1}{1.52}\right)^2$$

Durst (1960) estimated the uncertainty in his calculations of wind gust speed over durations shorter than one hour to be "about one mile per hour" (0.4 m/s). For a mean hourly wind speed of 80 mph (36 m/s), Durst (1960) calculated the 5-s wind gust speed to be 118 mph (53 m/s). The ratio of the 5-s wind gust speed to the hourly wind speed is (118 ± 1) / 80 = 1.475 ± 0.012. The uncertainty for the ratio 1.52 of the 3-s gust speed to the hourly wind speed can be considered to be ± 0.01.

7. Repeat for other zones, terrains and buildings.

Note there are two consecutive steps in the selection of the peak wind pressures for design purposes: selection of peaks over time (step 4), and selection of peaks over all wind directions (step 5). The selection of the peaks over all wind directions is inherent in the envelope method, as defined in the ASCE 7 Standard. Finally, the peaks corresponding to the most unfavorable combination of cells forming various areas A are chosen for the development of design specifications.

Duration ratio

The Sadek-Simiu (2002) method uses a duration ratio that is explained by the following example. The University of Western Ontario wind tunnel tests a 1/100 model of size D_m = 6.0 in (0.152 m), by exposing it to mean wind speed V_m = 30.0 ft/s (9.144 m/s) in open country, for a duration T_{ma} = 100 s. The mean wind speed is calculated over the duration of the test, and is measured at a reference height ($h_{ref} = 6.8$ ft $\times$ 100 = 680 ft = 207.26 m full scale), then converted to eave height ($H = 40$ ft = 12.19 m) by the relationship (Ho, Surry and Morrish 2003. For a discussion of this power law and various values of the exponent proposed over the years, see Simiu and Scanlan 1996 p. 46):

$$\frac{V_H}{V_{ref}} = \left(\frac{H}{h_{ref}}\right)^{1/7.446}$$

These data are used to design a building of size D_p = 50 ft (15.2 m) for a region with 3-s gust speed of 140 mi/h (225 km/h) measured at 33 ft (10 m) elevation. The hourly wind speed is $(140\ \text{mi/h})/1.52 = 92.11\,\text{mi/h} = 135.09\,\text{ft/s} = 41.17\,\text{m/s}$. The 33 ft (10 m) elevation is close enough to the eave height that no correction is required. Scaling laws require (Simiu and Scanlan 1996):

$$\left(\frac{D}{VT}\right)_m = \left(\frac{D}{VT}\right)_p$$

where subscripts *m* and *p* stand for model and prototype respectively. Thus:

$$T_m = T_p \frac{D_m}{D_p} \frac{V_p}{V_m} = 3600 \frac{1}{100} \frac{135.09}{30.0} = 162 \text{ s}$$

The following duration ratio must be applied in the extreme value procedure to obtain the proper estimate for peak wind gusts:

$$\frac{T_m}{T_{ma}} = \frac{162 \text{ s}}{100 \text{ s}} = 1.62$$

Results

Results are shown for two buildings in the UWO-NIST database, Building 7 (data set jp1) and Building 15 (data set eh1), tested in open country. Both buildings were modelled at a scale of 1:100, and data were collected for 100 s at 500 Hz.

Building 7 (Fig. 6c) is 40 ft (12.19 m) wide, 62.5 ft (19.05 m) long, 40 ft high (12.19 m, eave height) and has a roof slope of 1:12 (4.8°). It was tested for wind directions ranging from 0° to 90° and 270° to 360° every 5°. Due to building symmetry, only half of all possible wind directions need to be investigated. In Fig. 6c, 0° and 90° are in the +y and the +x directions respectively. Results are summarized in Table 1 and graphed in appendices A to D. Selected results covering ASCE zones 1 to 5 are discussed in this section.

Building 15 (Fig. E1b, Appendix E) is 80 ft (24.38 m) wide, 125 ft (38.10 m) long, 40 ft high (12.19 m, eave height) and has a roof slope of 1:12 (4.8°). It was tested for wind directions ranging from 180° to 360° every 5°. Results are summarized in Table 2 and graphed in appendices E to H.

Figure 6c (the appendices show complete sets of results, so Fig. 6 is also Fig. A5, Appendix A) shows an outline of Building 7, with dimensions in feet. Pressure sensors, or taps, are shown on half of the gable roof (called roof 3 here), and the interior zone (defined in ASCE 7-10 as zone 1) being investigated is delineated by blue lines. The area combination scheme of rectangles with aspect ratio less than or equal to 4 is used, and is also specialized to the case of squares (aspect ratio 1) that cover at least 4 taps. This last scheme has been used by other researchers (Morrison 2015). Each area combination results in a maximum and a minimum pressure coefficient (Figs. 6a, b). The current ASCE 7 specifications are plotted for comparison (+ means positive maxima, - means negative minima).

Figure 6a shows the current ASCE specifications underestimate negative pressures by a factor ranging from 1.3 for larger areas close to 1000 ft^2 (100 m^2) to 2.5 for smaller areas of 10 ft^2 (1 m^2) or less. The square area scheme also captures the same trend, albeit at fewer area combinations, as expected. Limiting the data areas including at least four taps results in a lower limit of 37 ft^2 (3.4 m^2), compared with the area of 10 ft^2 (1 m^2) below which ASCE specifies the pressure coefficients to remain constant. ASCE underestimates positive pressures by a factor of 2.0 for areas between 5 ft^2 (0.5 m^2) and 30 ft^2 (3m^2), but the pressures are small, and the ASCE specifications are acceptable for larger areas. Figure 6b will be discussed later in a separate section on aspect ratio.

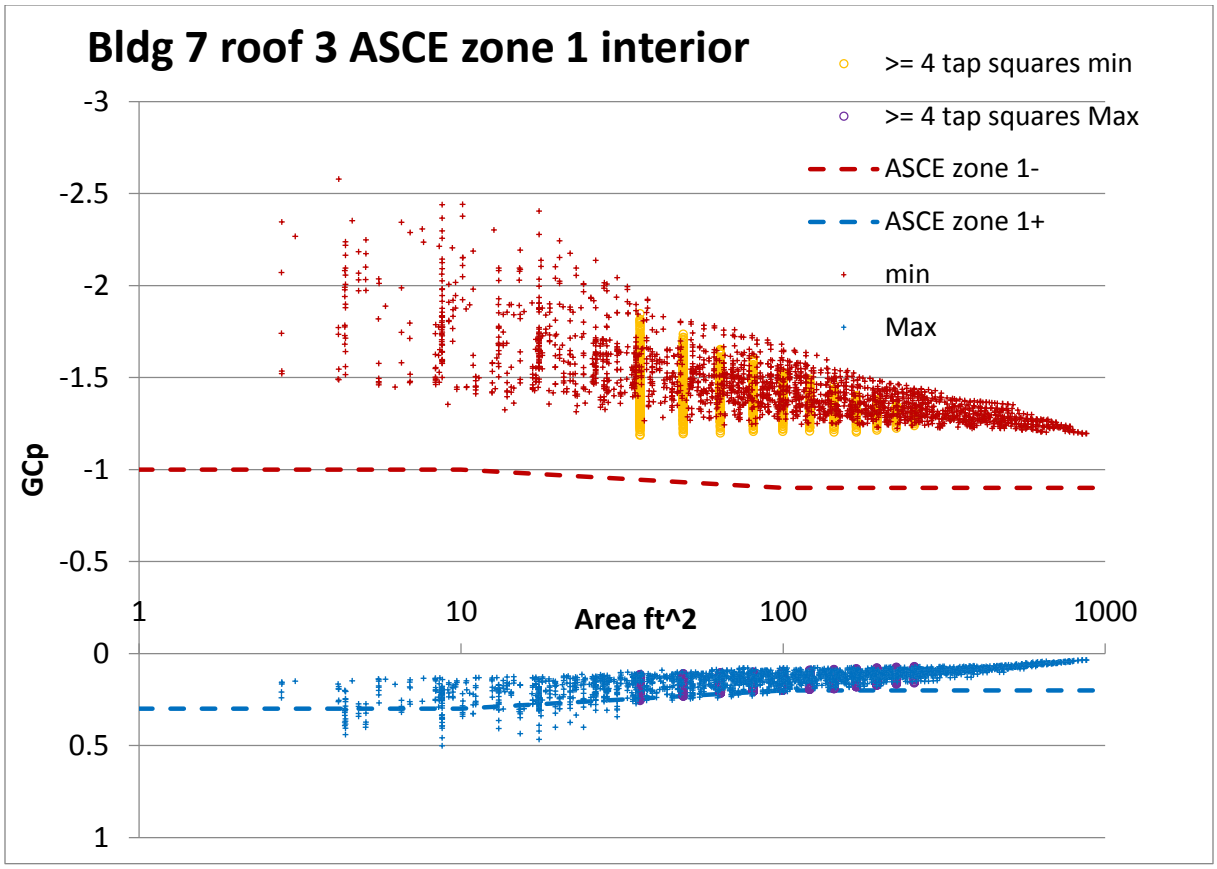
Bldg 7 roof 3 ASCE zone 1 interior
>= 4 tap squares min
>= 4 tap squares Max
ASCE zone 1-
ASCE zone 1+
min
Max
GCp
-3
-2.5
-2
-1.5
-1
-0.5
0
0.5
1
1
10
100
1000
Area ft^2

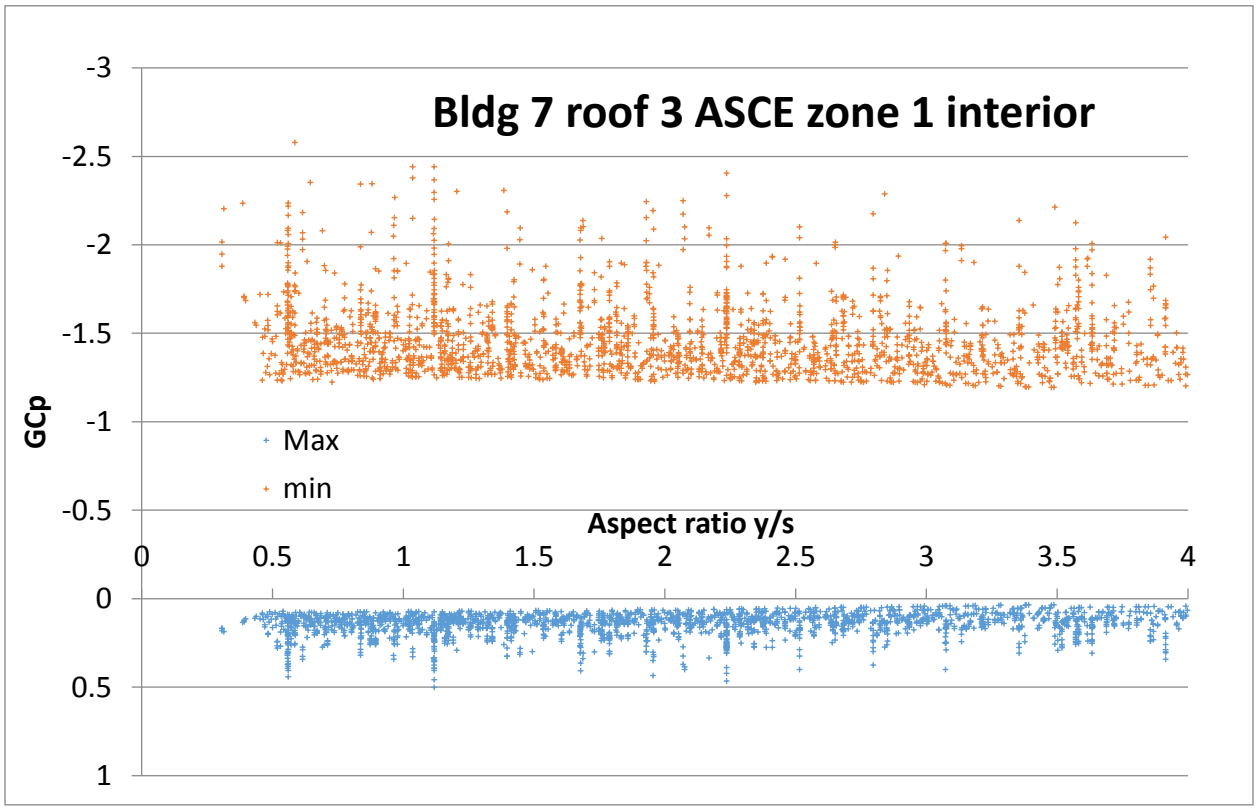
Bldg 7 roof 3 ASCE zone 1 interior
GCp
-3
-2.5
-2
-1.5
-1
-0.5
0
0.5
1
Max
min
Aspect ratio y/s
0
0.5
1
1.5
2
2.5
3
3.5
4

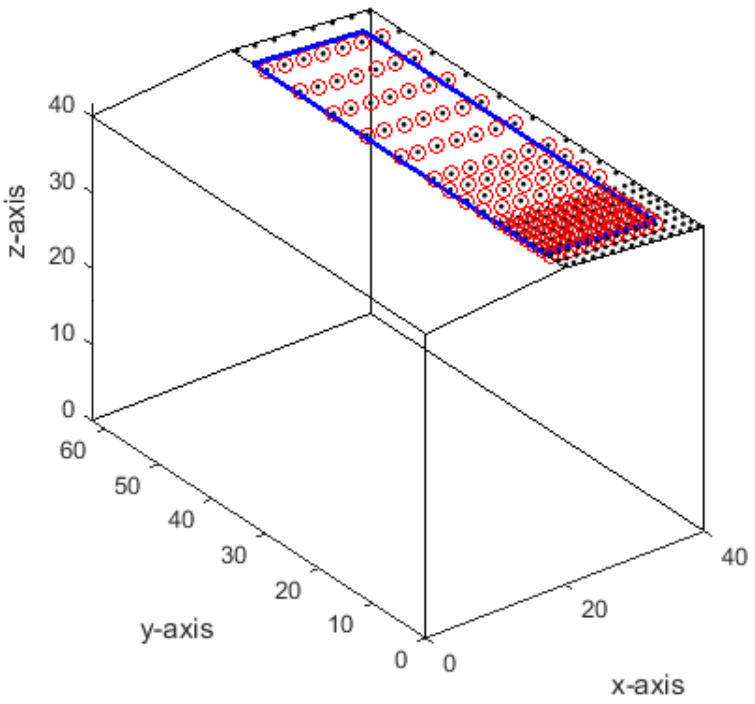

Fig. 6a, b, c Bldg 7 roof 3 ASCE zone 1 interior (1 ft^2 = 0.0929 m^2)

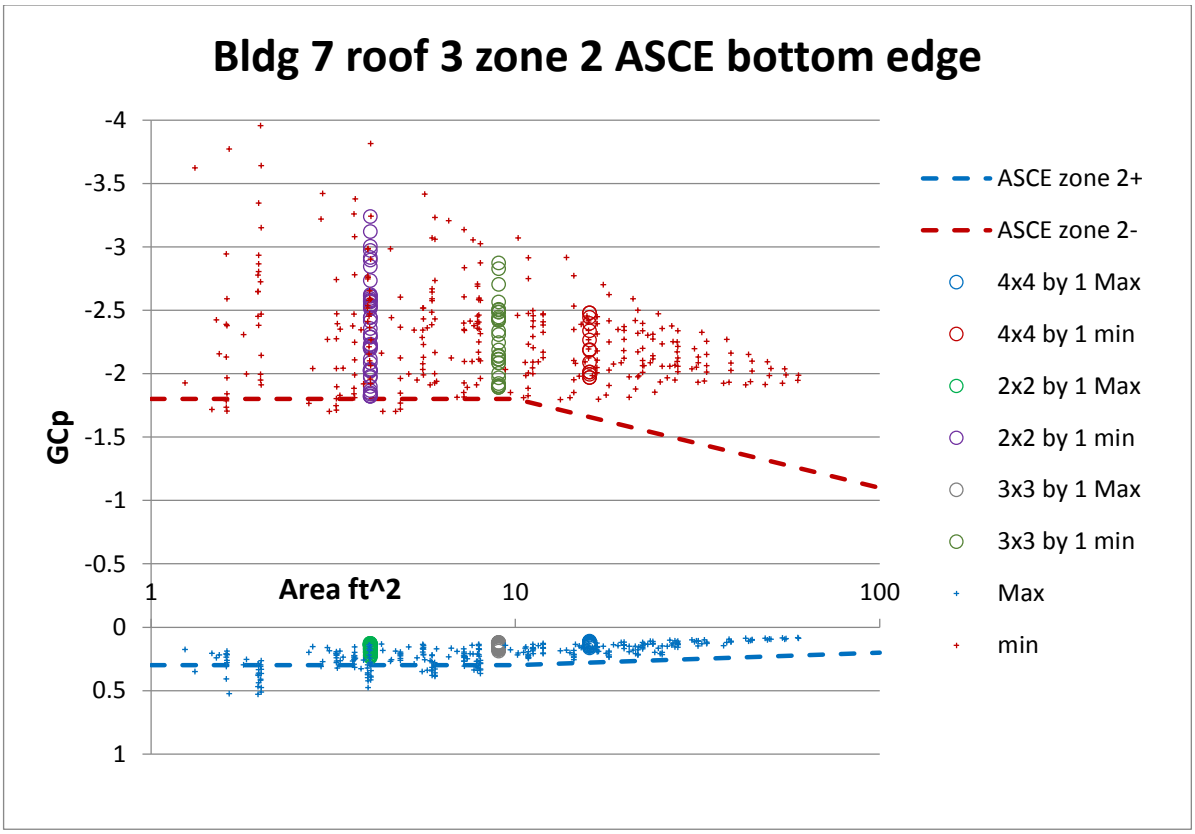

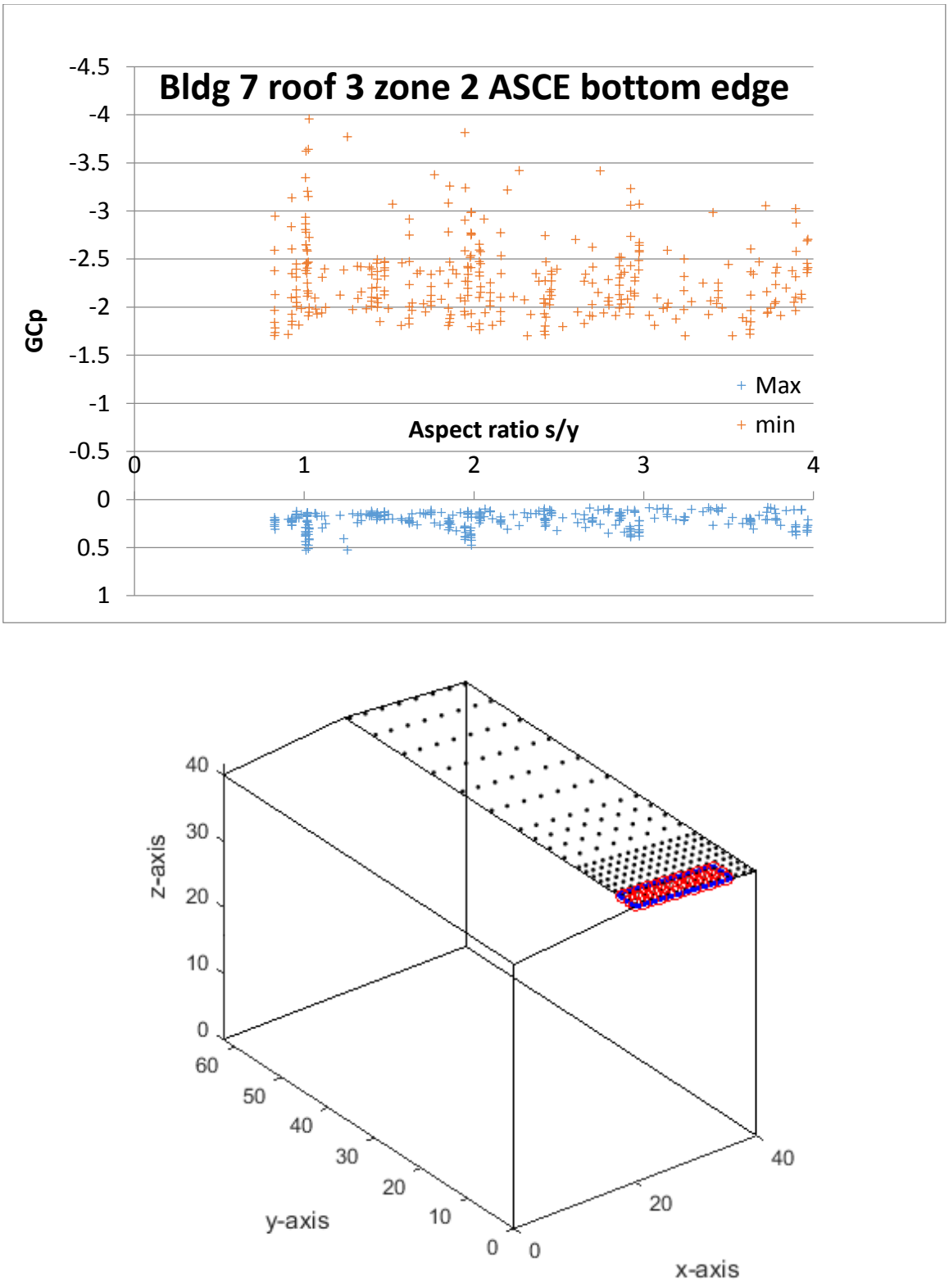

Fig. 7a, b, c Bldg 7 roof 3 ASCE zone 2 lower edge (1 ft^2 = 0.0929 m^2)

One particularly attractive feature of the NIST-UWO database is the high density of pressure taps on one part of the roof. This allows high resolution in edge and corner zones, shown in Figs. 7 and 8 for Building 7, roof 3 (in the DAD software, the roof gables are numbered 2 and 3, and the side walls 1 and 4. The DAD software focuses on structural response in the transverse direction x and does not use the end wall pressure data). The upper corner of roof 3 (x = 40, y = 62.5) does not have a sufficient number of taps for meaningful results.

Figure 7 (also Fig. A4, Appendix A) shows the results for the roof edge on the windward side in the UWO tests. Observations are consistent with those regarding the interior zone just discussed. For negative pressures, current ASCE specifications underestimate the measurements by a factor ranging from 1.6 for the larger areas (60 ft^2 or 6 m^2) to 2.2 for the smaller areas (2 ft^2 or 0.2 m^2). ASCE underestimates positive pressures by a factor of 1.7 for areas smaller than 3 ft^2 (0.3 m^2), but the pressures are small, and the ASCE specifications are acceptable for larger areas. The notation "2×2 by 1 min" indicates negative pressures (or minima) estimated from square areas with a 2×2 arrangement of pressure taps, with the squares being shifted by 1 ft (0.30 m) in consecutive steps in both directions of the planar surface to cover all possible areas within the study zone. Similar notation holds for the maxima and other size squares.

Figure 8 (also Fig. A1, Appendix A) shows that ASCE specifications underestimate negative pressures over virtually all of the areas within the corner zone, by up to a factor of 2.3. For areas that include at least four taps, the underestimation is by 1.5. On the other hand, positive pressure specifications are adequate. This corner is on the windward side in the UWO tests.

Figure 9 (also Fig. C3, Appendix C) shows results for the left edge, part of ASCE zone 5, of Wall 1 of Building 7. ASCE underestimates negative pressures and positive pressures by a factor of 1.6. Note the tap density is not high in this zone, which is less than two-cell wide. The peaks of negative pressure occur for wind directions between 50° and 65°, and the peaks of positive pressures occur for wind directions of 10° (0° is +y and 90° is +x). Since the tests were conducted only for wind directions between 0° and 90° and 270° and 360°, the corresponding peaks for both positive and negative pressure were missed for the right edge of Wall 1, as a comparison of Figs. C2 and C3, Appendix C, confirms.

Fig. 10 (also Fig. C1, Appendix C) shows that for the interior, zone 4, of Wall 1 of Building 7, ASCE 7-10 specifications underestimate negative pressures by a factor ranging from 1.2 for areas of 1100 ft^2 (110 m^2) to 1.9 for areas 60 ft^2 (6 m^2); and underestimate positive pressures by a factor of 1.8 over all areas. The rest of the results are summarized in Table 1 for Building 7, and Table 2 for Building 15.

Aspect ratio

The choice of aspect ratios of 4 or less makes more effective use of the UWO data than, say 3 or less. Results show a slight decreasing trend of GC_p as the aspect ratio increases (Figs. 6b, 7b, A2b, A3b, A4b and A5b). This is true for edge zones as well as interior zones, and validates the ASCE 7-10 Commentary. The envelope of GC_p is not affected by extending the aspect ratio from 3 to 4. (It had been expected that, along the edges of roofs and walls, and for certain wind

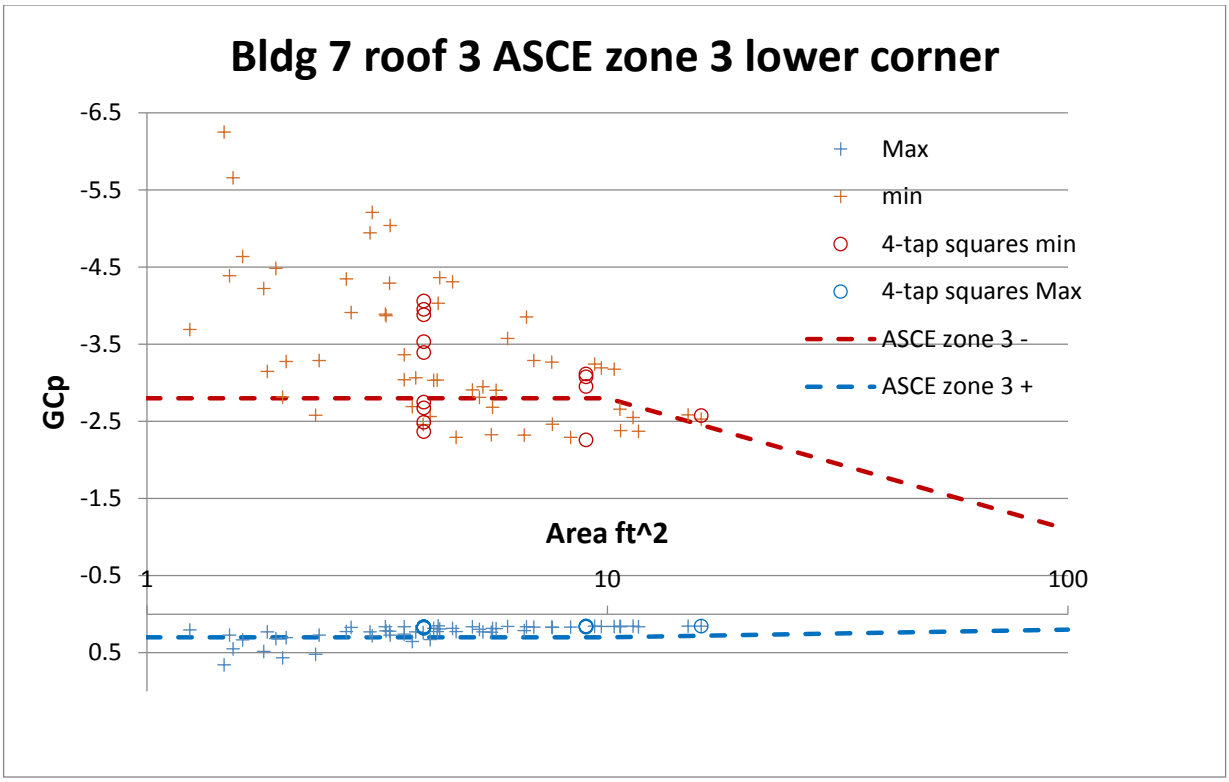

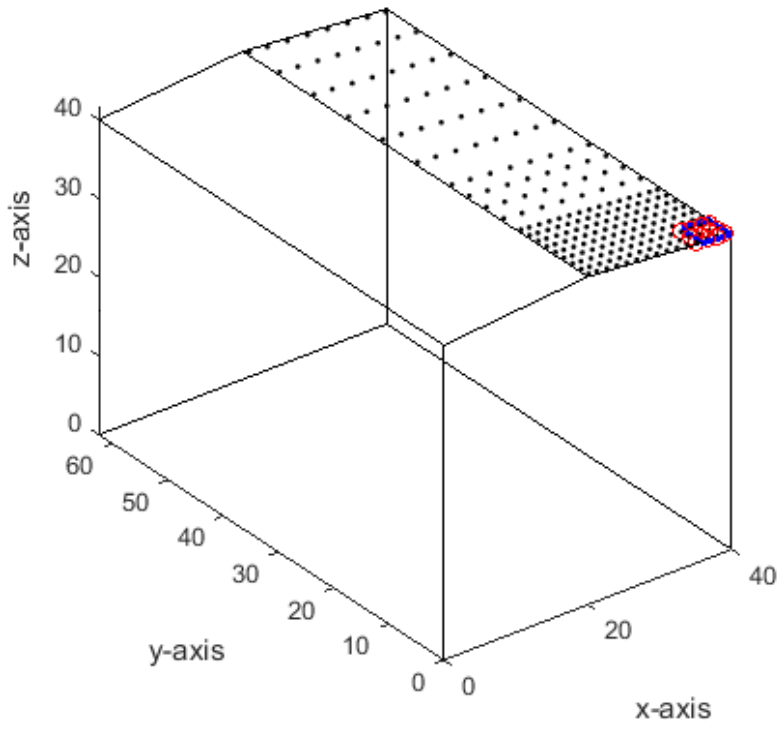

Fig. 8a, b Bldg 7 roof 3 ASCE zone 3 lower corner (1 ft^2 = 0.0929 m^2)

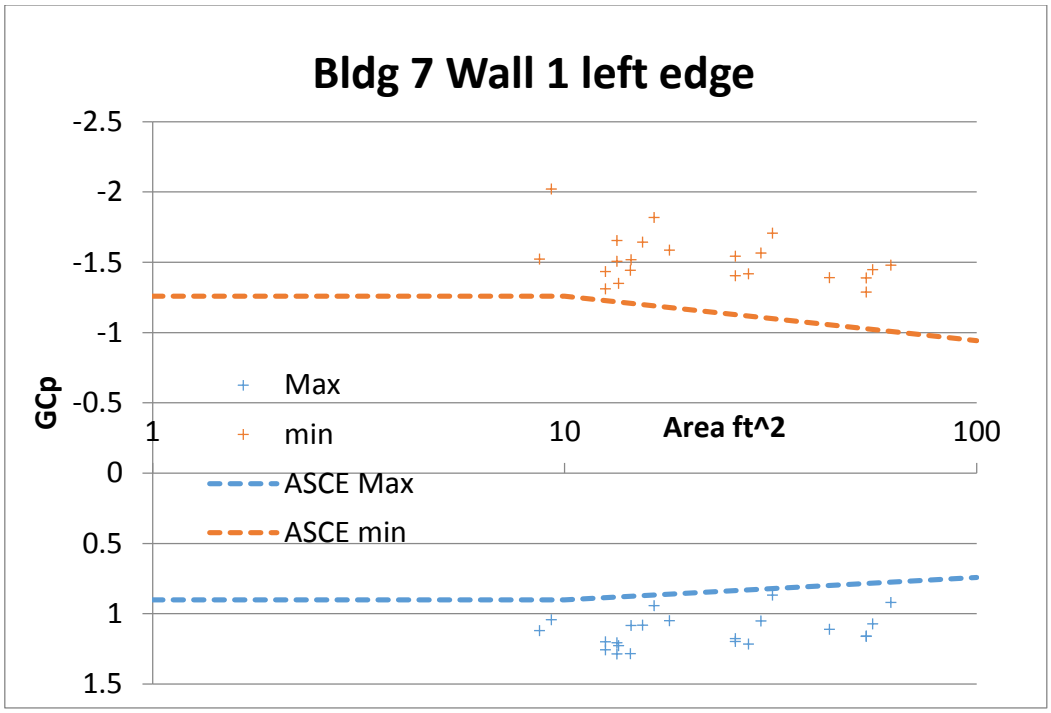

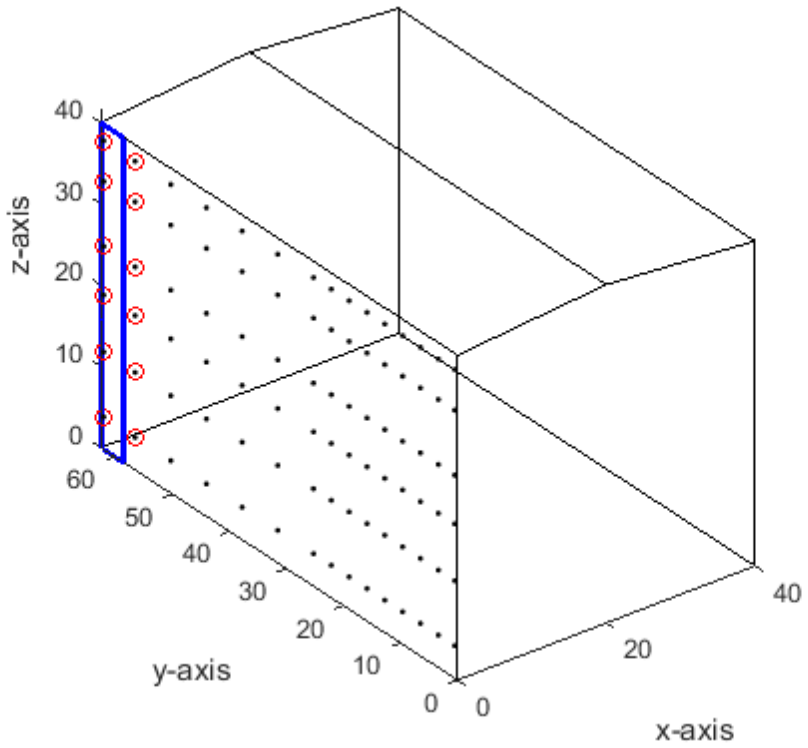

Fig. 9a, b Building 7 Wall 1 ASCE zone 5 – left edge (1 ft^2 = 0.0929 m^2)

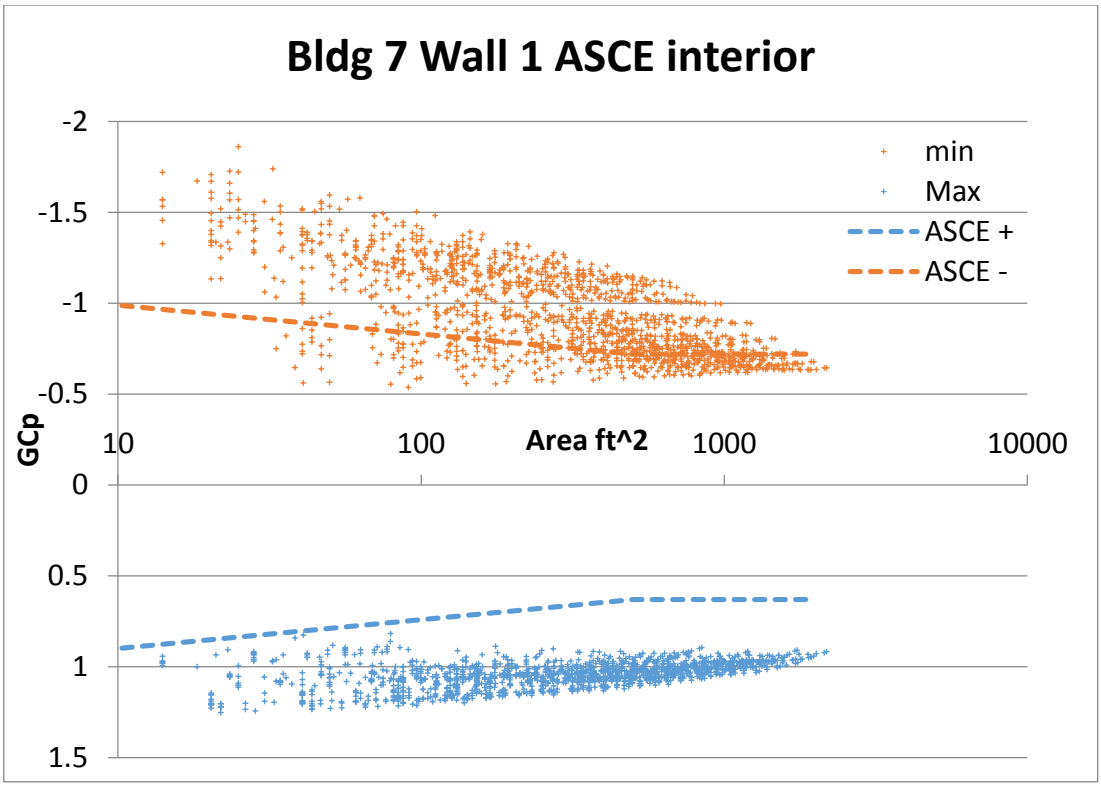

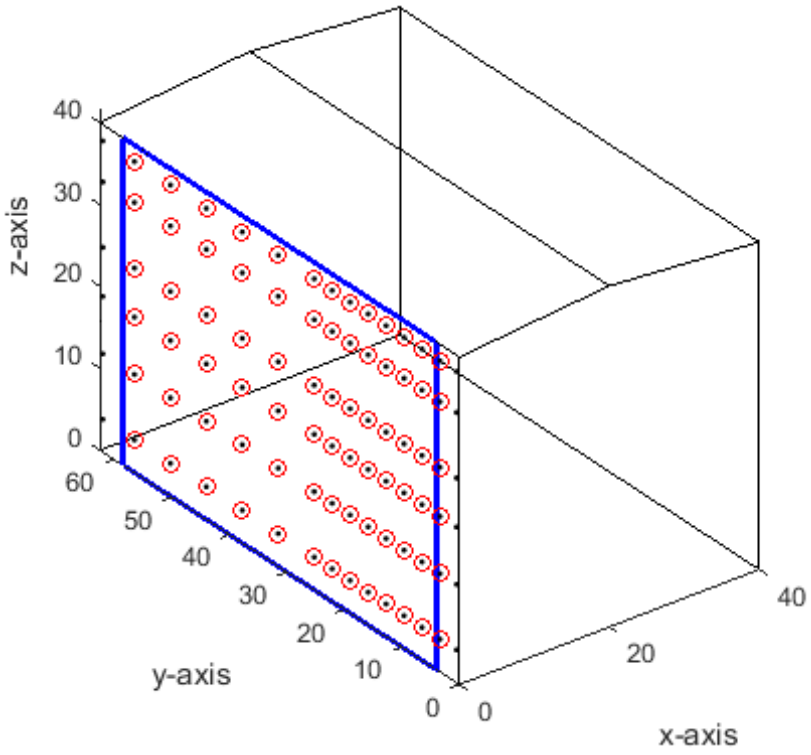

Fig. 10a, b Building 7 Wall 1 ASCE zone 4 - interior (1 ft^2 = 0.0929 m^2)

Table 1 Results for Building 7
(ASCE underestimates by *n* means the ratio of the envelope of the data to the ASCE specification for that area is *n*.)

Fig.	part	zone	- pressure	+ pressure
A1 8	Roof 3	Lower corner	ASCE underestimates by 1.5 for A > 4 cells, by 2.3 for smaller areas.	ASCE acceptable.
A2	Roof 3	Side edge	ASCE underestimates by 1.8 for A = 70 ft^2 (7 m^2) to 2.0 for A = 7 ft^2 (0.7 m^2).	ASCE acceptable.
A3	Roof 3	Upper edge	ASCE underestimates by 1.1. This edge is on the leeward side.	ASCE acceptable
A4 7	Roof 3	Lower edge	ASCE underestimates by 1.6 for larger areas (60 ft^2 or 6 m^2) and 2.2 for smaller areas (2 ft^2 or 0.2 m^2).	ASCE underestimates by 1.7 for A $\leq$ 3 ft^2 (0.3 m^2), acceptable for larger areas.
A5 6	Roof 3	Interior	ASCE underestimates by 1.3 for A = 1000 ft^2 (100 m^2) to 2.5 for A = 10 ft^2 (1 m^2)	ASCE underestimates by 1.7 for 5 $ft^2 \leq A \leq 30$ ft^2 (0.5 $m^2 \leq A \leq 3$ m^2)
B1	Roof 2	Side edge	ASCE underestimates by 1.8 for A = 70 ft^2 (7 m^2) to 2.0 for A = 7 ft^2 (0.7 m^2).	ASCE acceptable
B2	Roof 2	Upper edge	ASCE acceptable. This edge is on the leeward side.	ASCE acceptable
B3	Roof 2	Lower edge	ASCE underestimates by 1.5 for A = 70 ft^2 (7 m^2) to 2.0 for A = 7 ft^2 (0.7 m^2).	ASCE acceptable
B4	Roof 2	Interior	ASCE underestimates by1.3 for A = 1000 ft^2 (93 m^2) to 2.5 for A = 8 ft^2 (0.8 m^2).	ASCE acceptable
B5	Roof 2	Corners	ASCE underestimates by 1.6 for A = 5 ft^2 (0.5 m^2), acceptable for A $\geq$ 10 ft^2 (1 m^2).	ASCE acceptable
The lower corner, on the windward side, records higher suction than the upper corner.				
C1 10	Wall 1	Interior	ASCE underestimates between 1.2 for A = 1100 ft^2 (110 m^2) and 1.9 for A = 60 ft^2 (6 m^2).	ASCE underestimates by 1.8
C2	Wall 1	Right edge	ASCE underestimates by 1.2.	ASCE acceptable
The most demanding wind directions are not tested for the right edge.				
C3 9	Wall 1	Left edge	ASCE underestimates by 1.6. - peaks for wind between 50° and 65°.	ASCE underestimates by 1.6. + peaks for wind directions of 10°.
D1	Wall 4	Interior	ASCE underestimates by 2.1 for A = 20 ft^2 (2 m^2), 1.4 for A = 1000 ft^2 (90 m^2). Linear trend of log A in between.	ASCE underestimates by 1.8 for A = 20 ft^2 (2 m^2), 2.0 for A = 500 ft^2 (50 m^2).
D2	Wall 4	Left edge	ASCE underestimates by 1.6. - peaks for wind between 330° and 360°.	ASCE underestimates by 1.6. + peaks between 290° and 335°.
D3	Wall 4	Right edge	ASCE underestimates by 1.2.	ASCE *overestimates* by 1.2.
The most demanding wind directions are not tested for the right edge.				

Table 2 Results for Building 15

Fig.	part	zone	- pressure	+ pressure
E1	Roof 3	Interior	ASCE acceptable for A = 3000 ft^2 (300 m^2), underestimates by 2.5 for A = 10 ft^2 (1 m^2). Linear trend of log A in between.	ASCE acceptable
E2	Roof 3	Lower edge	ASCE underestimates by 1.5 for A = 200 ft^2 (20 m^2), by 2.2 for A = 8 ft^2 (0.8 m^2). Linear trend of log A in between.	ASCE acceptable
E3	Roof 3	Upper edge	ASCE underestimates by 1.4 for A = 200 ft^2 (20 m^2), by 1.7 for A = 10 ft^2 (1 m^2). Linear trend of log A in between.	ASCE acceptable
E4	Roof 3	Side edge	ASCE underestimates by 1.5 for A = 200 ft^2 (20 m^2), by 1.7 for A = 10 ft^2 (1 m^2). Linear trend of log A in between.	ASCE acceptable
E5	Roof 3	Lower corner	ASCE underestimates by 1.4 for A = 60 ft^2 (6 m^2), by 1.8 for A = 7 ft^2 (0.7 m^2).	ASCE acceptable
E6	Roof 3	Upper corner	ASCE underestimates by 1.7 for A $\geq$ 20 ft^2 (2 m^2), by 1.2 for A = 8 ft^2 (0.8 m^2).	ASCE acceptable
F1	Roof 2	Interior	ASCE *overestimates* by 2.0 for A = 2000 ft^2 (200 m^2), underestimates by 2.2 for A = 30 ft^2 (3 m^2). Linear trend of log A in between.	ASCE acceptable
F2	Roof 2	Lower edge	ASCE underestimates by 1.2 for A = 200 ft^2 (20 m^2), by 1.5 for A = 15 ft^2 (1.5 m^2).	ASCE acceptable
F3	Roof 2	Upper edge	ASCE underestimates by 1.2 for A = 200 ft^2 (20 m^2), by 1.4 for A = 7 ft^2 (0.7 m^2).	ASCE acceptable
F4	Roof 2	Side edge	ASCE underestimates by 1.2.	ASCE acceptable
F5	Roof 2	Lower Corner	ASCE underestimates by 1.3 for A = 70 ft^2 (7 m^2) to 1.5 for A = 12 ft^2 (1.2 m^2).	ASCE *overestimates* by 2.5, but pressures are small.
For lower corner, -peaks for wind at 360°, +peaks for wind between 180° and 260°. Symmetrical directions were covered for upper corner.				
F6	Roof 2	Upper Corner	ASCE *overestimates* by 1.6 for A < 10 ft^2 (1 m^2).	ASCE *overestimates* by 2.5, but pressures are small.
G1	Wall 1	Interior	ASCE *overestimates* by 1.3 for A = 4000 ft^2 (400 m^2), underestimates by 2.0 for A = 60 ft^2 (6 m^2). Linear trend of log A in between.	Negligible on leeward side.
Wall 1 is on leeward side.				
G2	Wall 1	Left edge	ASCE underestimates by 1.4.	Negligible on leeward side.
G3	Wall 1	Right edge	ASCE underestimates by 1.3.	Negligible on leeward side.
H1	Wall 4	Interior	ASCE *overestimates* by 1.8 for A = 3000 ft^2 (300 m^2), underestimates by 2.4 for A = 60 ft^2 (6 m^2).	ASCE underestimates by 2.0 for A = 1000 ft^2 (100 m^2), by 1.6 for A = 60 ft^2 (6 m^2).
H2	Wall 4	Left edge	ASCE underestimates by 1.4	ASCE underestimates by 1.5.
H3	Wall 4	Right edge	ASCE underestimates by 1.4.	ASCE underestimates by 1.7.

directions, the spatial coherence of wind pressure may extend over longer shapes than those mentioned in the Commentary.)

Uncertainty

The design of buildings for wind involves many uncertainties in the micrometeorological, wind climatological and aerodynamic elements that determine wind loads (see, e.g., Simiu 2011, p. 229, Duthinh and Simiu 2011). A fundamental difficulty in achieving reproducible wind tunnel measurements of wind effects, especially on low-rise buildings, is the simulation of atmospheric flows (Simiu, 2009). Ho et al. (2003, 2003, 2005) discussed the methodology used in the NIST-UWO tests in modelling the terrain, characterizing the modelled wind, and measuring wind pressures by a tubing system. They found it difficult to arrive at an overall uncertainty factor, but they compared wind tunnel measurements to full scale measurements of a building at Texas Tech University (TTU), and concluded that "mean pressures compared well", but root mean square "rms pressures… showed significant differences."

In the analysis of the wind pressure data, it was discovered that a few pressure taps malfunctioned, and their records have been replaced by the average of neighboring taps. The area-averaging method is not unique, but similar methods produced comparable results (Gierson et al. 2015, Morrison 2015).

Finally, statistics is an essential element in the definition of wind effects for design purposes, especially for the determination of peak wind pressures induced by a given wind speed. For the Sadek-Simiu method used here, the goodness of the peak estimation depends on the goodness of fit of the distributions to the peaks of the tails of the time series. A future publication that discusses alternative methods, using the Generalized Extreme Value distribution, is planned.

Conclusion

This note presents a methodology used to exploit wind tunnel pressure measurements to arrive at graphs of peak positive and negative pressure coefficients corresponding to various areas over all wind directions. Such plots will eventually lead to specifications required for the design of components and cladding by the envelope method. According to the results shown here for two buildings and one terrain exposure, the *negative* wind pressure coefficients (suction) specified by ASCE 7-10 for gable roofs of low-rise buildings are too small, by factors ranging from 1.3 to 2.5, whereas the *positive* coefficients appear adequate. For walls, both positive and negative pressures are underestimated by current ASCE specifications, by factors ranging from 1.5 to 2.0 and 1.2 to 2.4, respectively. Future work will include the checking of these conclusions by using alternative methods for the estimation of peaks.

All buildings in the NIST-UWO database are being investigated, together with those in other publicly available databases such as the Tokyo Polytechnic Institute (Gierson et al. 2015). Only at the conclusion of the study can more definitive recommendations be made, including possibly changes in the number, size, shape and location of the various wind pressure zones, together with their associated pressure coefficients. This will be the subject of a future paper.

References

ASCE 7-10 (2010) "Minimum Design Loads for Buildings and Other Structures," American Society of Civil Engineers, Reston, VA

Durst, C.S. (1960) "Wind Speeds Over Short Periods of Time," *Meteor. Mag.* **89**, 181-187

Duthinh, D. and Simiu, E. (2011) "The Use of Wind Tunnel Measurements in Building Design," *Wind Tunnels and Experimental Fluid Dynamics Research,* Jorge Colman Lerner and Ulfilas Boldes (Eds.), Ch. 13, pp. 281-300, InTech - Open Access, DOI: 10.5772/18670

Gavanski, E., Kordi, B., Kopp, G.A. and Vickery, P.J. (2013a) "Wind Loads on Roof Sheathing of Houses," J. Wind Eng. & Ind. Aerodyn., **114**, 106-121

Gavanski, E., Kopp, G.A. and Vickery, P.J. (2013b) "Roof Sheathing Wind Loads on Wood-Frame Residential Houses," 12th Americas Conf. on Wind Eng. (12ACWE), Seattle, WA, June

Gavanski, E. and Uematsu, Y. (2014) "Local Wind Pressures Acting on Walls of Low-Rise Buildings and Comparisons to the Japanese and US Wind Loading Provisions," J. Wind Eng. & Ind. Aerodyn., **132**, 77-91

Gierson, M.L., Phillips, B.M. and Duthinh, D. (2015) "Evaluation of ASCE 7-10 Wind Velocity Pressure Coefficients on the Components and Cladding of Low-rise Buildings Using Recent Wind Tunnel Testing Data," 6th Int. Conf. on Advances in Experimental Structural Engineering, and 11th Int. Workshop on Advanced Smart Materials and Smart Structural Technology, Urbana, IL

Habte, F., Chowdhury, A. G. and Park, S. (2015) "The Use of Demand-to-Capacity Indexes for the Iterative Design of Rigid Structures for Wind," NIST Technical Note, National Institute of Standards and Technology, Gaithersburg, MD

Ho, T.C.E., Surry, D., and Morrish, D. (2003) "NIST/TTU Cooperative Agreement – Windstorm Mitigation Initiative: Wind Tunnel Experiments on Generic Low Buildings" University of Western Ontario, London, ON, Canada

Ho, T.C.E., Surry, D., and Nywening, M. (2003) "NIST/TTU Cooperative Agreement – Windstorm Mitigation Initiative: Further Experiments on Generic Low Buildings" University of Western Ontario, London, ON, Canada

Ho, T.C.E., Surry, D., Morrish, D., and Kopp, G.A. (2005) "The UWO Contribution to the NIST Aerodynamic Database for Wind Loads on Low Buildings Part 1: Archiving Format and Basic Aerodynamic Data" J. Wind Eng. Ind. Aerodyn., **93** (1),1-30

Lieblein, J. (1974) "Efficient Methods of Extreme Value Methodology," NBSIR74-602, National Bureau of Standards, Washington, DC

Main, J.A. (2011) "Special-Purpose Software: MATLAB Functions for Estimation of Peaks from Time Series," www.itl.nist.gov/div898/winds/homepage.htm, National Institute of Standards and Technology, Gaithersburg, MD

Main, J. and Fritz, W.P. (2006) "Database-Assisted Design for Wind: Concepts, Software, and Examples for Rigid and Flexible Buildings," NIST Building Science Series 180, National Institute of Standards and Technology, Gaithersburg, MD

Meecham, D. (1988) "Wind Action on Low-Rise Buildings," M.E.Sc. Thesis, The University of Western Ontario, London, ON, Canada

Morrison, M. (2015) "Wind Pressure on Cladding of Low-Rise Buildings," private communication

NIST (2004) "Extreme Winds and Wind Effects on Structures" (Aerodynamic Database for Rigid Buildings) www.itl.nist.gov/div898/winds/homepage.htm, National Institute of Standards and Technology, Gaithersburg, MD, created 03/05/2004, last updated 05/22/2015, last accessed 09/04/2015

Sadek, F. and Simiu, E. (2002) "Peak Non-Gaussian Wind Effects for Database-Assisted Low-Rise Building Design," ASCE J. Eng. Mech. **128** (5), 530-539, May

Simiu, E. (2011) "Design of Buildings for Wind," 2nd ed. John Wiley, Hoboken, N.J.

Simiu, E. (2009). "Toward A Standard on the Wind Tunnel Method," NIST Technical Note 1655, National Institute of Standards and Technology, Gaithersburg, MD

Simiu, E. and Scanlan, R.H. (1996) "Wind Effects on Structures," 3rd ed. Wiley, New York, N.Y.

Stathopoulos, T. (1979) "Turbulent Wind Action on Low-Rise Buildings," Ph.D. Thesis, The University of Western Ontario, London, ON, Canada

Stathopoulos, T., Wang, K. and Wu, H. (1999) "Wind Standard Provisions for Low-Building Gable Roof Revisited," 10th Int. Conf. on Wind Eng., Copenhagen, Denmark, 155-162

Tamura, Y. (2012) "Aerodynamic Database for Low-Rise Buildings," (Database) Global Center of Excellence Program, Tokyo Polytechnic University, Tokyo, Japan

Vickery, P.J., Kopp, G.A. and Twisdale, L.A. (2013) "Component and Cladding Wind Pressures on Hip and Gable Roofs: Comparisons to the US Wind Loading Provisions," 12th Americas Conf. on Wind Eng. (12ACWE), Seattle, WA, June

Appendix A Building 7, roof 3

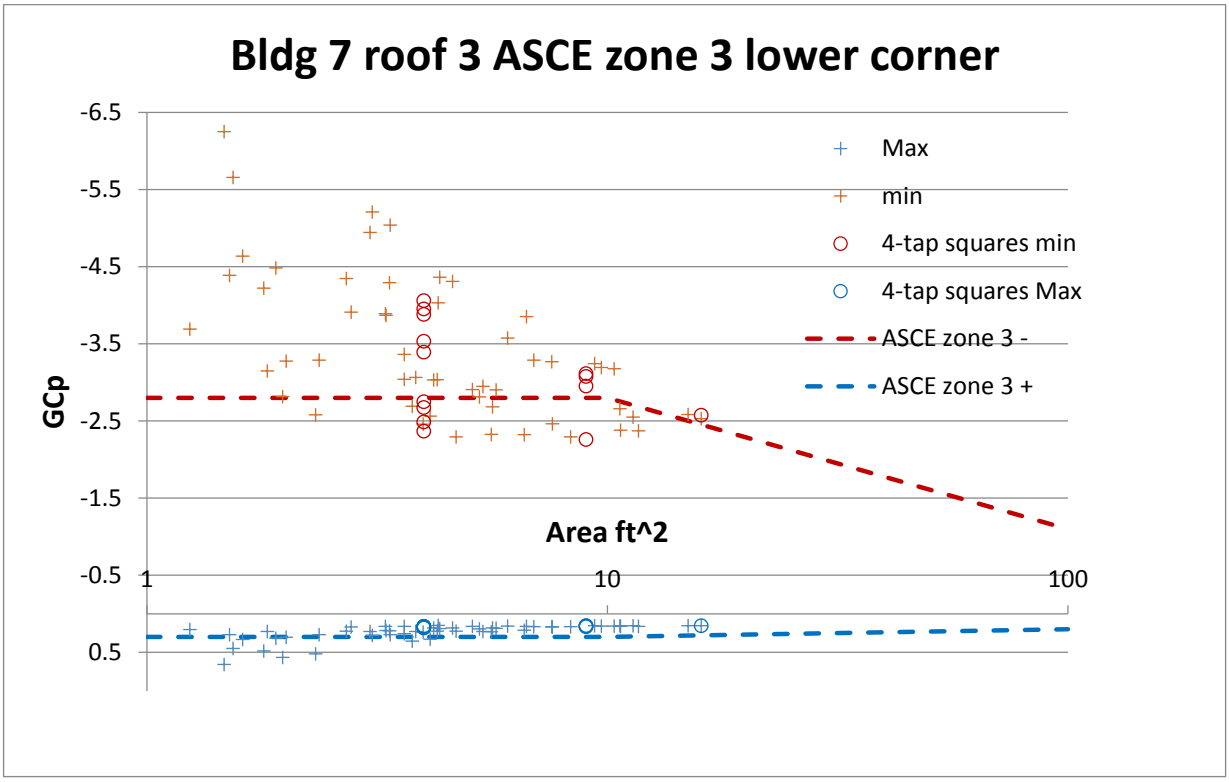

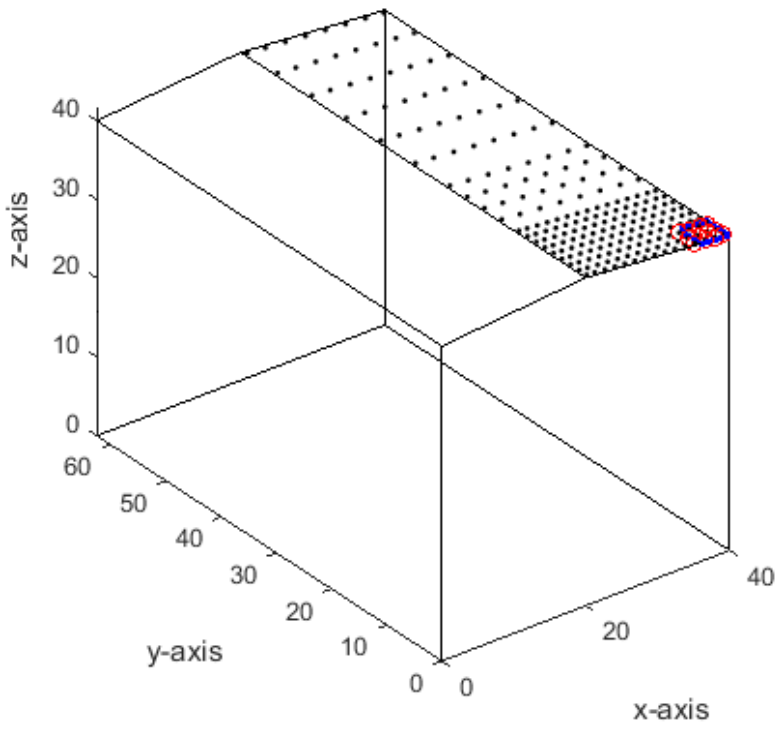

Fig. A1a, b Bldg 7 roof 3 ASCE zone 3 lower corner (1 ft^2 = 0.0929 m^2)

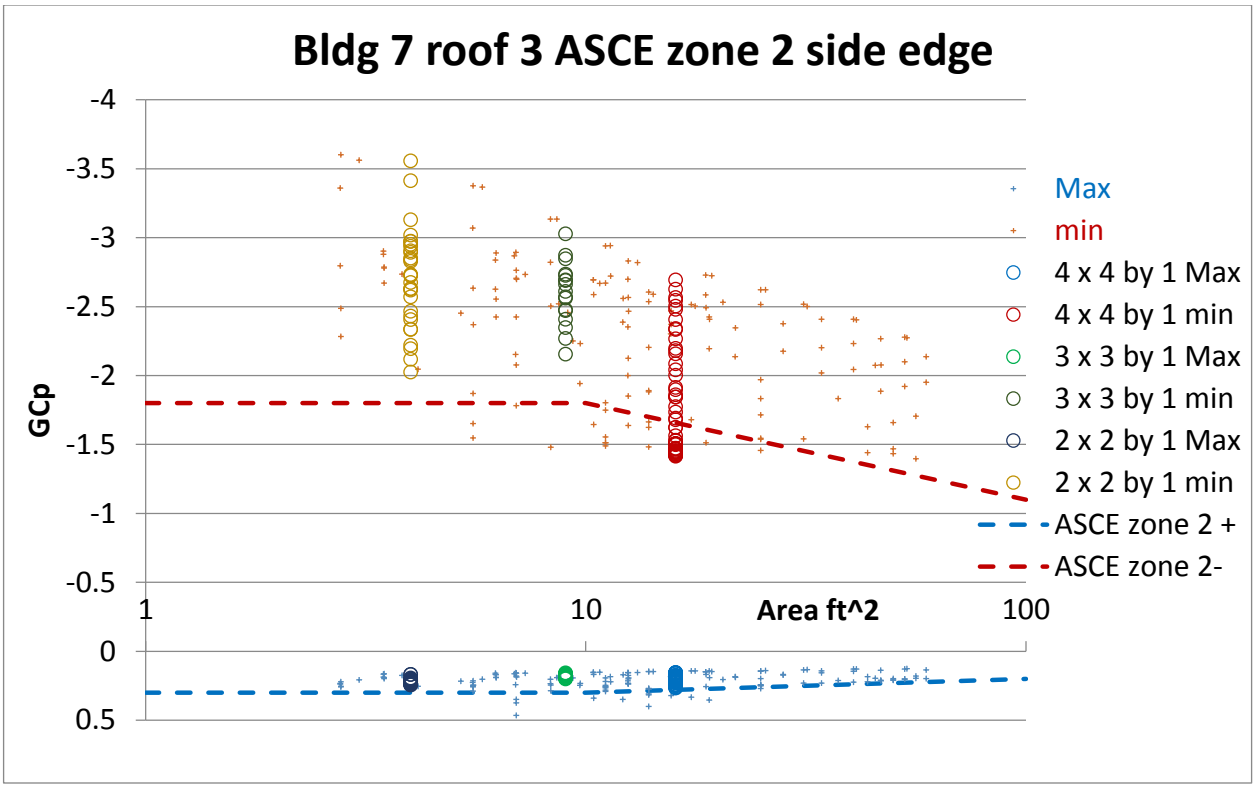
Bldg 7 roof 3 ASCE zone 2 side edge
GCp
-4
-3.5
-3
-2.5
-2
-1.5
-1
-0.5
0
0.5
1
10
100
Area ft^2
Max
min
4 x 4 by 1 Max
4 x 4 by 1 min
3 x 3 by 1 Max
3 x 3 by 1 min
2 x 2 by 1 Max
2 x 2 by 1 min
ASCE zone 2 +
ASCE zone 2-

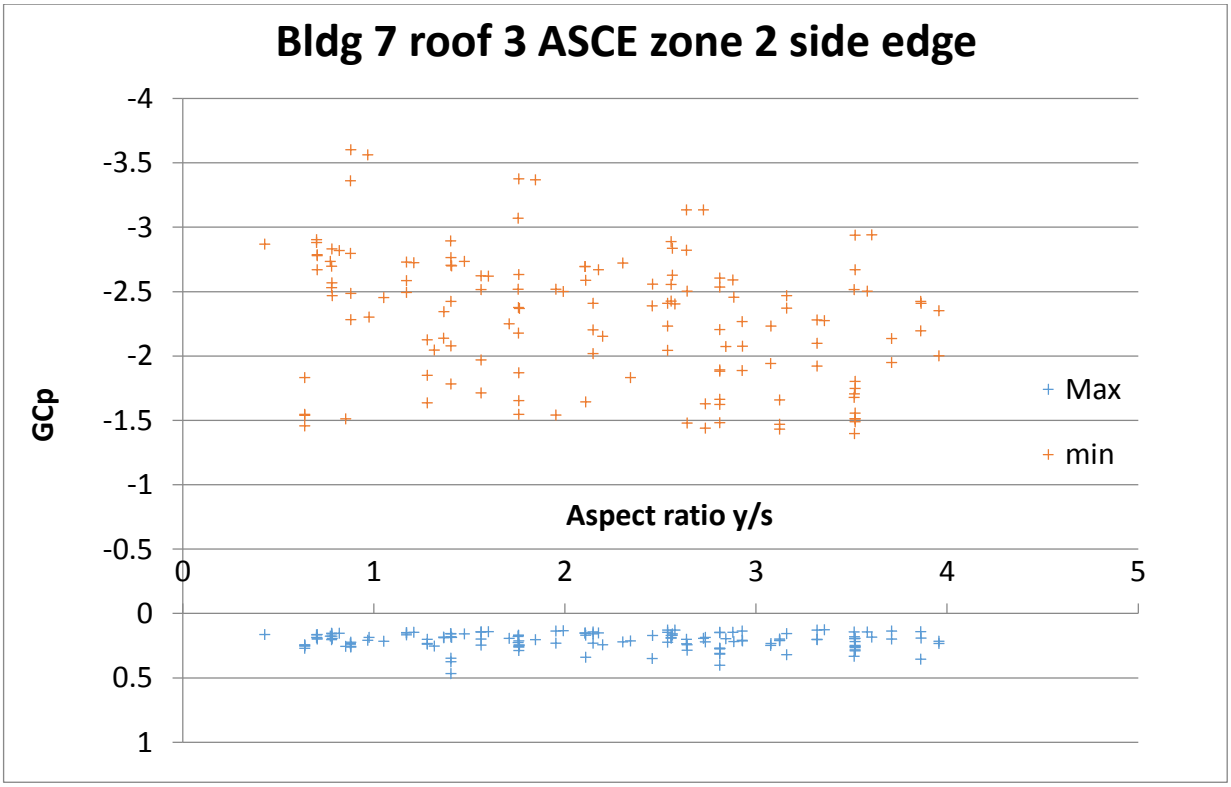
Bldg 7 roof 3 ASCE zone 2 side edge
GCp
-4
-3.5
-3
-2.5
-2
-1.5
-1
-0.5
0
0.5
1
0
1
2
3
4
5
Aspect ratio y/s
Max
min

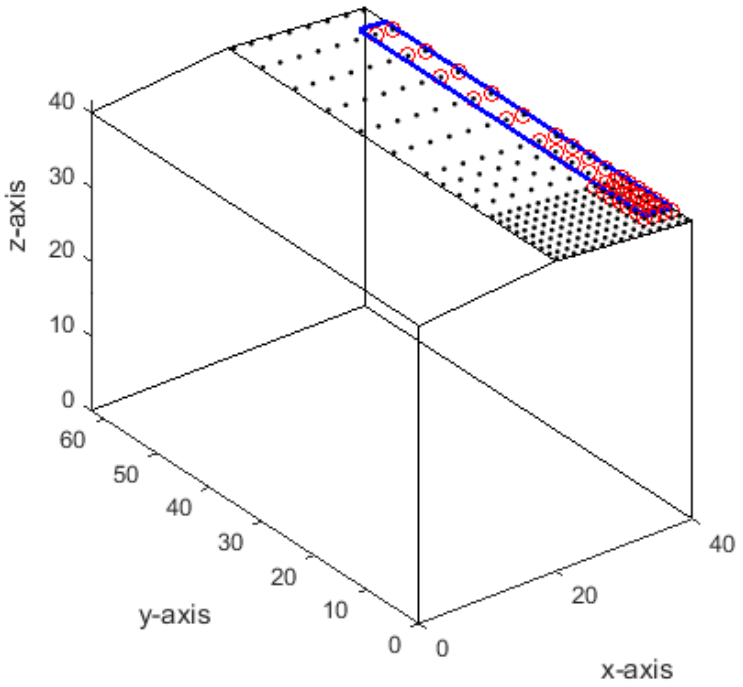

Fig. A2a, b, c Bldg 7 roof 3 ASCE zone 2 side edge (1 ft^2 = 0.0929 m^2)

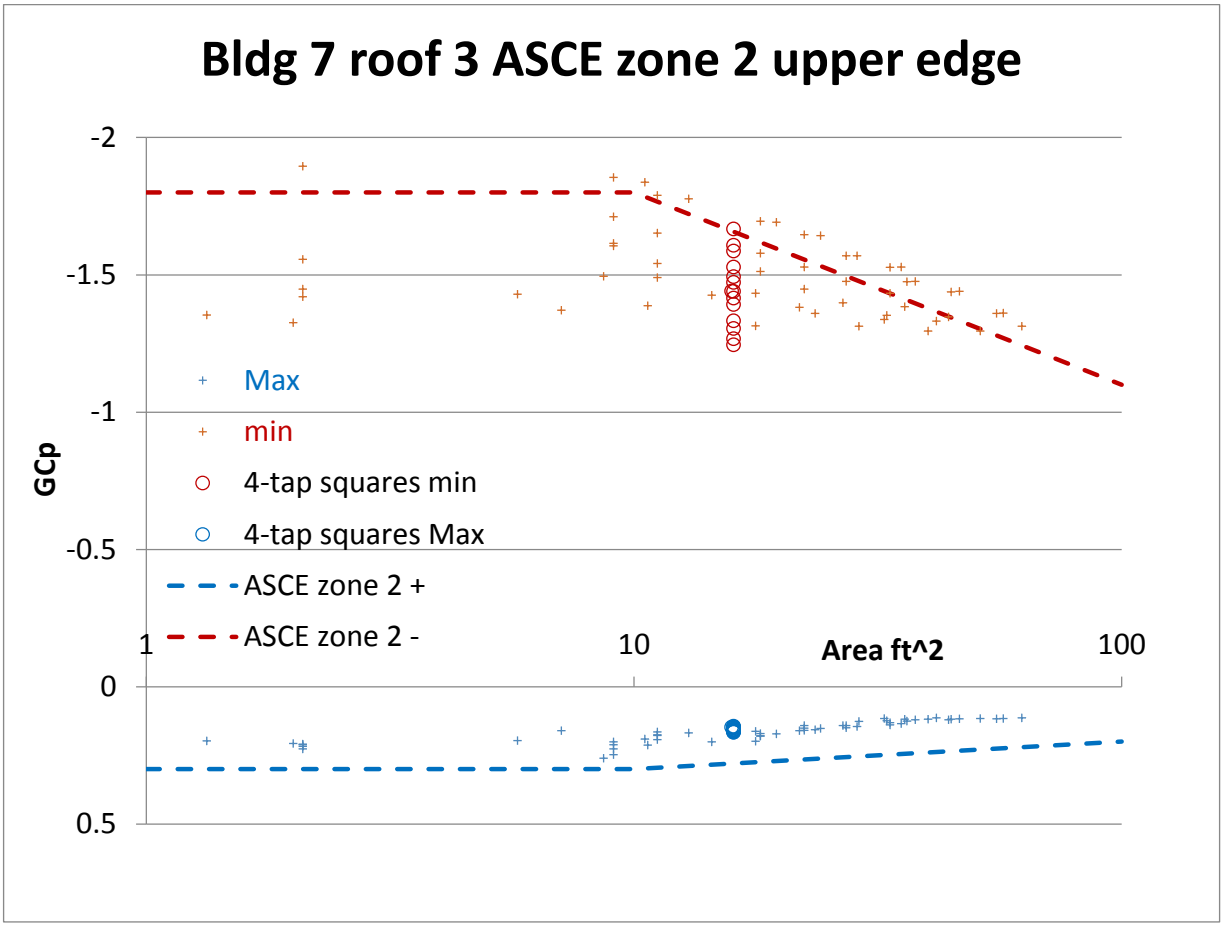

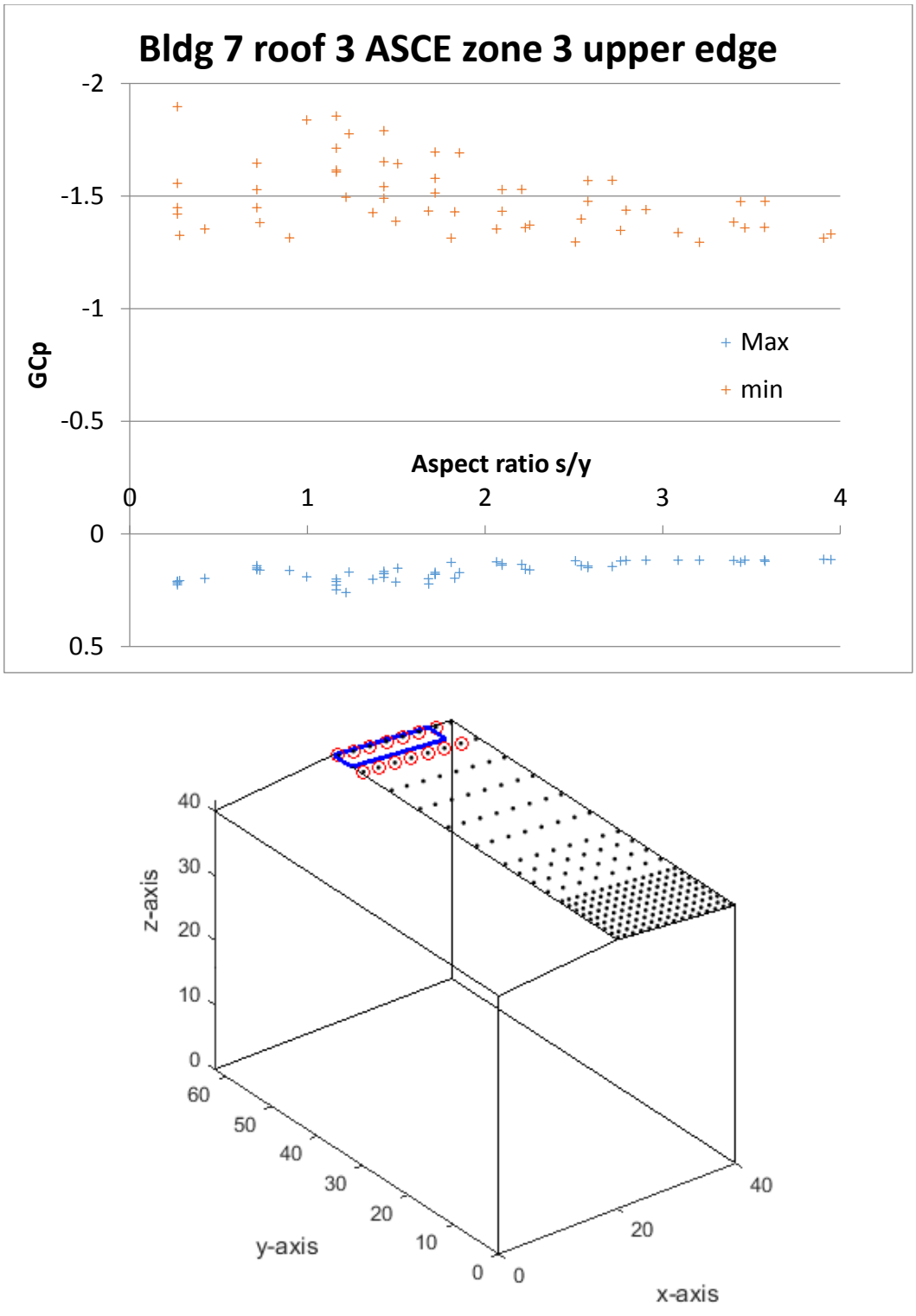

Fig. A3a, b, c Bldg 7 roof 3 ASCE zone 2 upper edge (1 ft^2 = 0.0929 m^2)

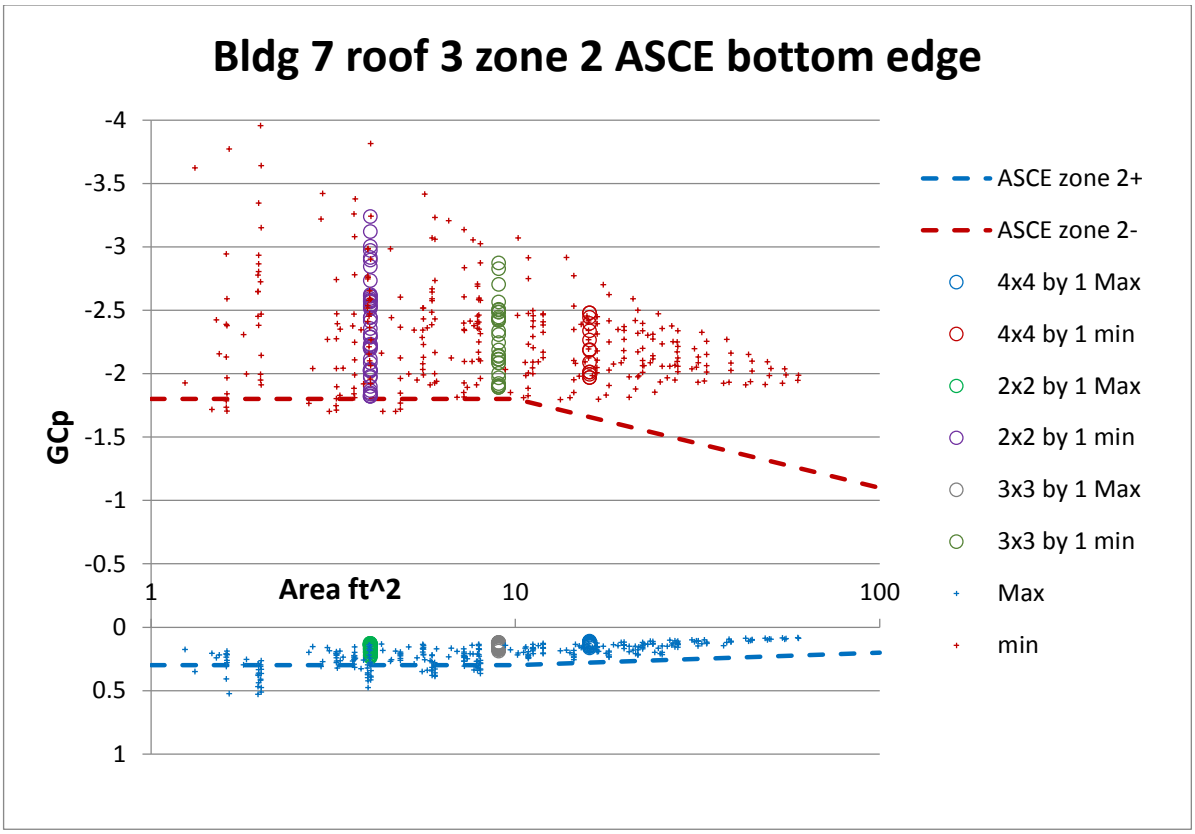
Bldg 7 roof 3 zone 2 ASCE bottom edge
GCp
-4
-3.5
-3
-2.5
-2
-1.5
-1
-0.5
0
0.5
1
1
10
100
Area ft^2
ASCE zone 2+
ASCE zone 2-
4x4 by 1 Max
4x4 by 1 min
2x2 by 1 Max
2x2 by 1 min
3x3 by 1 Max
3x3 by 1 min
Max
min

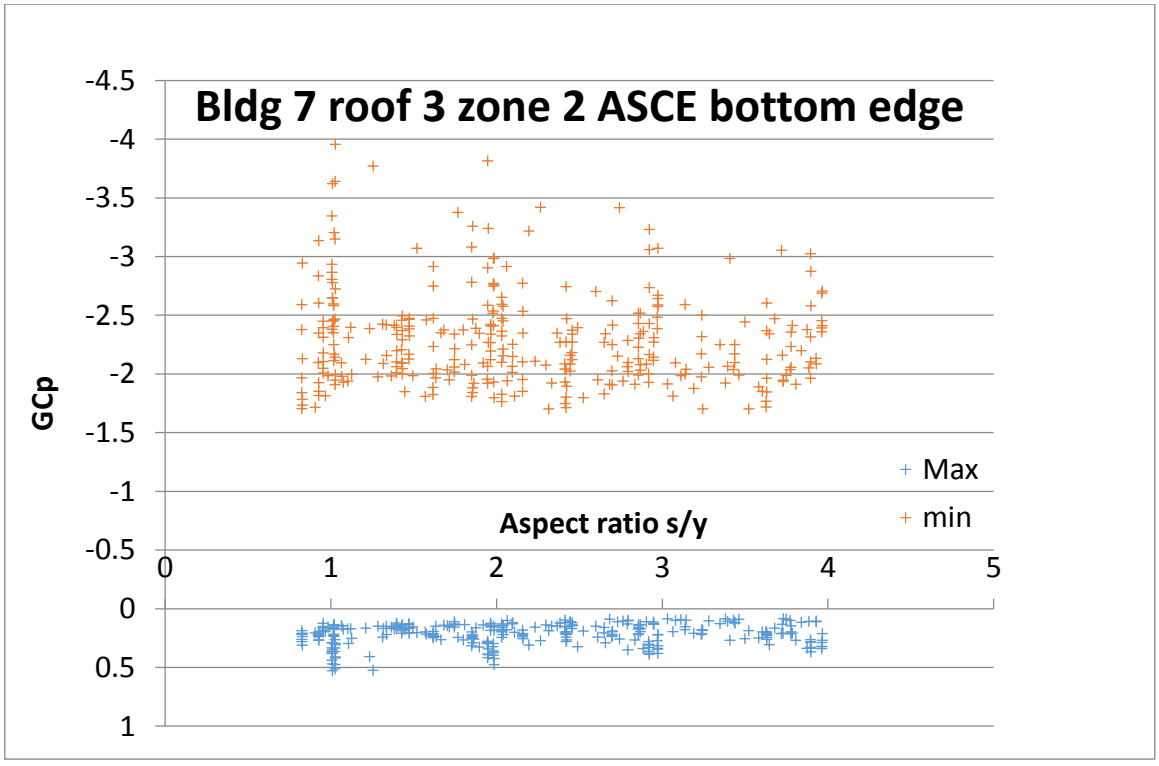
Bldg 7 roof 3 zone 2 ASCE bottom edge
GCp
-4.5
-4
-3.5
-3
-2.5
-2
-1.5
-1
-0.5
0
0.5
1
0
1
2
3
4
5
Aspect ratio s/y
Max
min

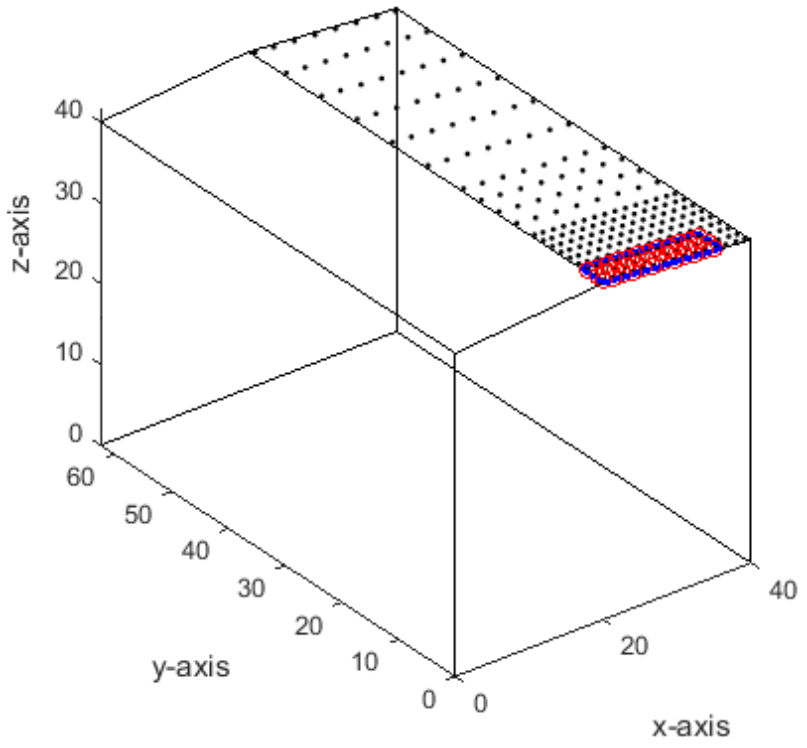

Fig. A4a, b, c Bldg 7 roof 3 ASCE zone 2 lower edge (1 ft^2 = 0.0929 m^2)

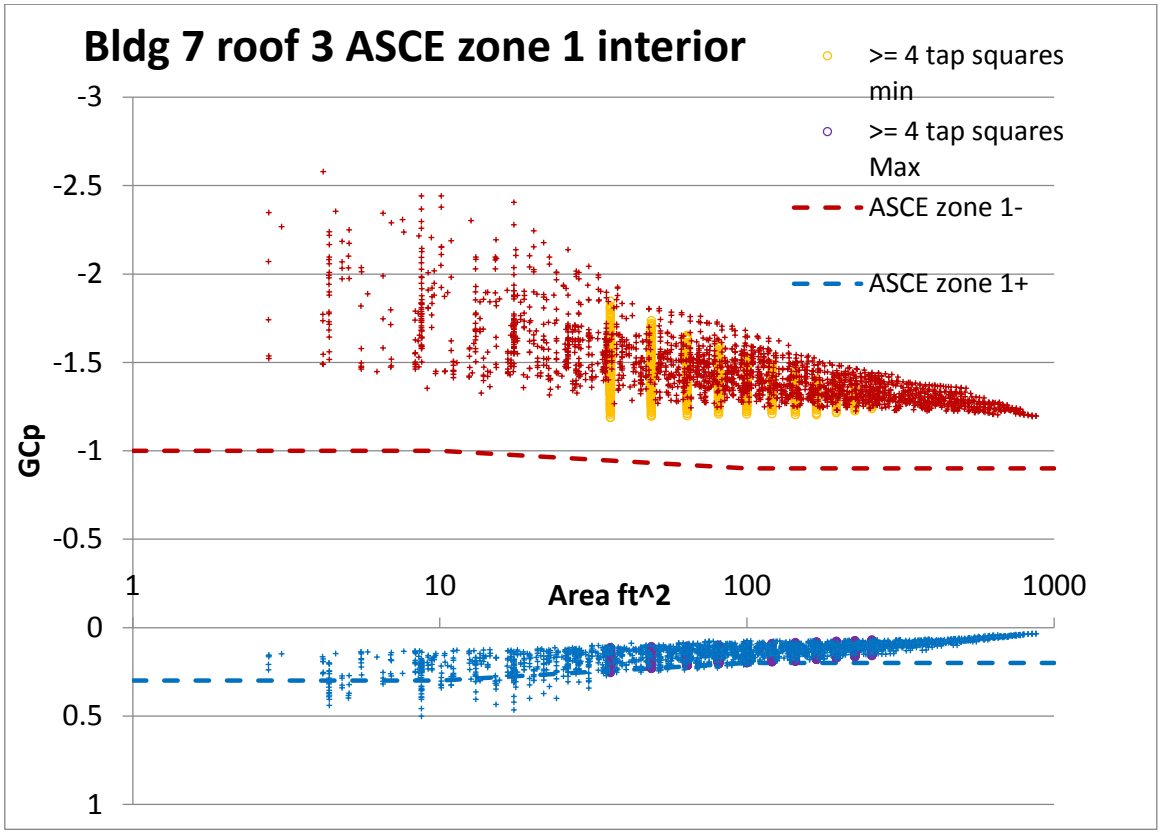

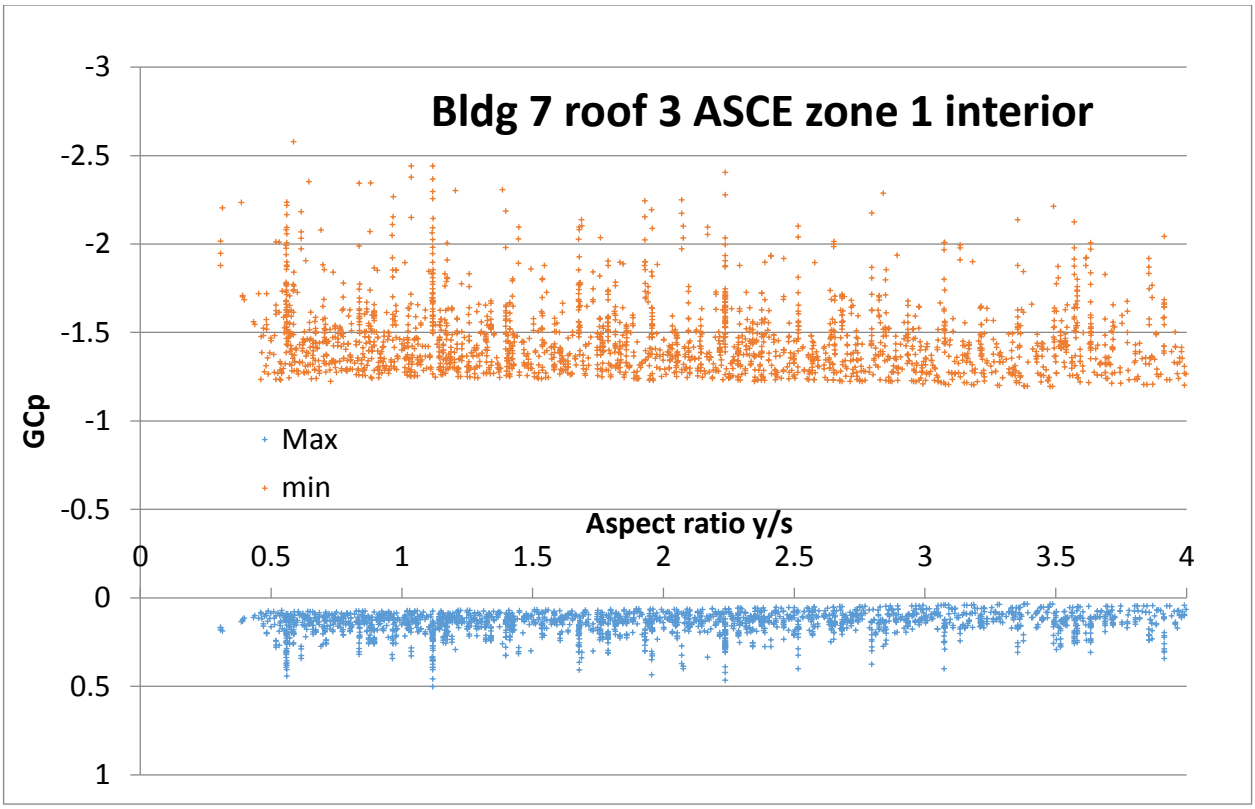

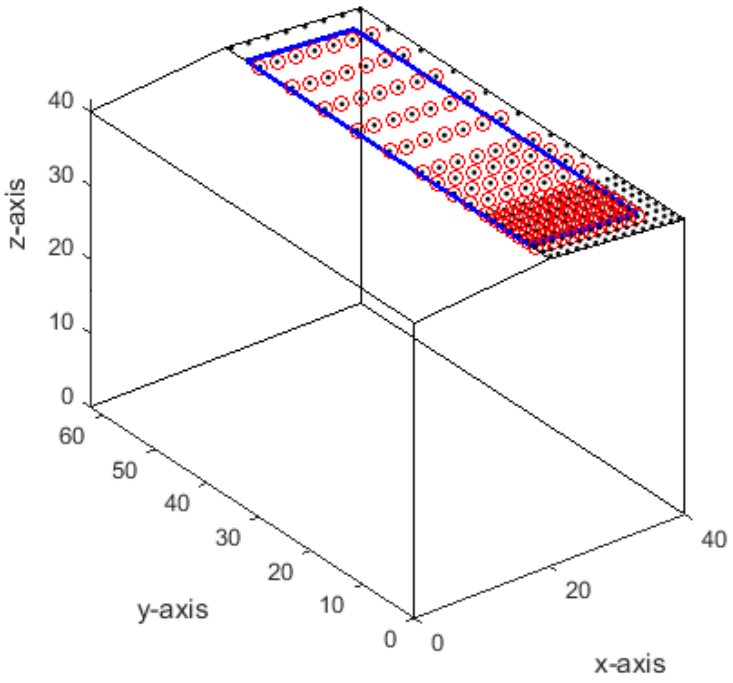

Fig. A5a, b, c Bldg 7 roof 3 ASCE zone 1 interior (1 ft^2 = 0.0929 m^2)

Appendix B Building 7, roof 2

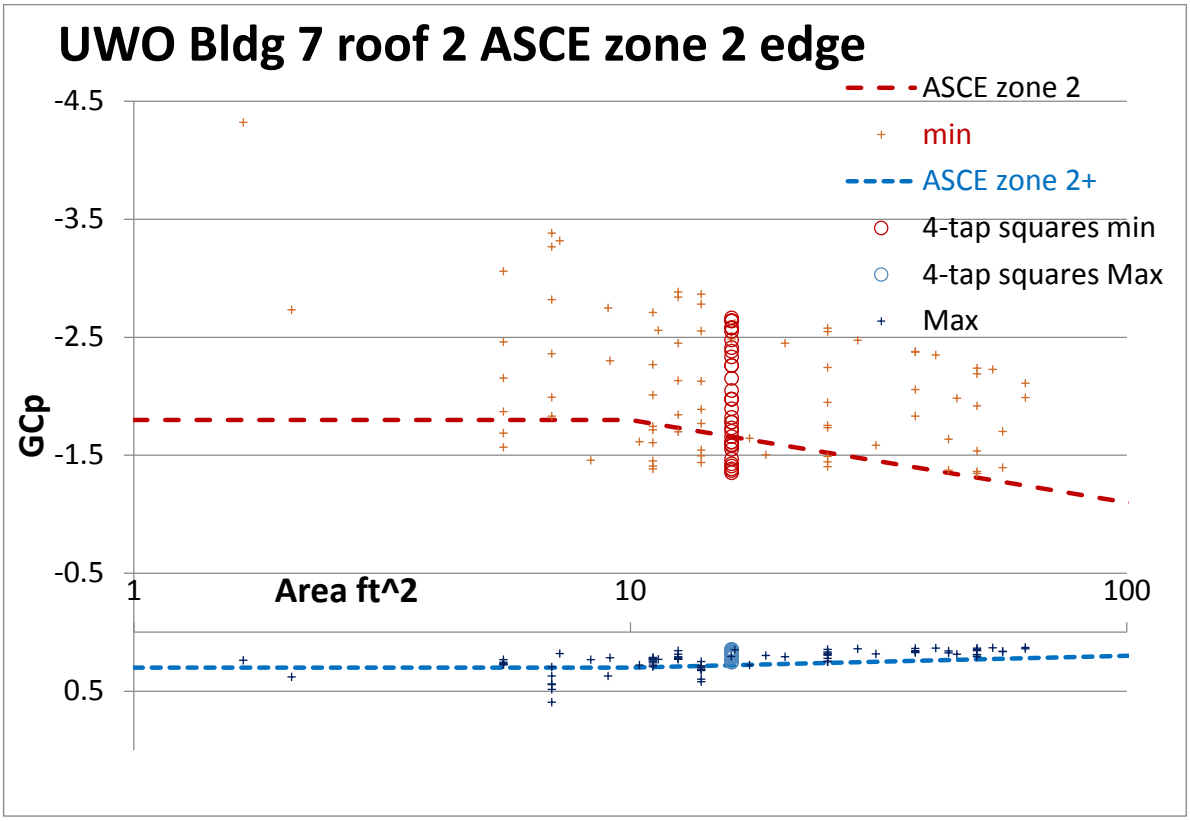

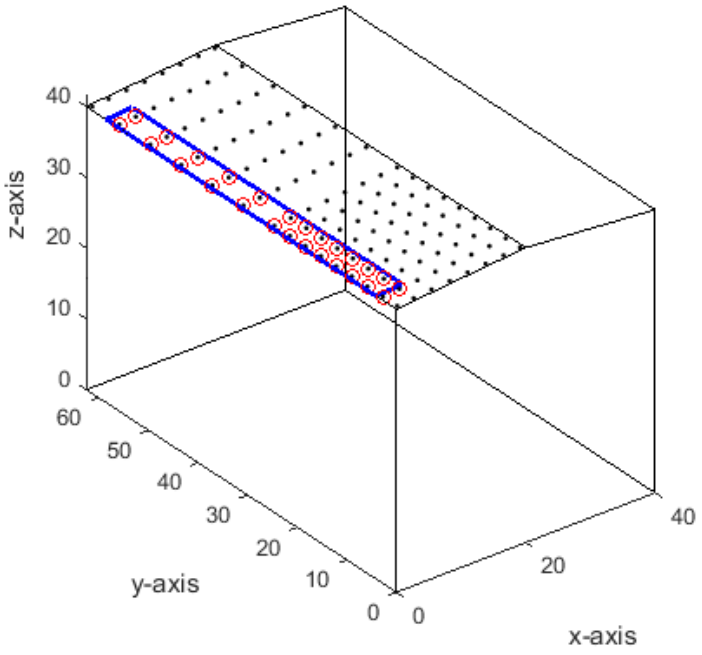

Fig. B1 UWO Bldg 7 roof 2 ASCE zone 2 edge (1 ft^2 = 0.0929 m^2)

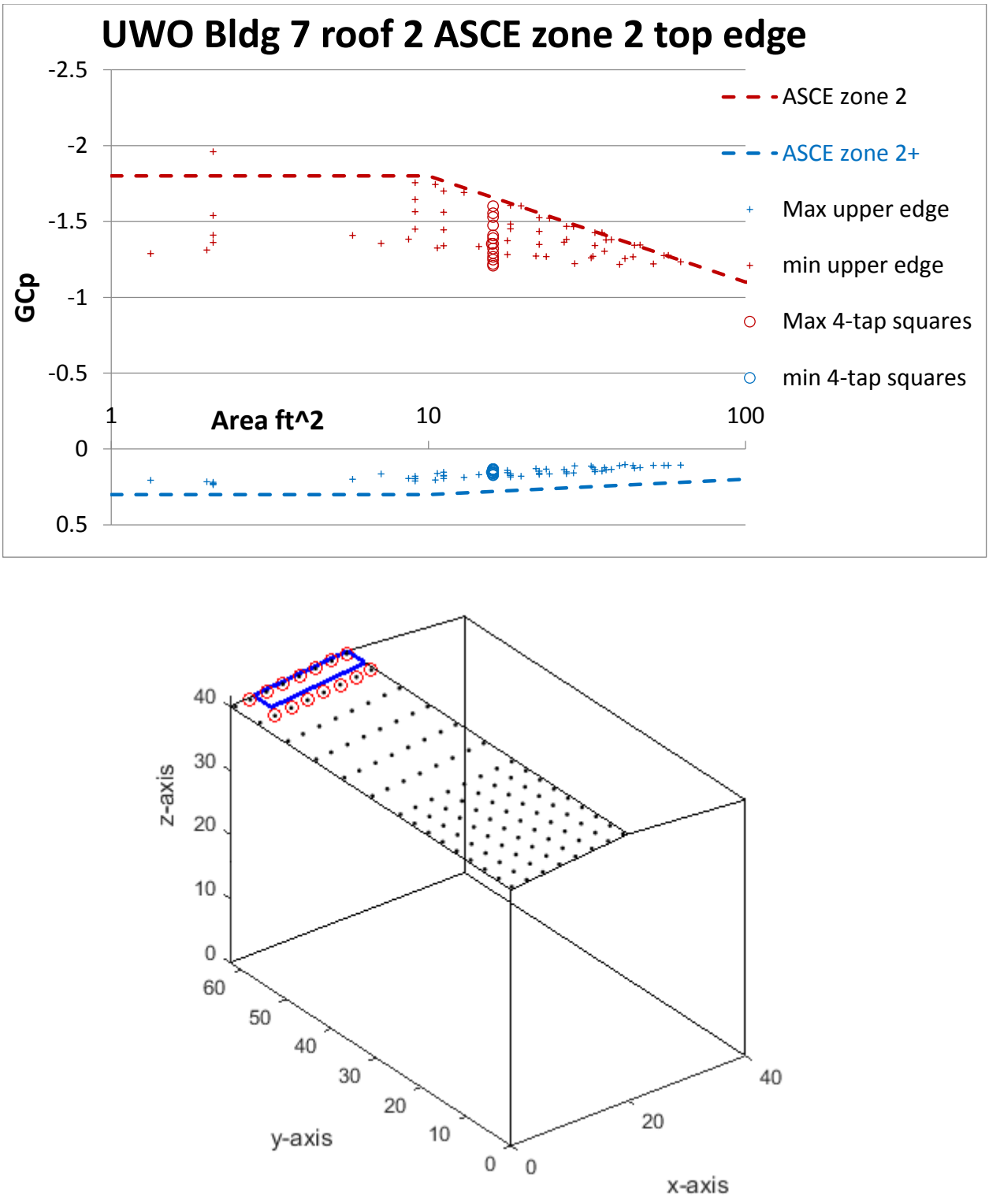

Fig. B2 UWO Bldg 7 roof 2 ASCE zone 2 top edge (1 ft^2 = 0.0929 m^2)

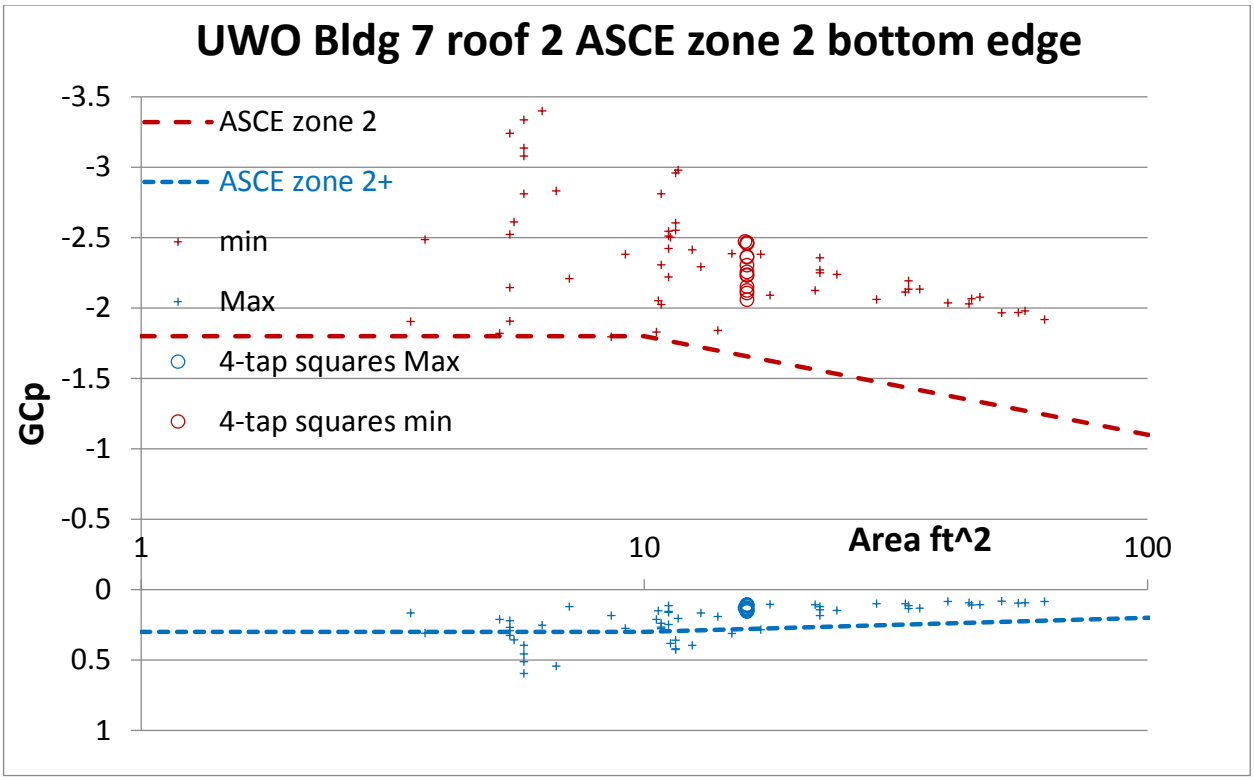

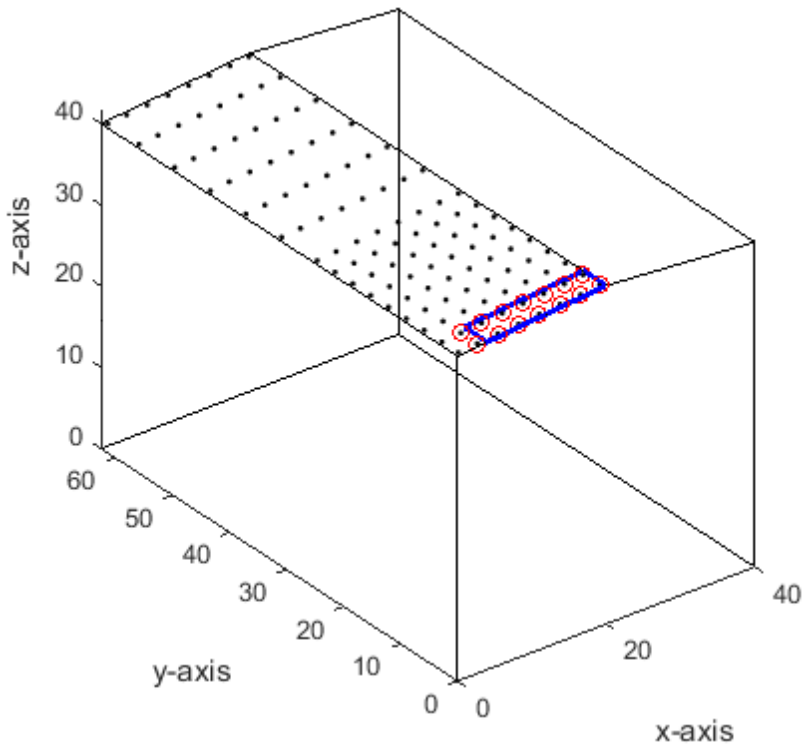

Fig. B3 UWO Bldg 7 roof 2 ASCE zone 2 bottom edge (1 ft^2 = 0.0929 m^2)

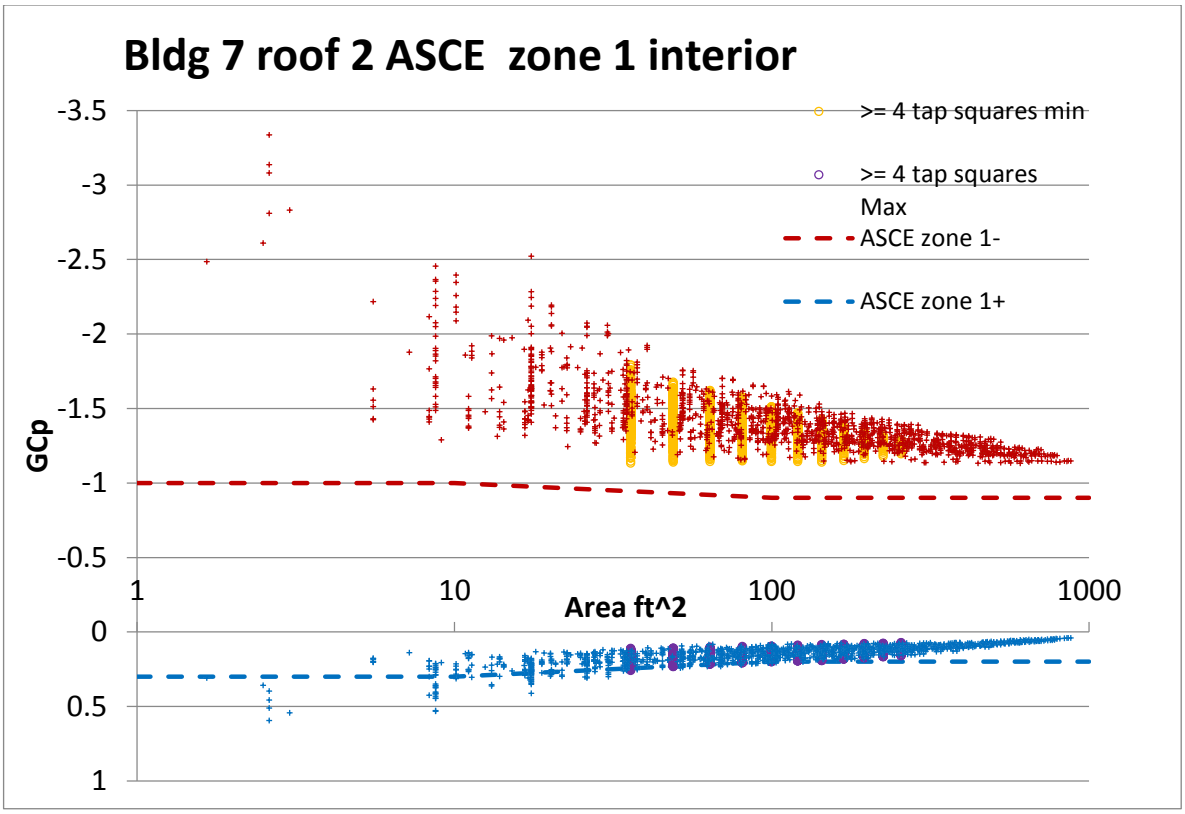

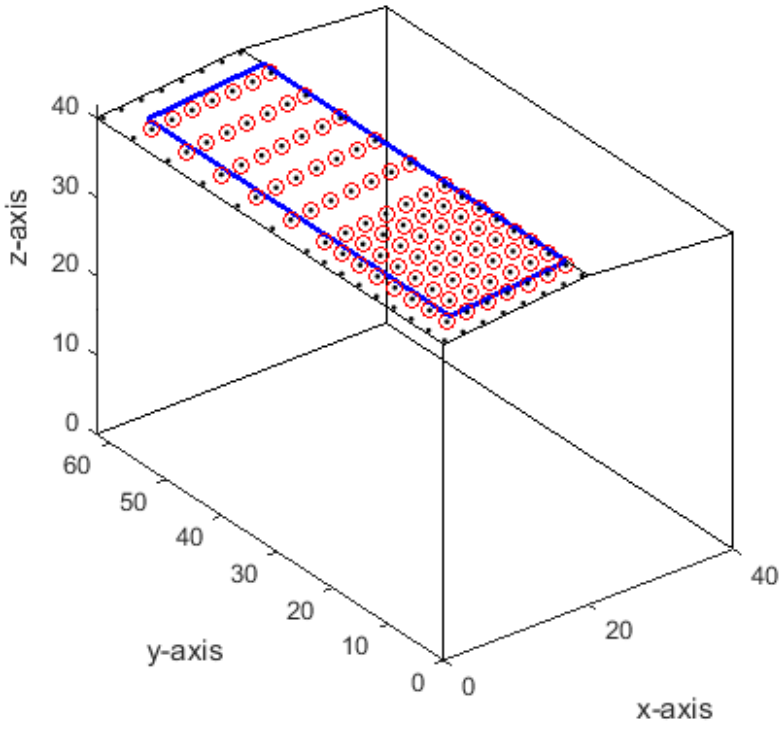

Fig. B4 Bldg 7 roof 2 ASCE zone 1 interior (1 ft^2 = 0.0929 m^2)

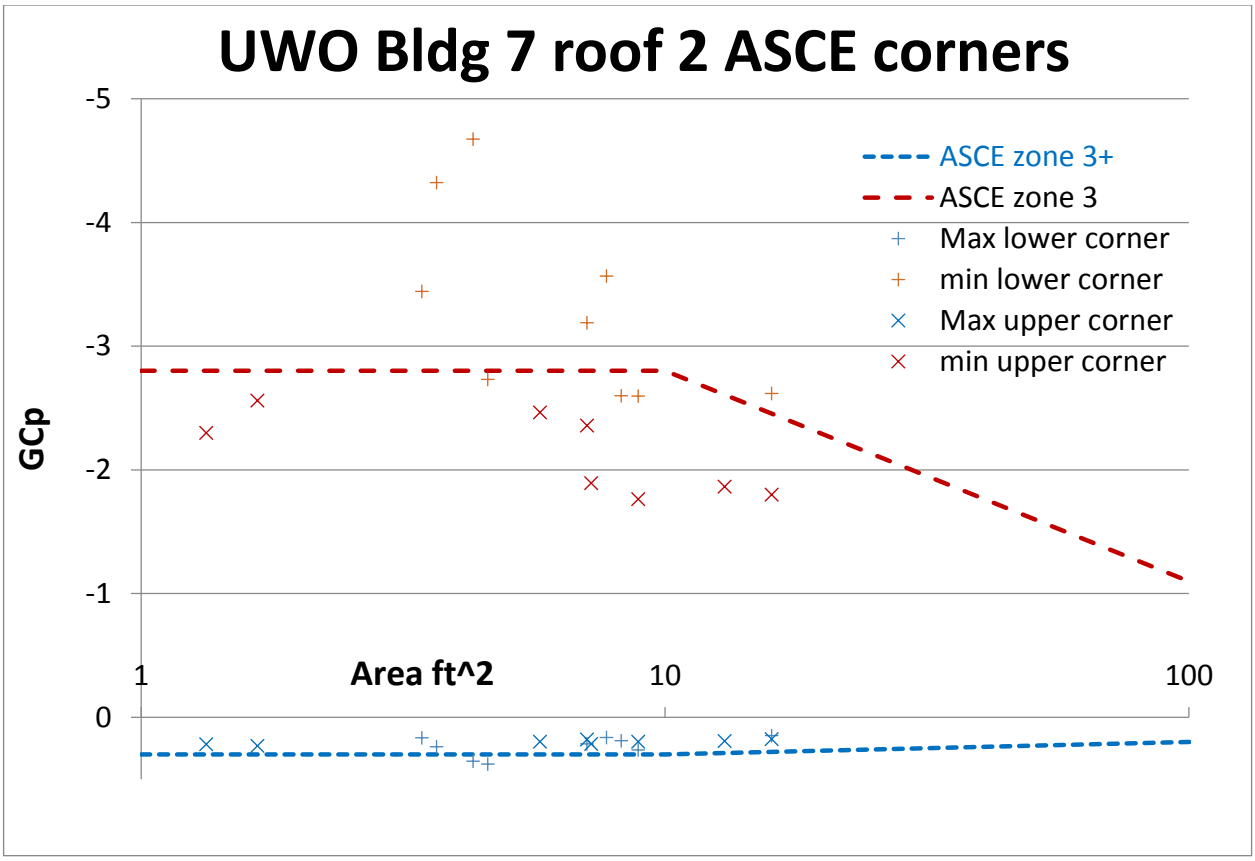

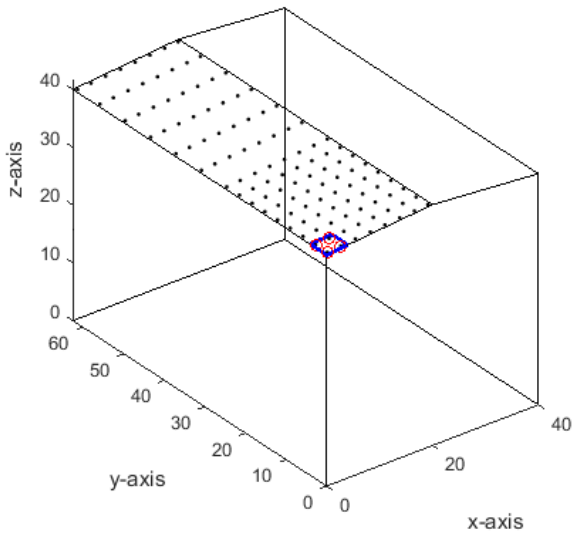

Lower corner

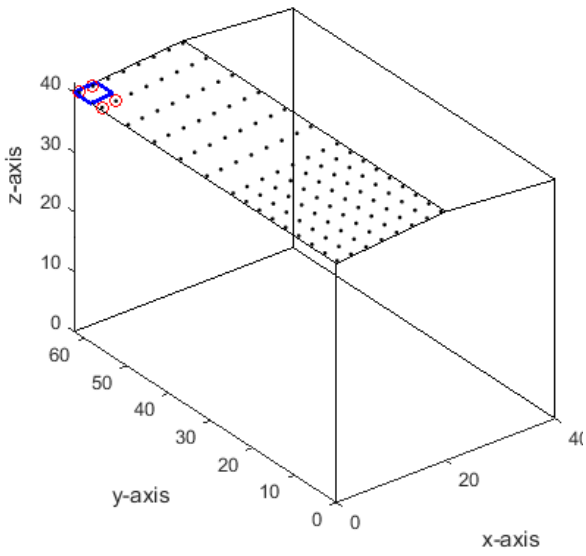

Upper corner

Fig. B5a, b Bldg 7 roof 2 ASCE zone 3 corners (1 ft^2 = 0.0929 m^2)

Appendix C Building 7 Wall 1

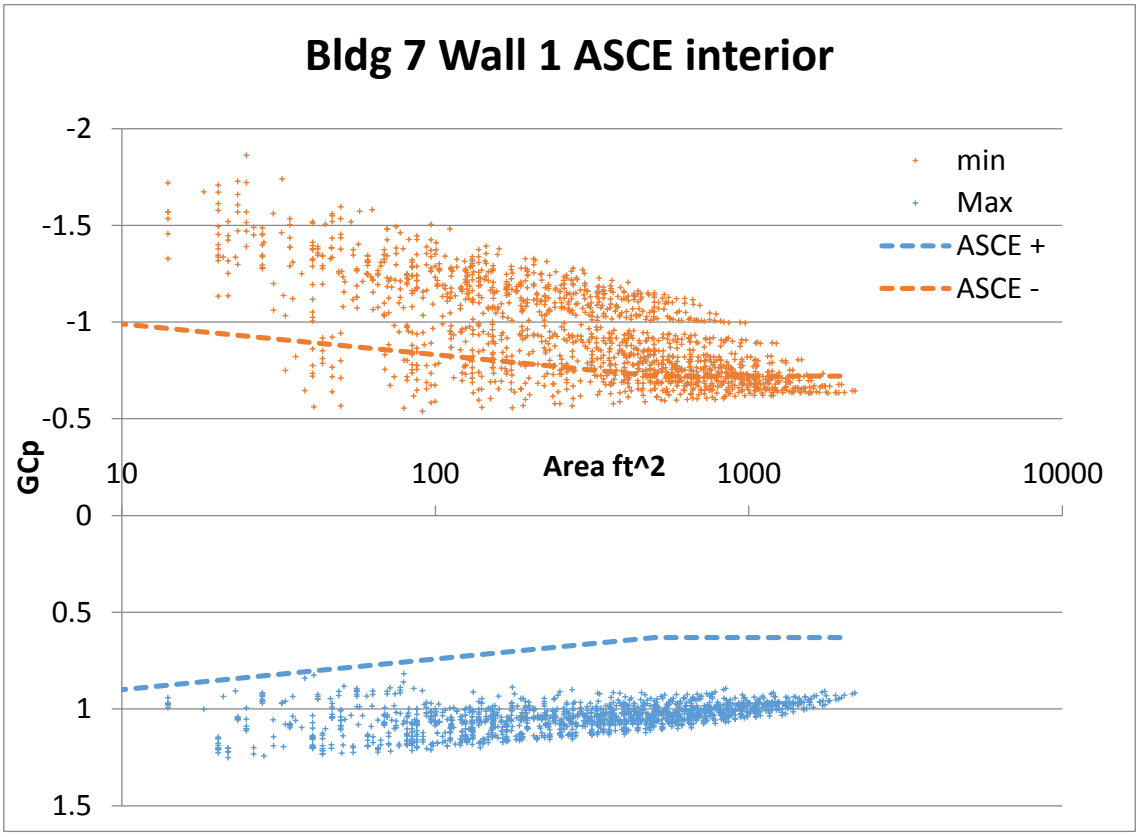

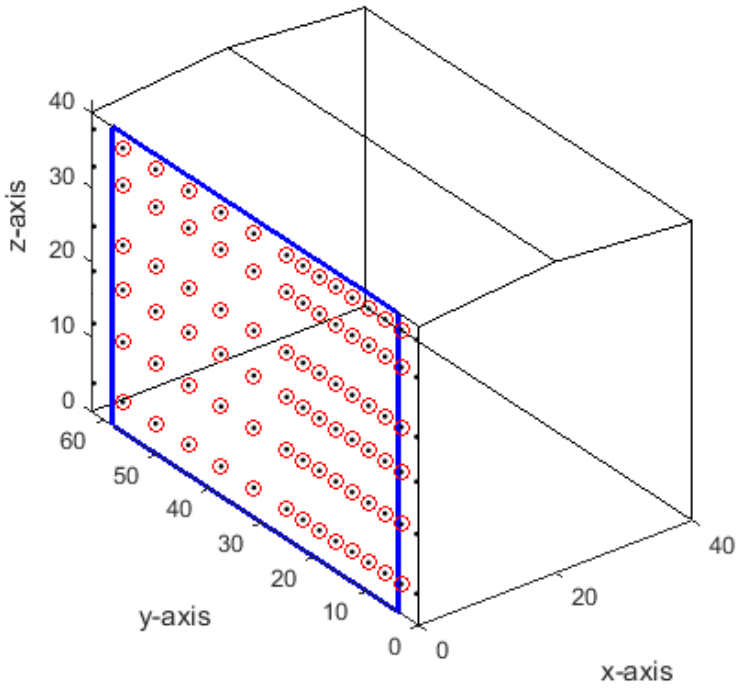

Fig. C1a, b Building 7 Wall 1 ASCE interior (1 ft^2 = 0.0929 m^2)

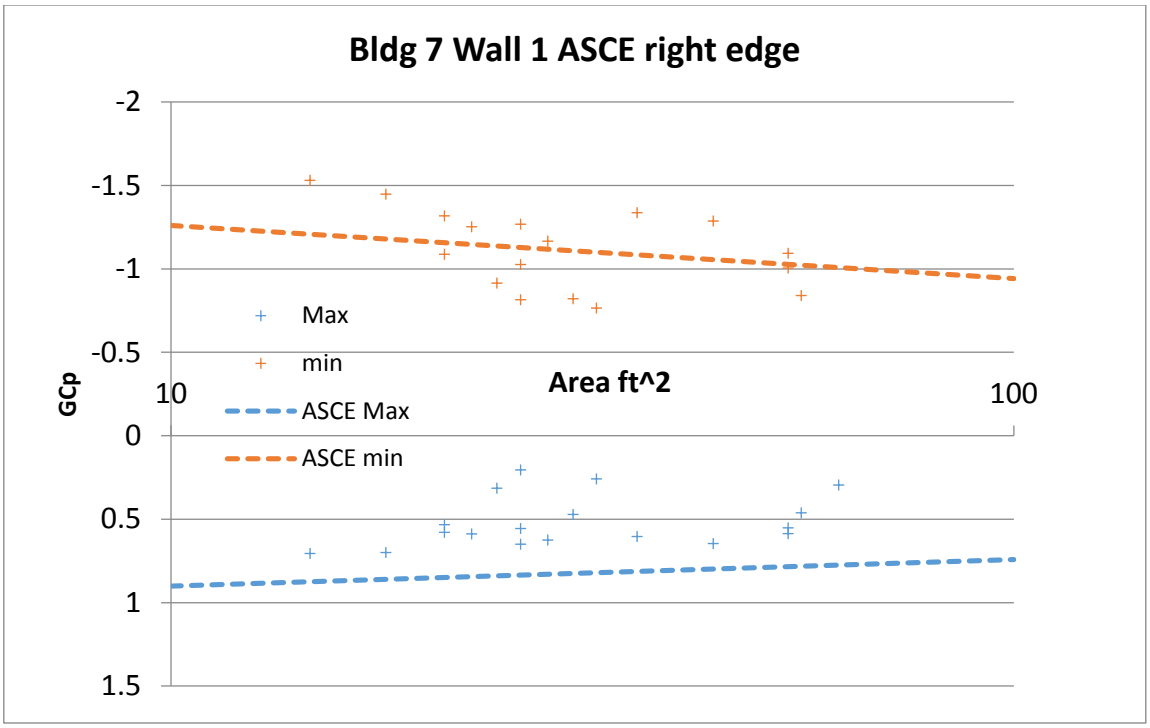

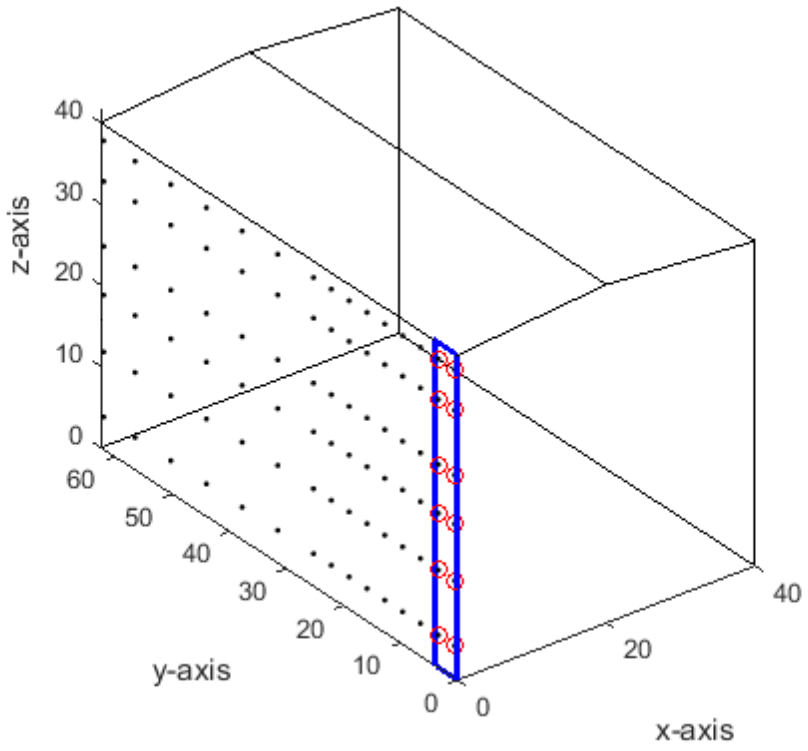

Fig. C2a, b Building 7 Wall 1 ASCE right edge (1 ft^2 = 0.0929 m^2)

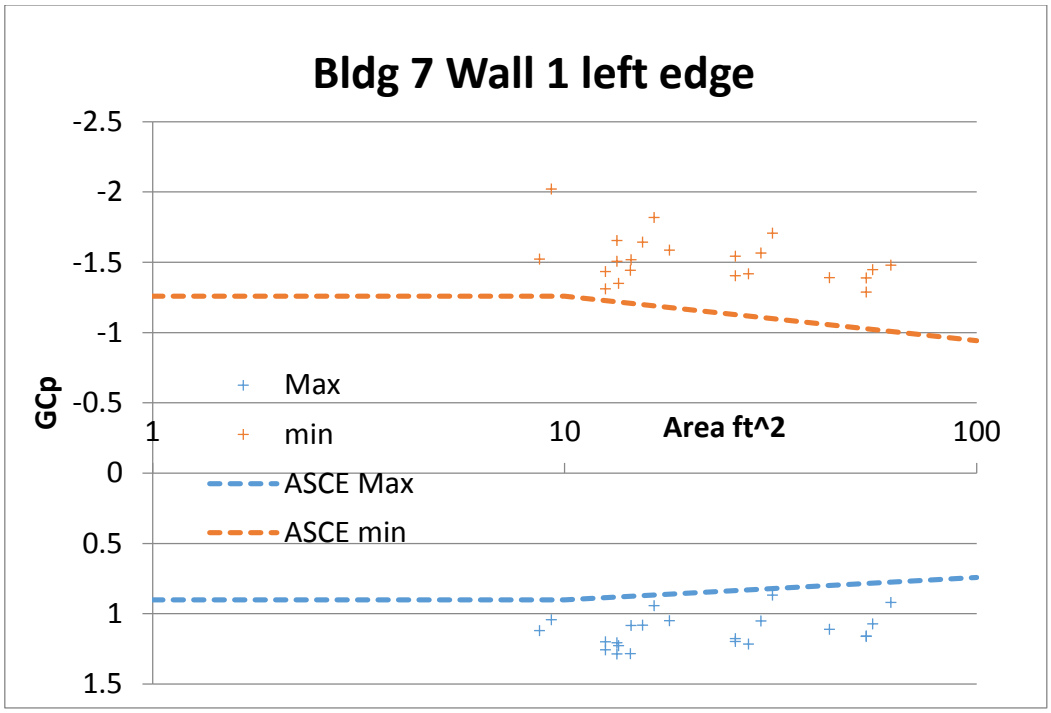

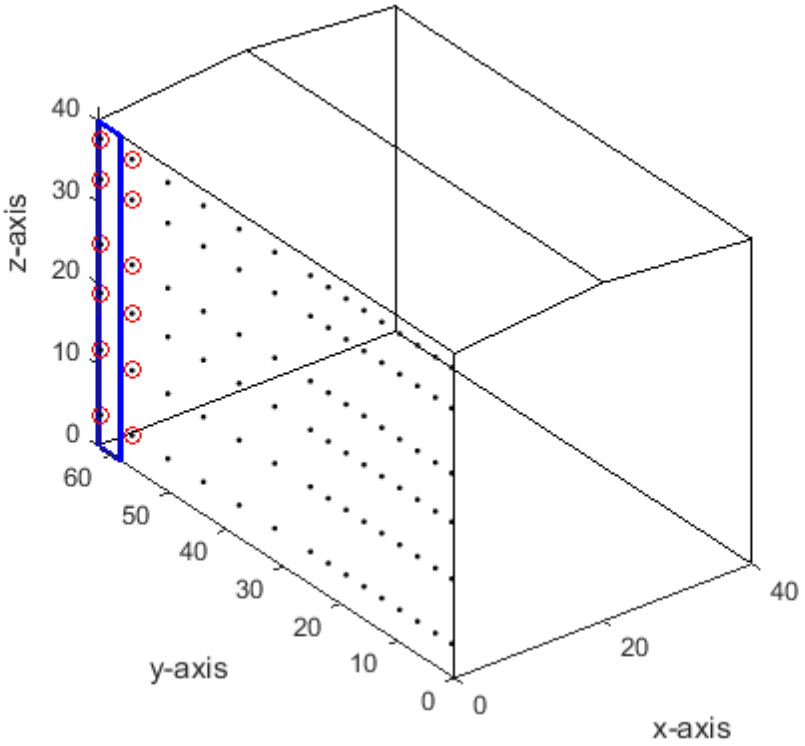

Fig. C3a, b Building 7 Wall 1 ASCE left edge (1 ft^2 = 0.0929 m^2)

Appendix D Building 7 Wall 4

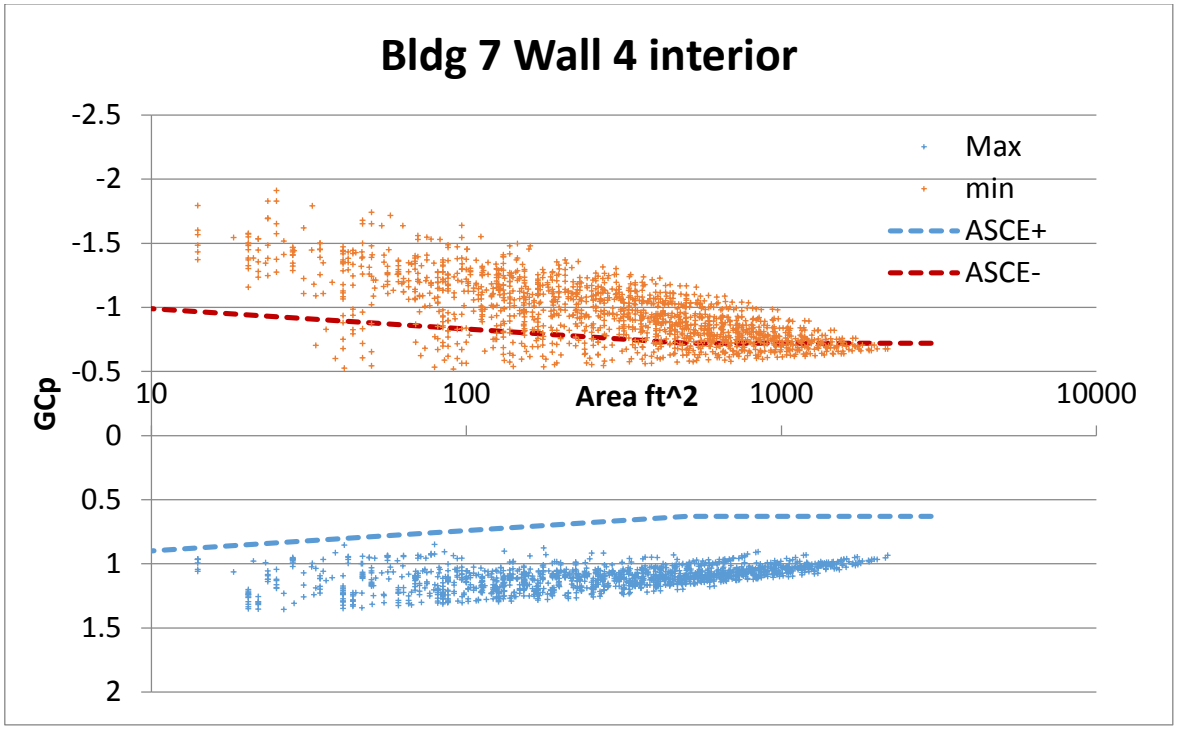

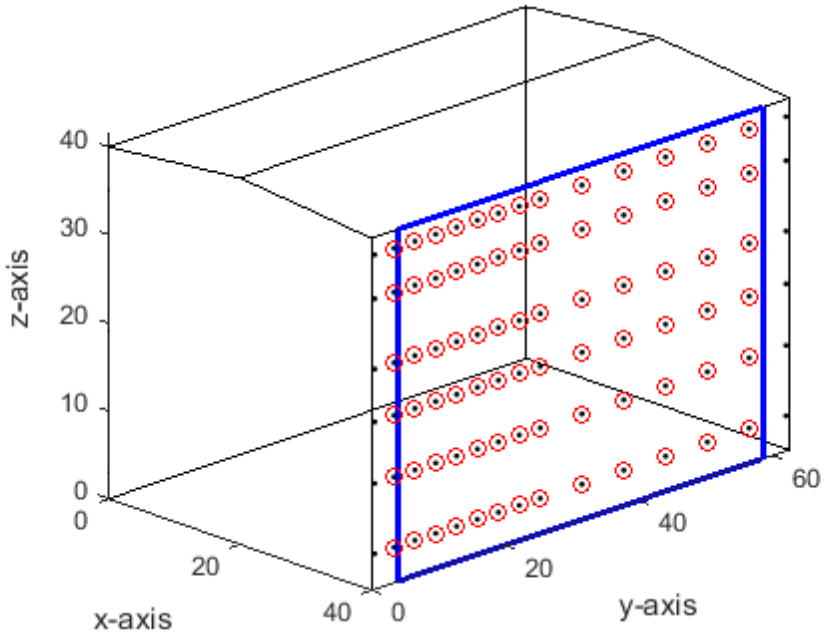

Fig. D1 Building 7 Wall 4 ASCE interior (1 ft^2 = 0.0929 m^2)

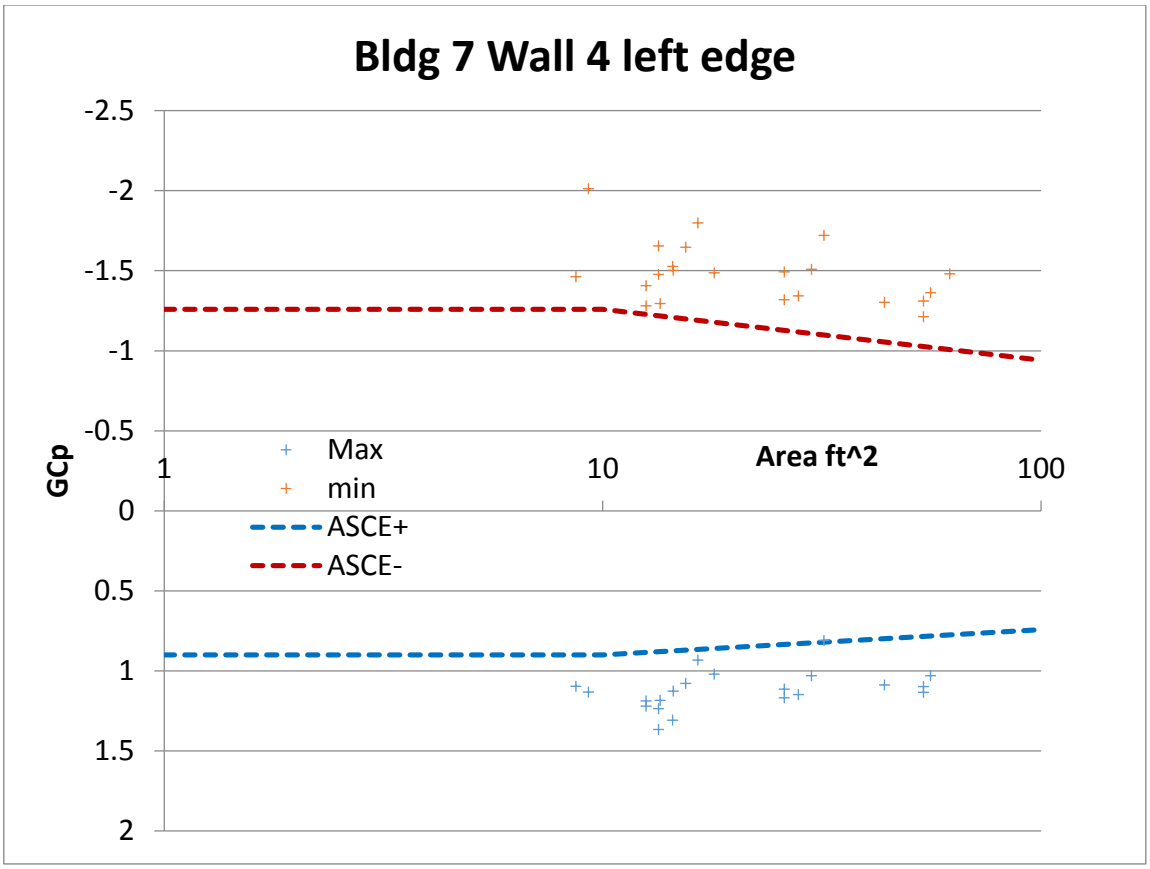

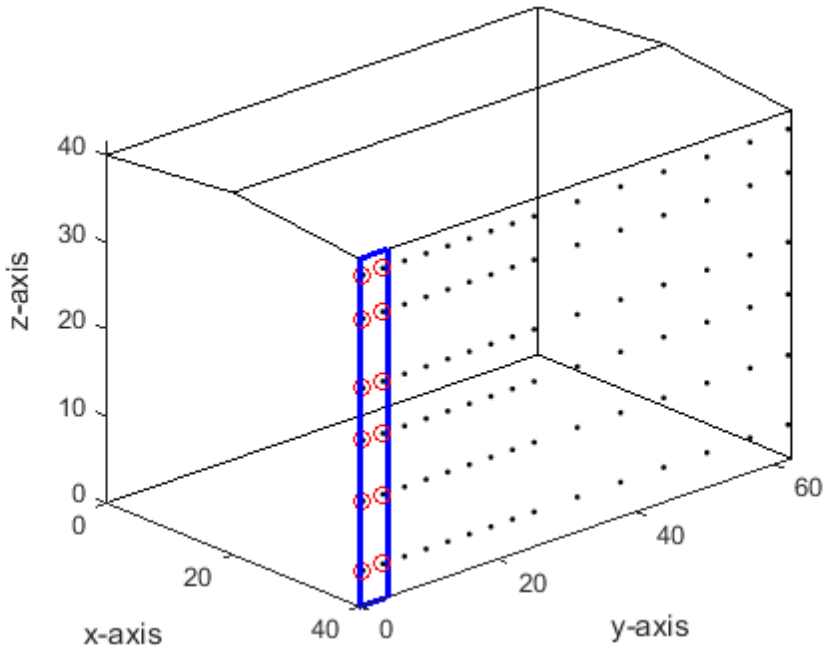

Fig. D2 Building 7 Wall 4 ASCE left edge (1 ft^2 = 0.0929 m^2)

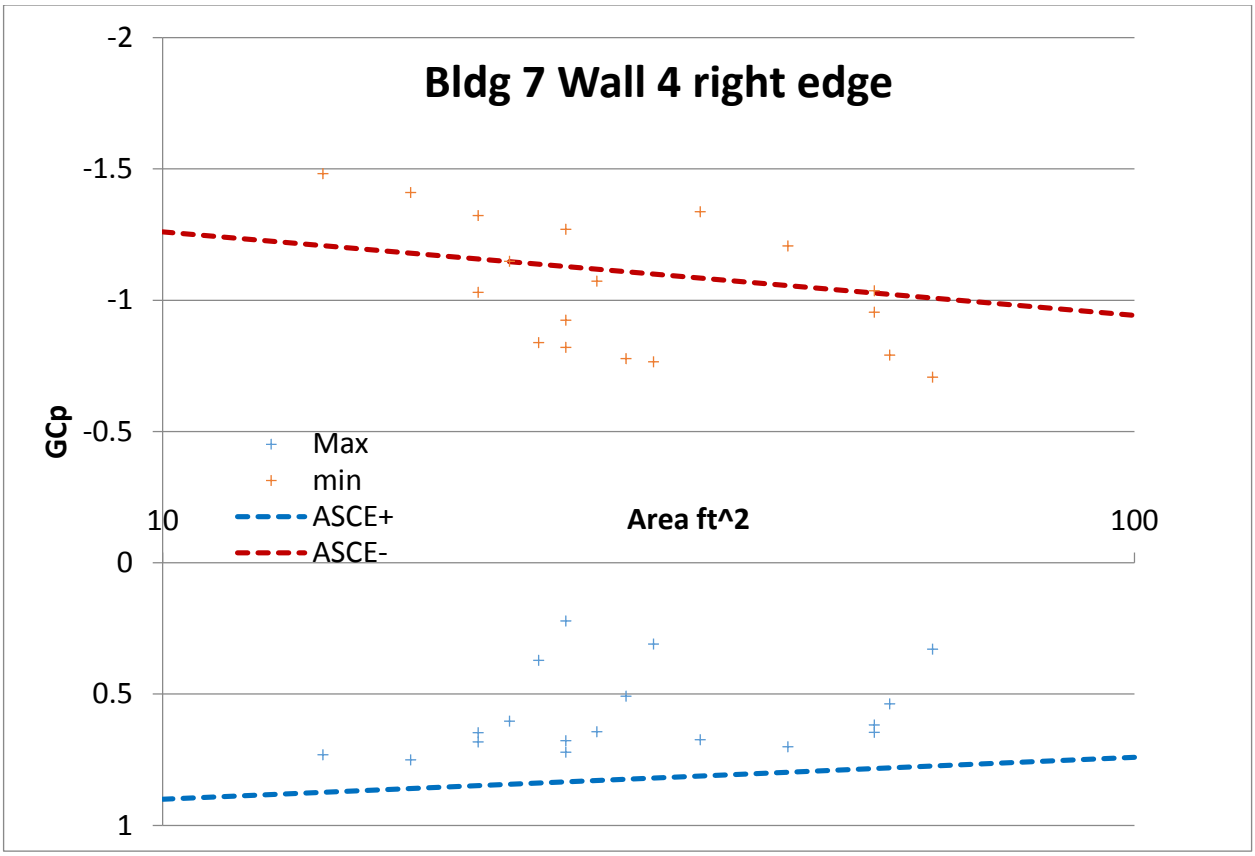

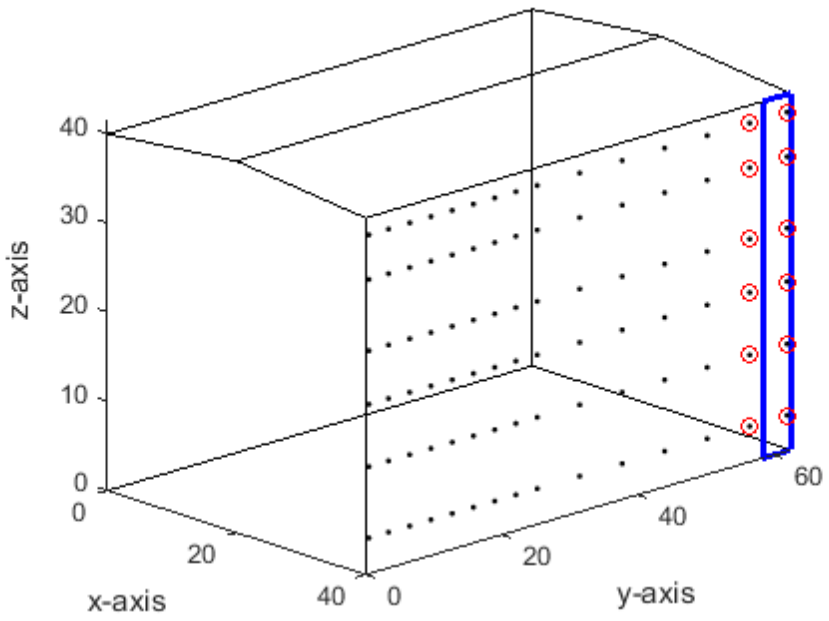

Fig. D3 Building 7 Wall 4 ASCE right edge (1 ft^2 = 0.0929 m^2)

Appendix E Building 15, roof 3

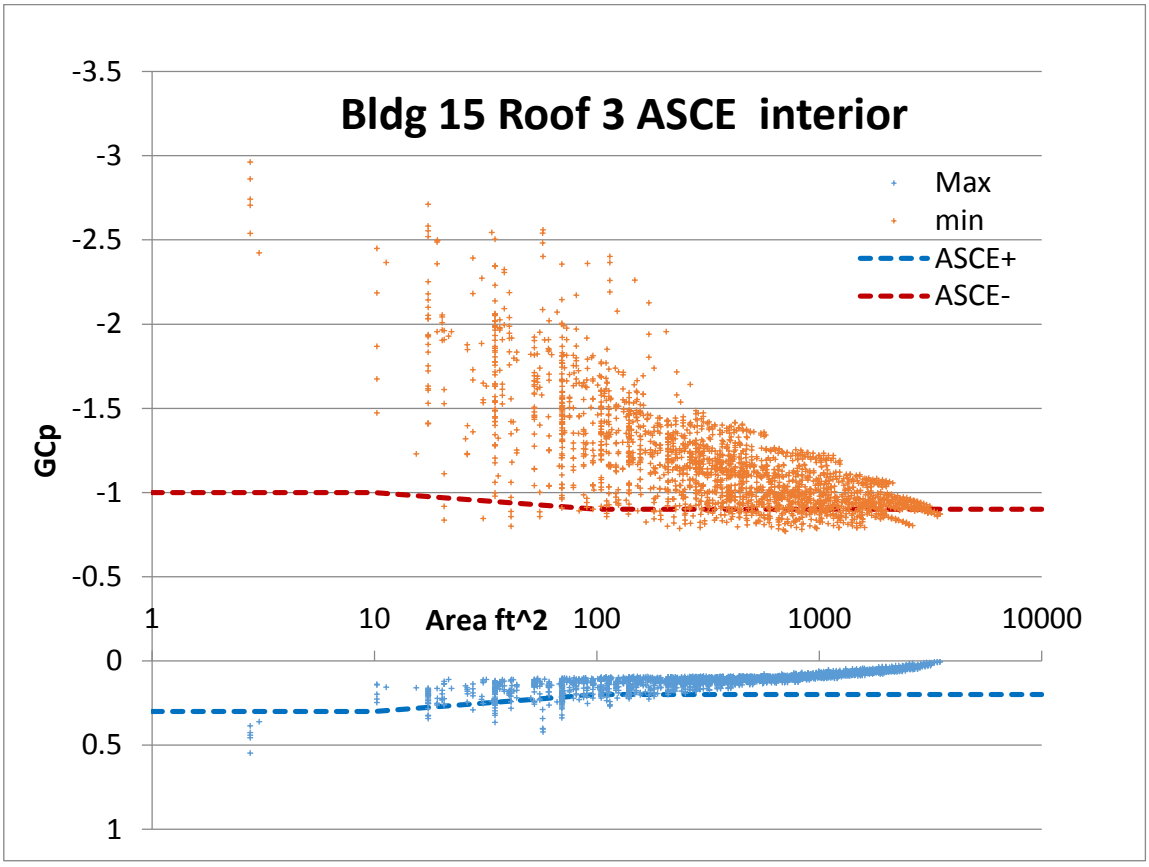

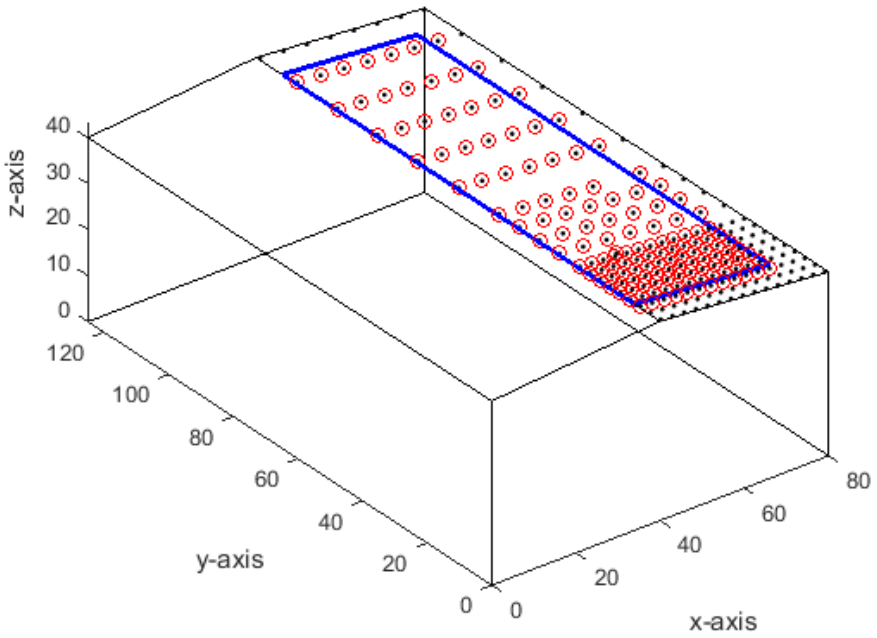

Fig. E1a, b Bldg 15 Roof 3 ASCE interior (1 ft^2 = 0.0929 m^2)

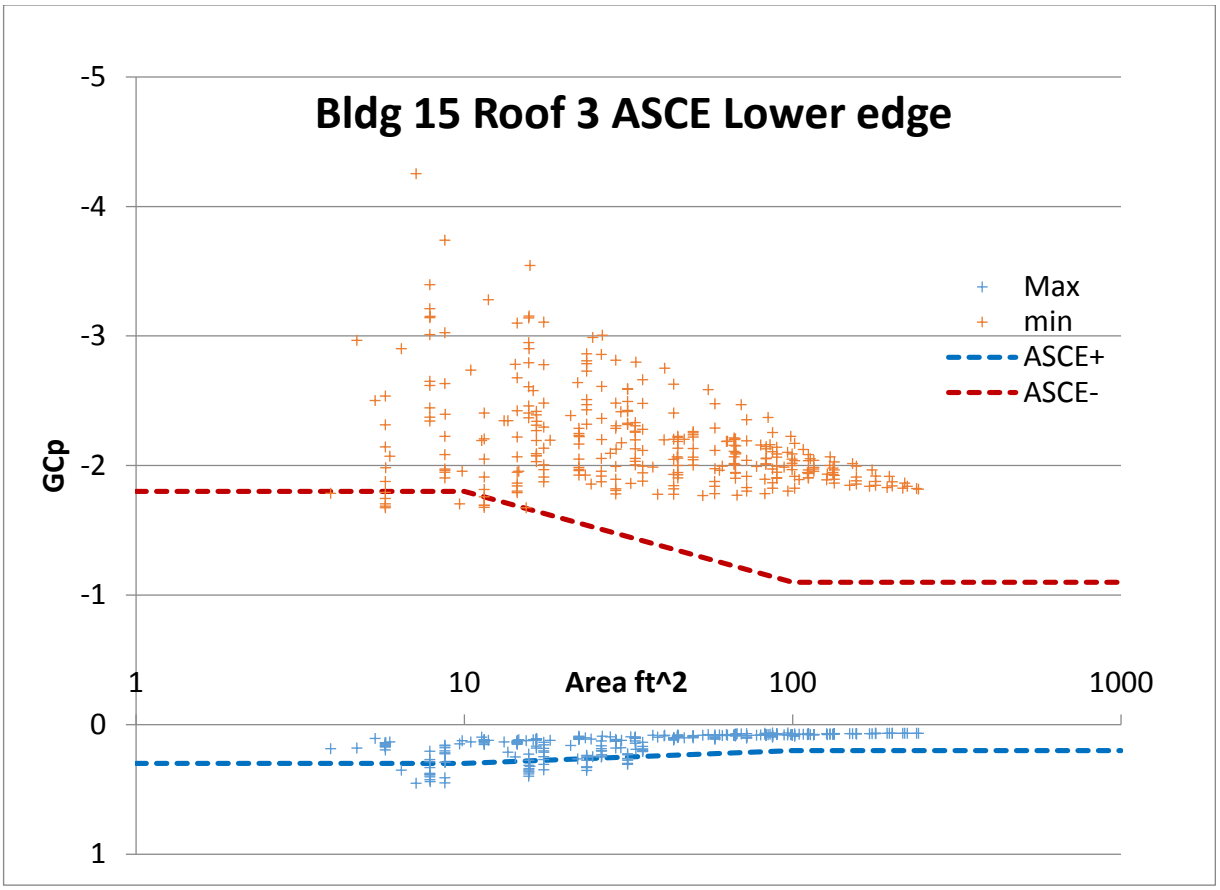

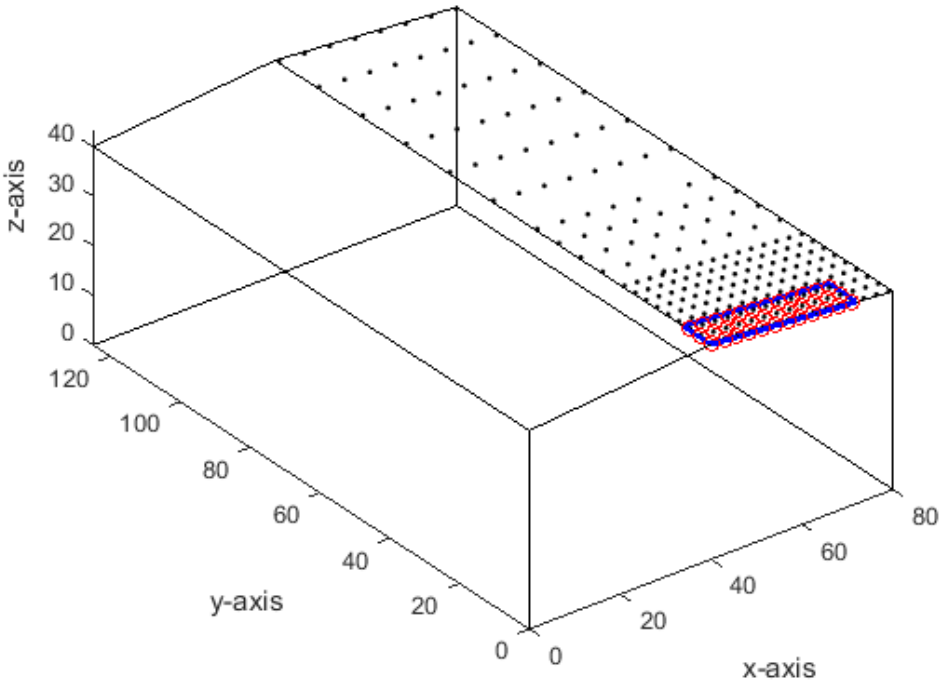

Fig. E2a,b Bldg 15 Roof 3 ASCE lower edge (1 ft^2 = 0.0929 m^2)

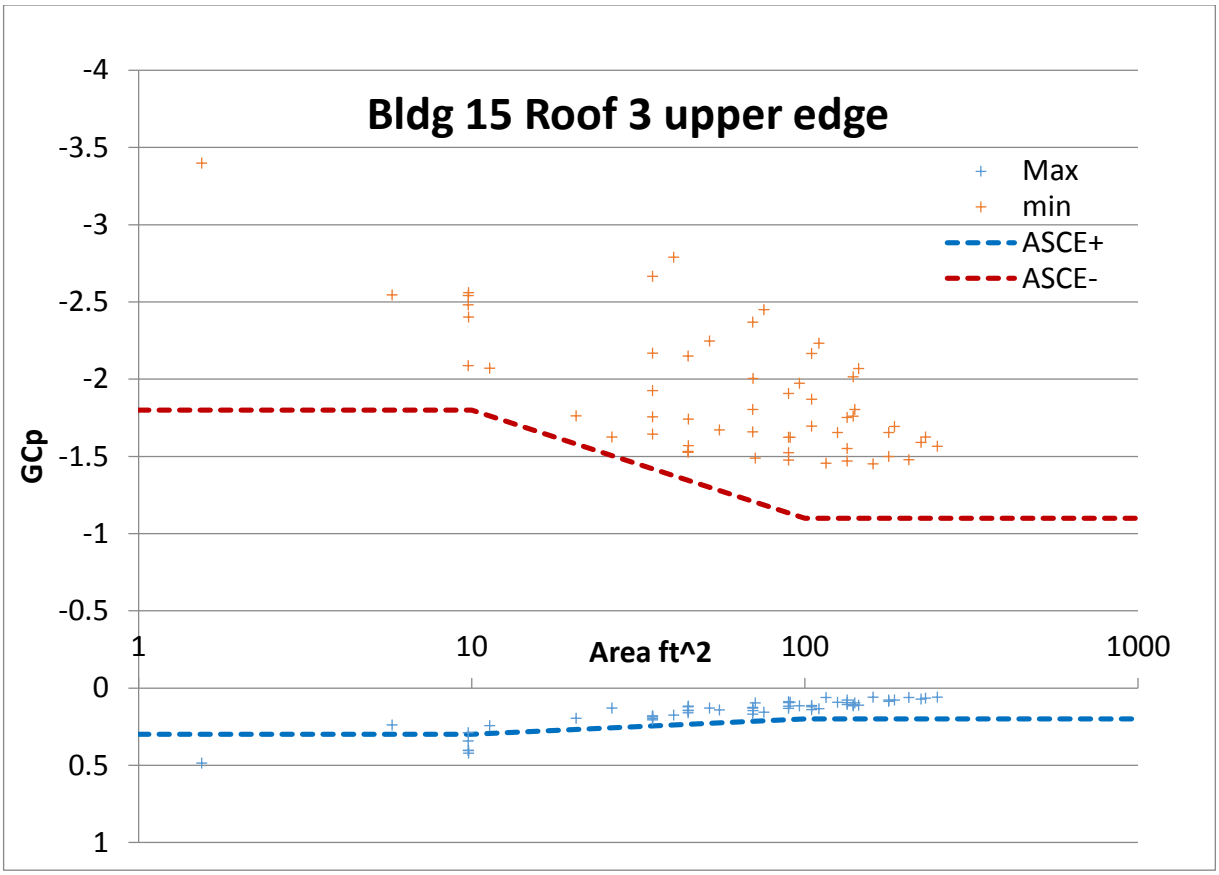

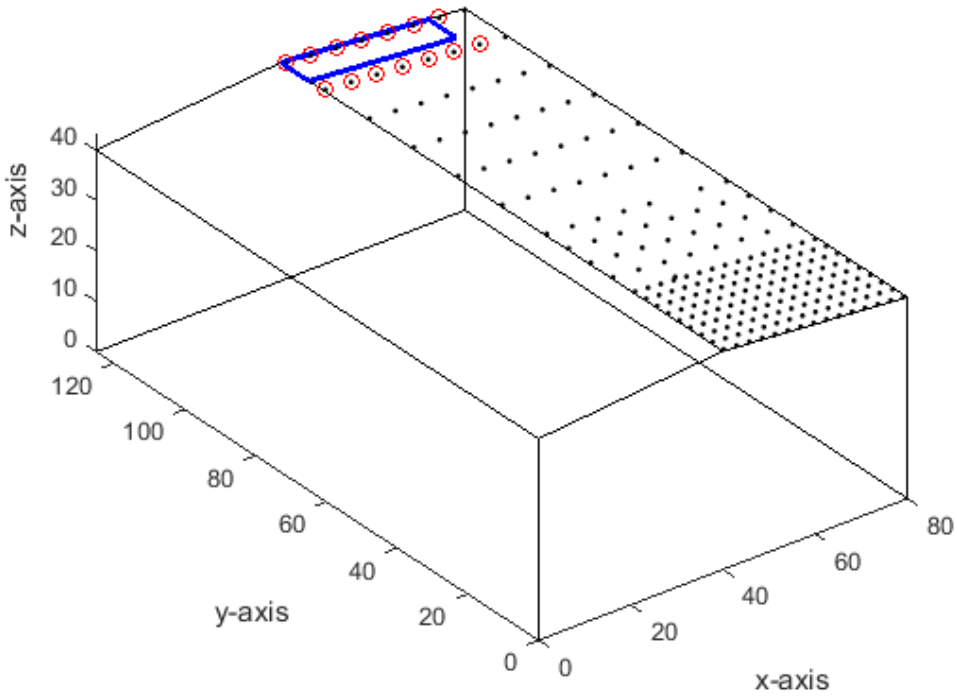

Fig. E3a, b Bldg 15 Roof 3 ASCE lower edge (1 ft^2 = 0.0929 m^2)

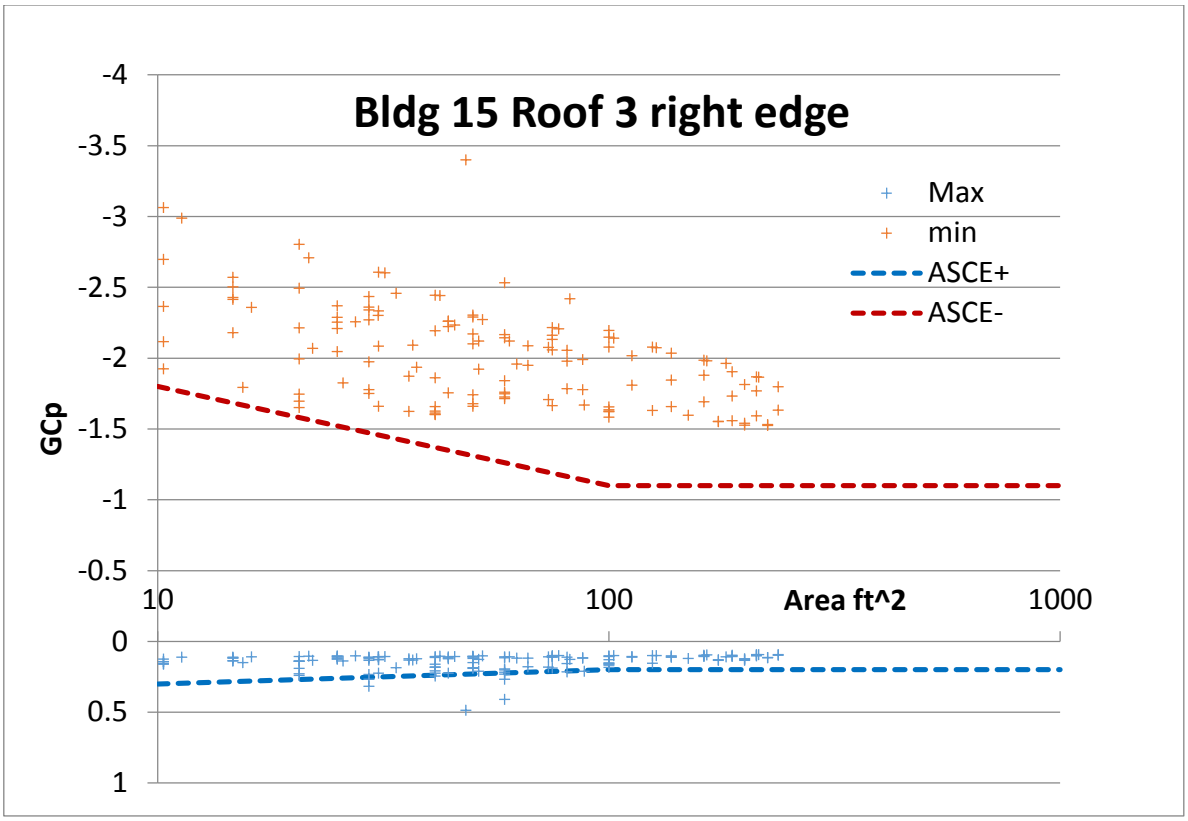

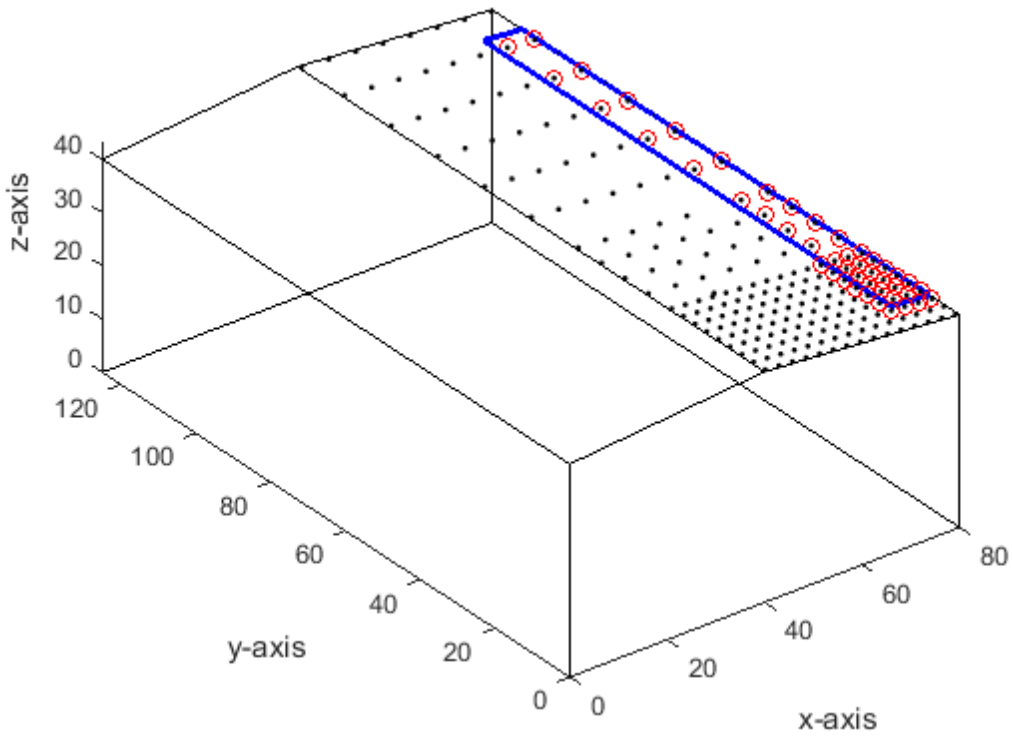

Fig. E4a,b Bldg 15 Roof 3 ASCE right edge (1 ft^2 = 0.0929 m^2)

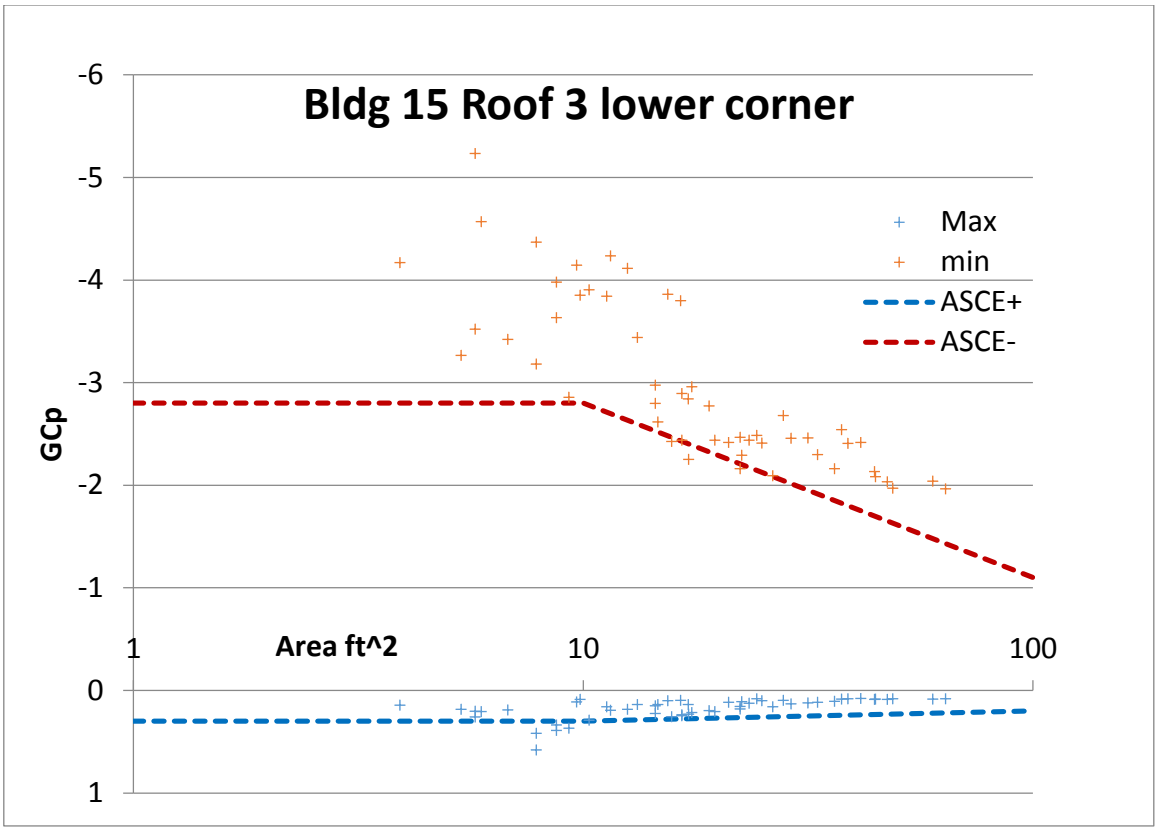

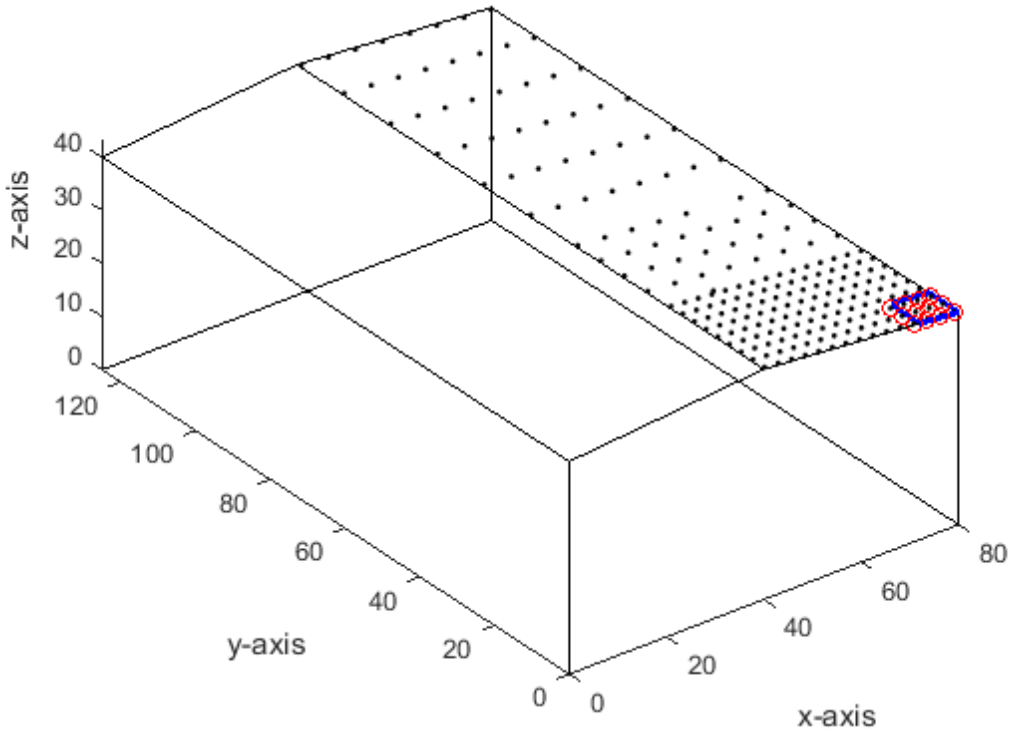

Fig. E5a, b Bldg 15 Roof 3 ASCE lower corner (1 ft^2 = 0.0929 m^2)

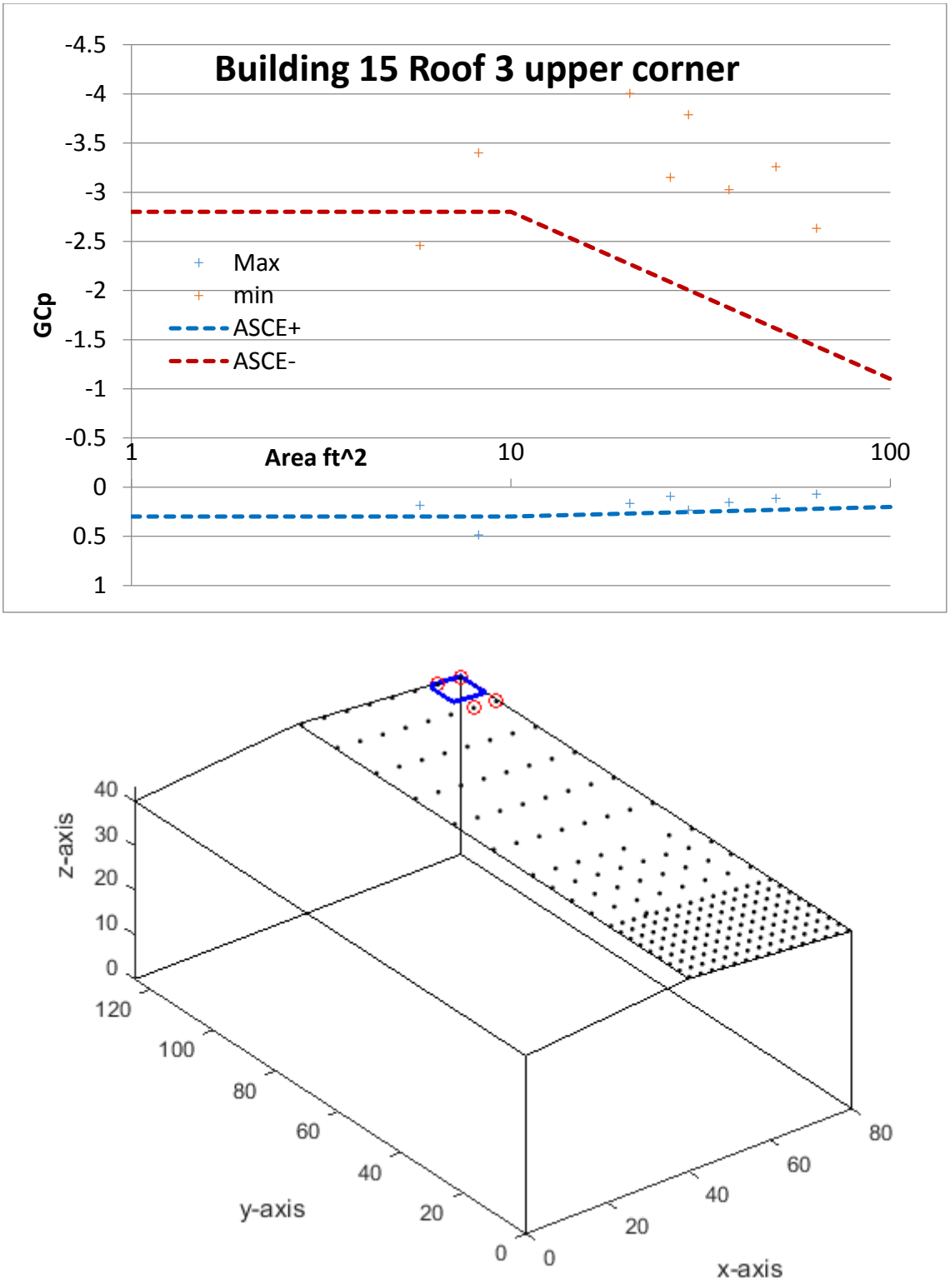

Fig. E6a, b Bldg 15 Roof 3 ASCE upper corner (1 ft^2 = 0.0929 m^2)

Appendix F Building 15, roof 2

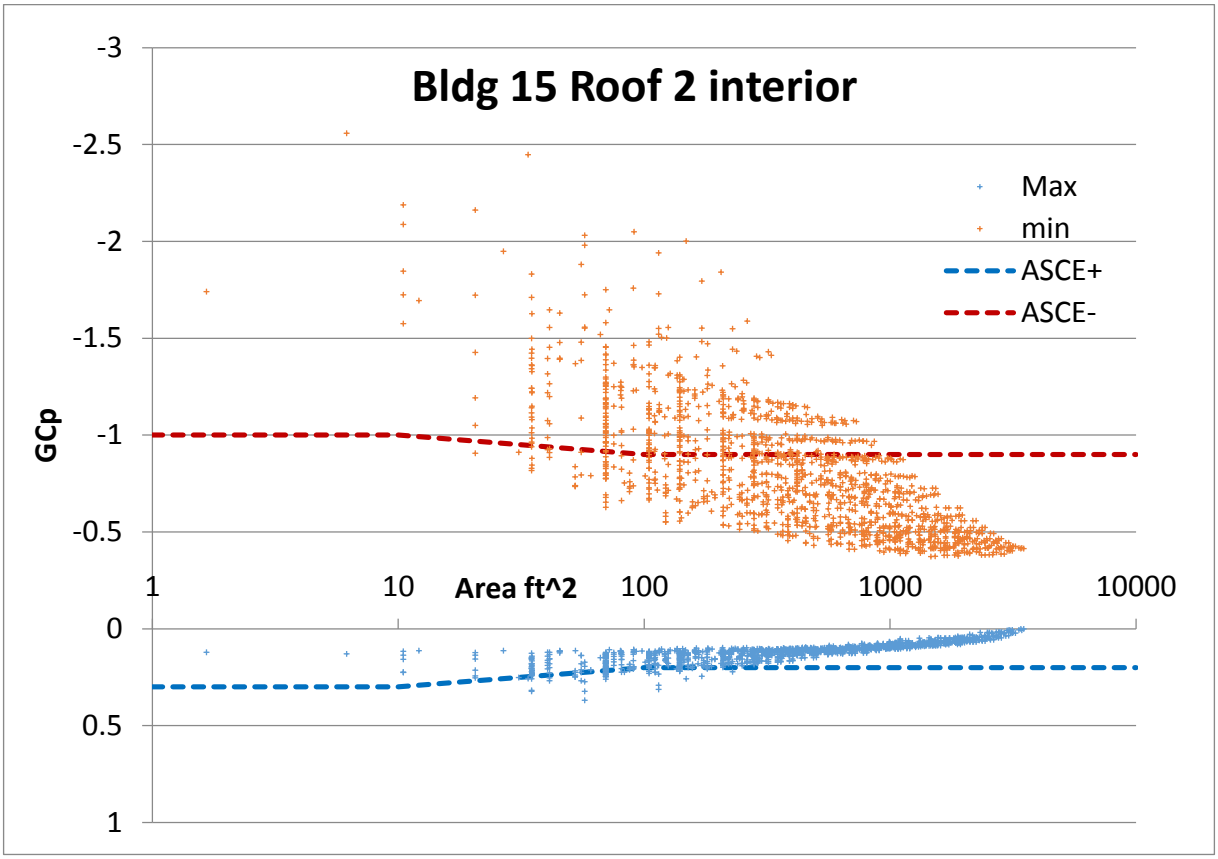

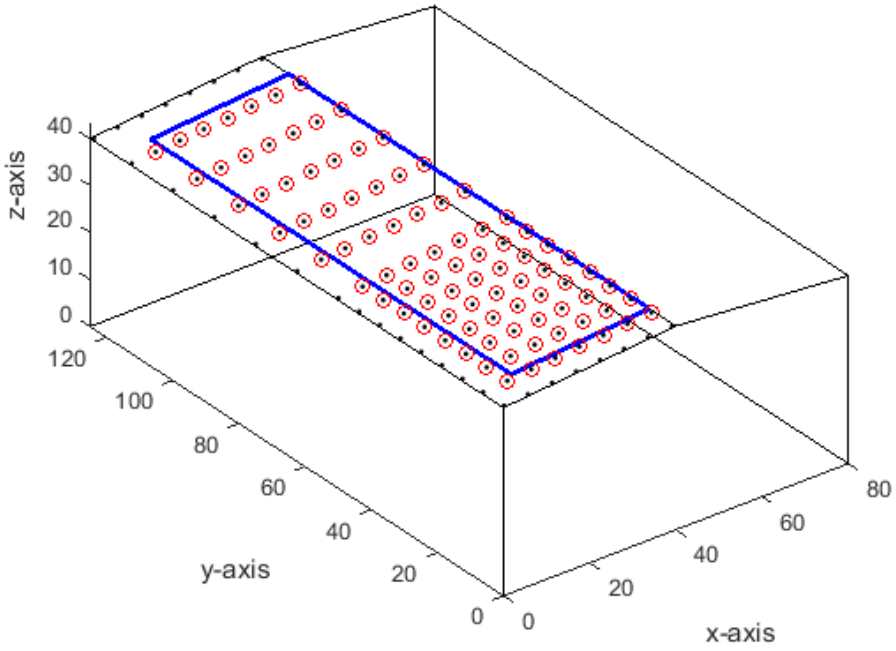

Fig. F1a,b Bldg 15 Roof 2 ASCE interior (1 ft^2 = 0.0929 m^2)

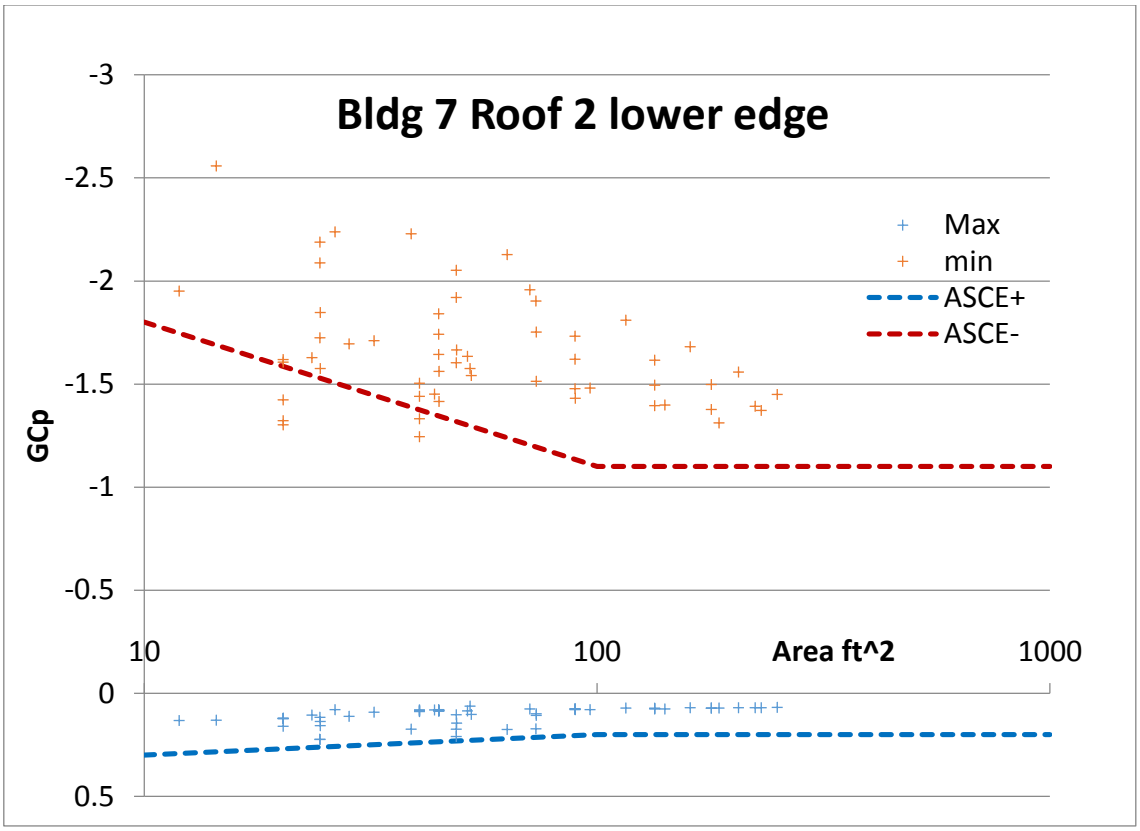

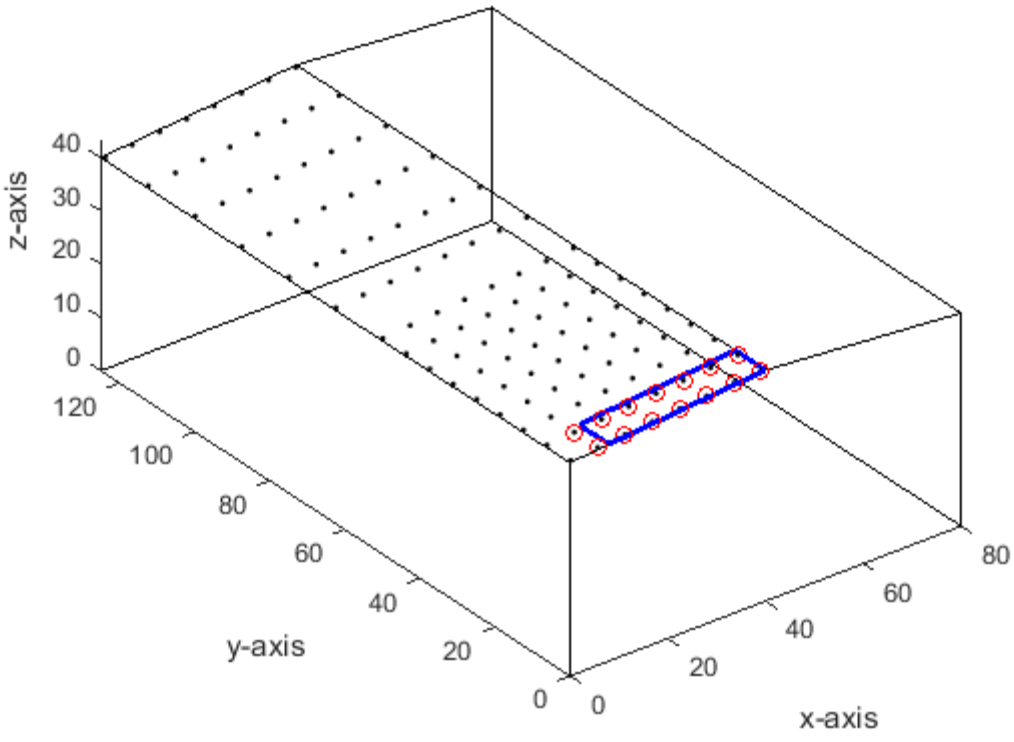

Fig. F2a, b Bldg 15 Roof 2 lower edge (1 ft^2 = 0.0929 m^2)

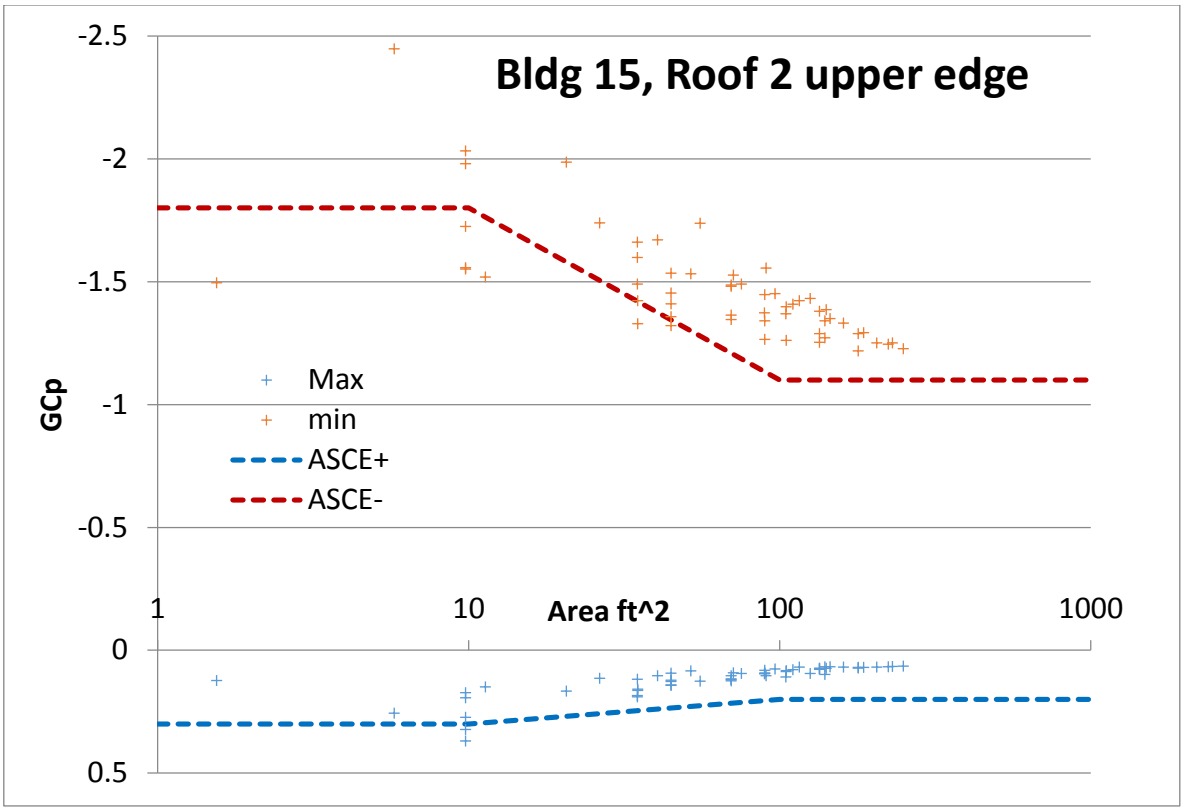

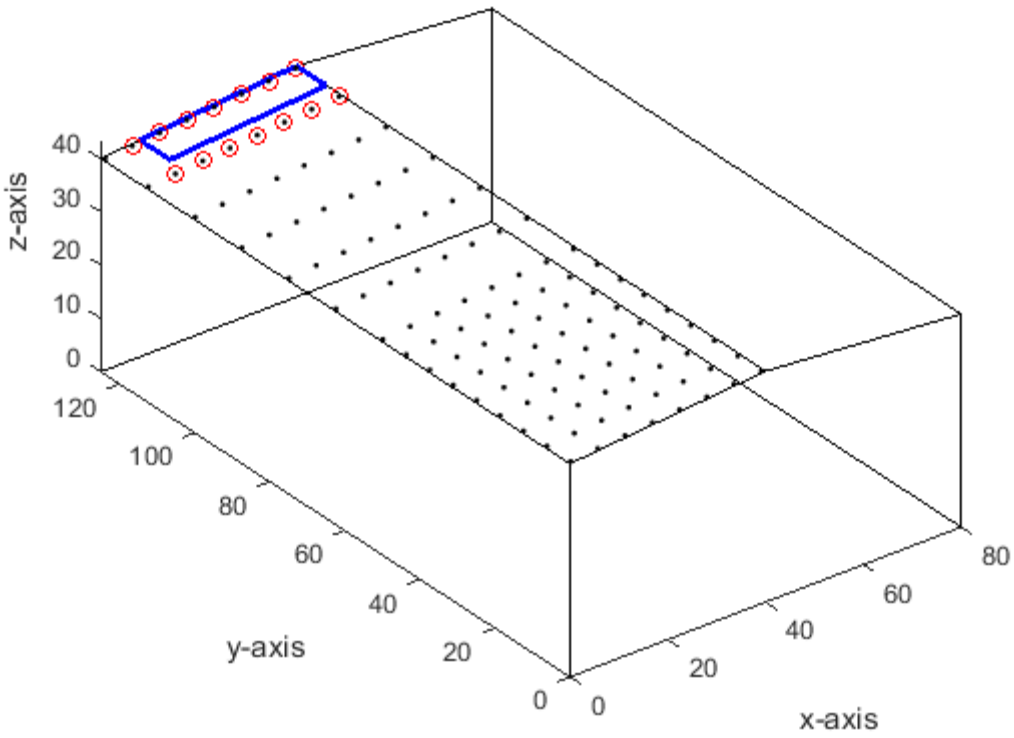

Fig. F3a,b Bldg 15 Roof 2 upper edge (1 ft^2 = 0.0929 m^2)

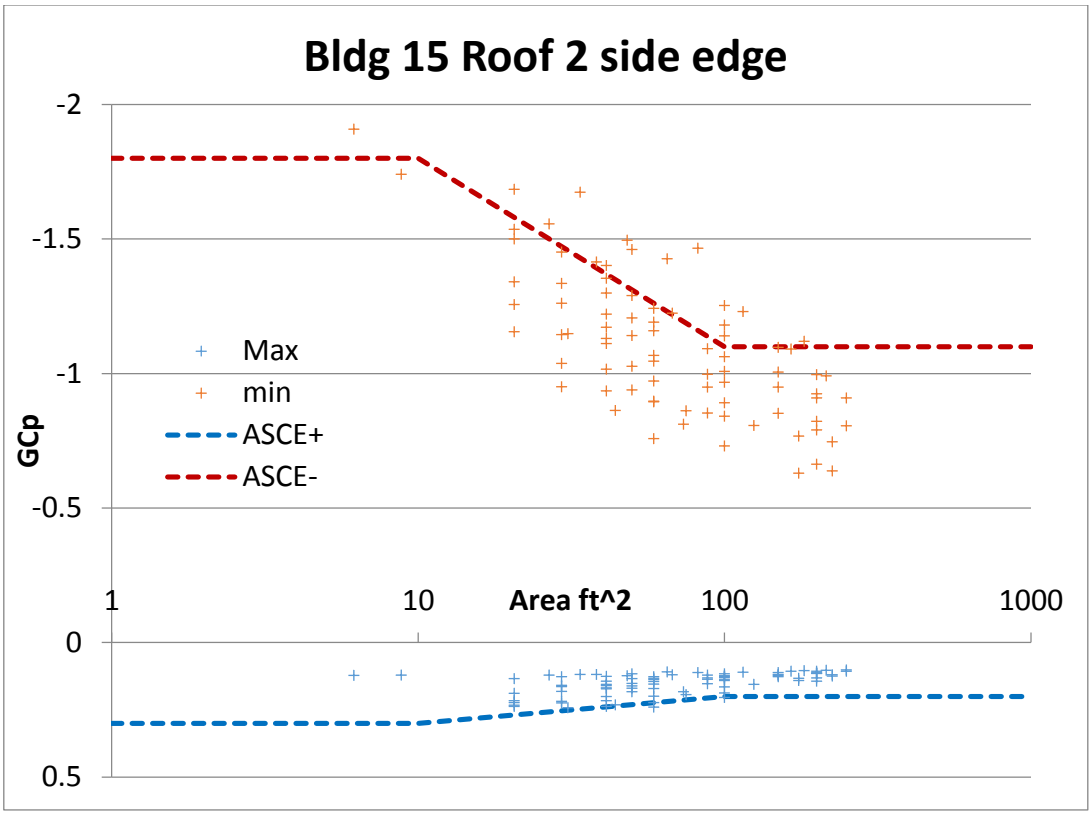

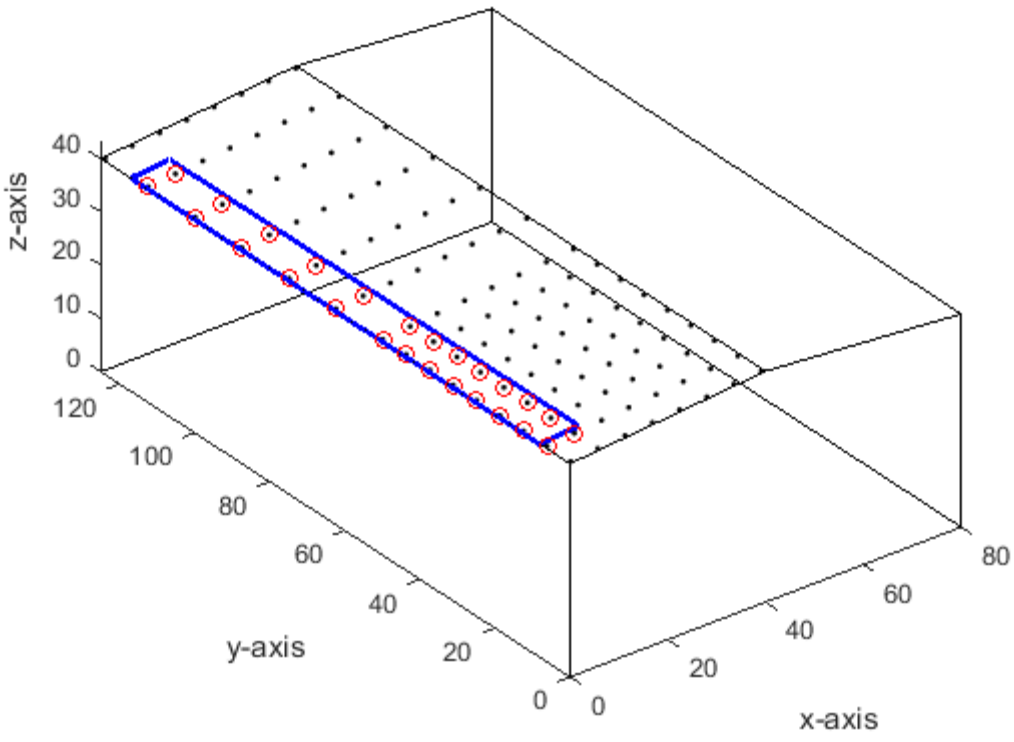

Fig. F4a, b Bldg 15 Roof 2 side edge (1 ft^2 = 0.0929 m^2)

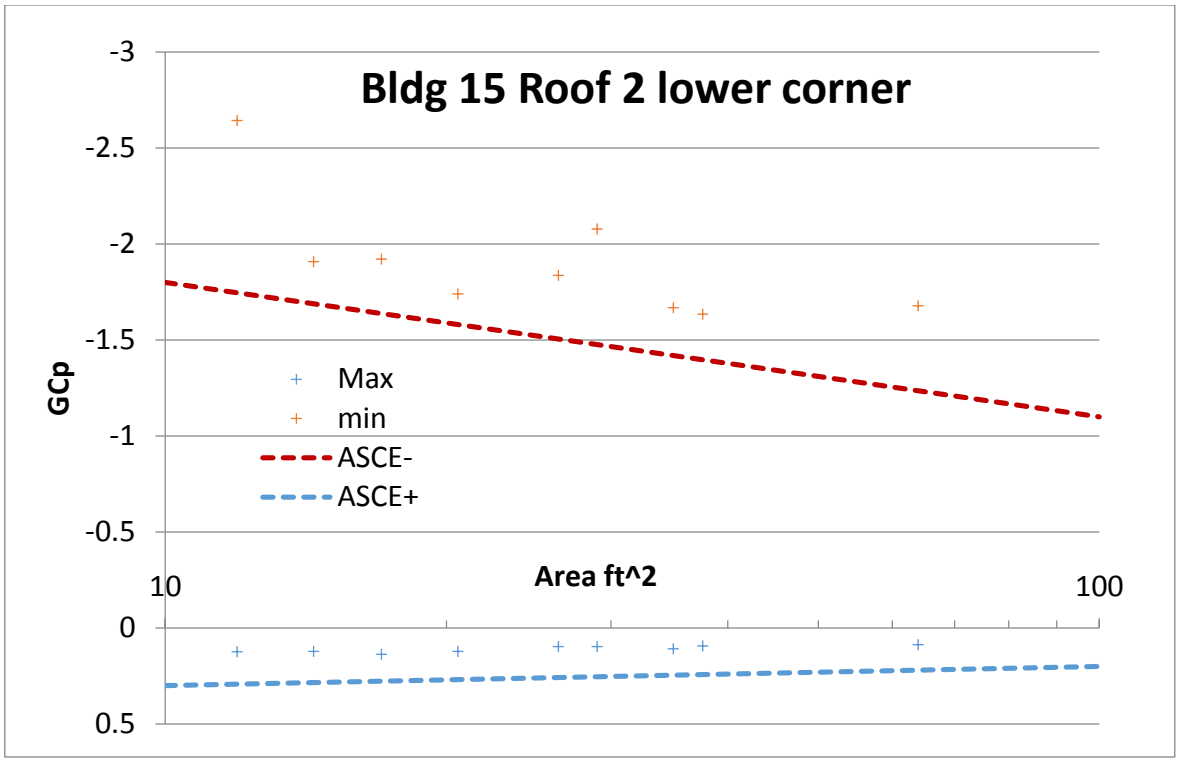

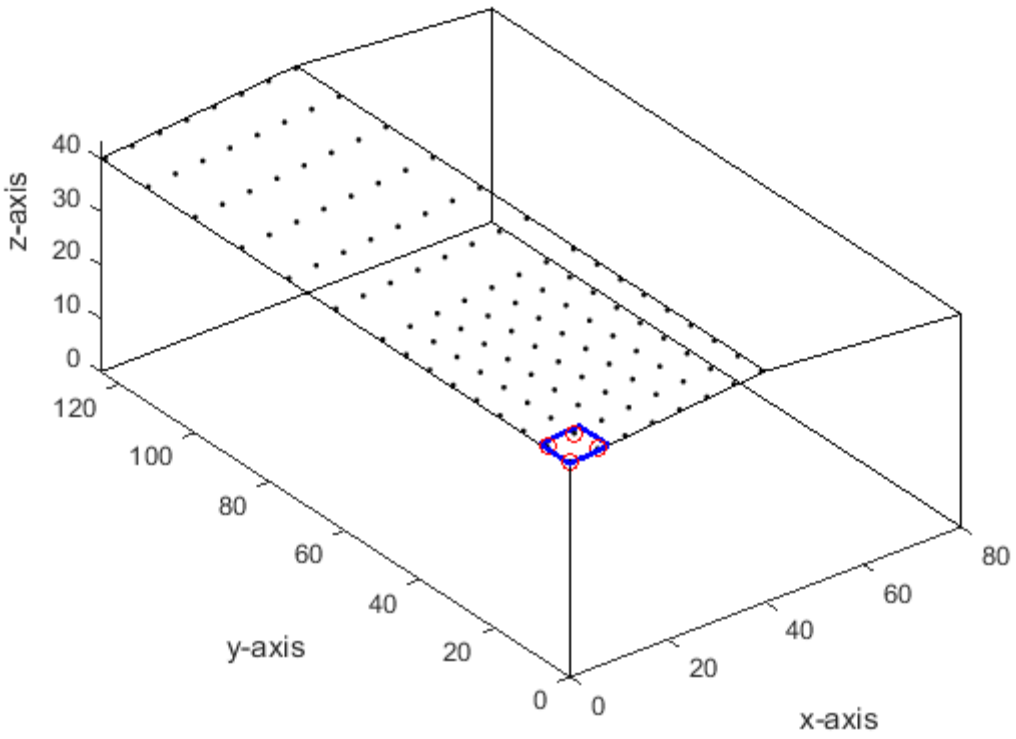

Fig. F5a, b Bldg 15 Roof 2 lower corner (1 ft^2 = 0.0929 m^2)

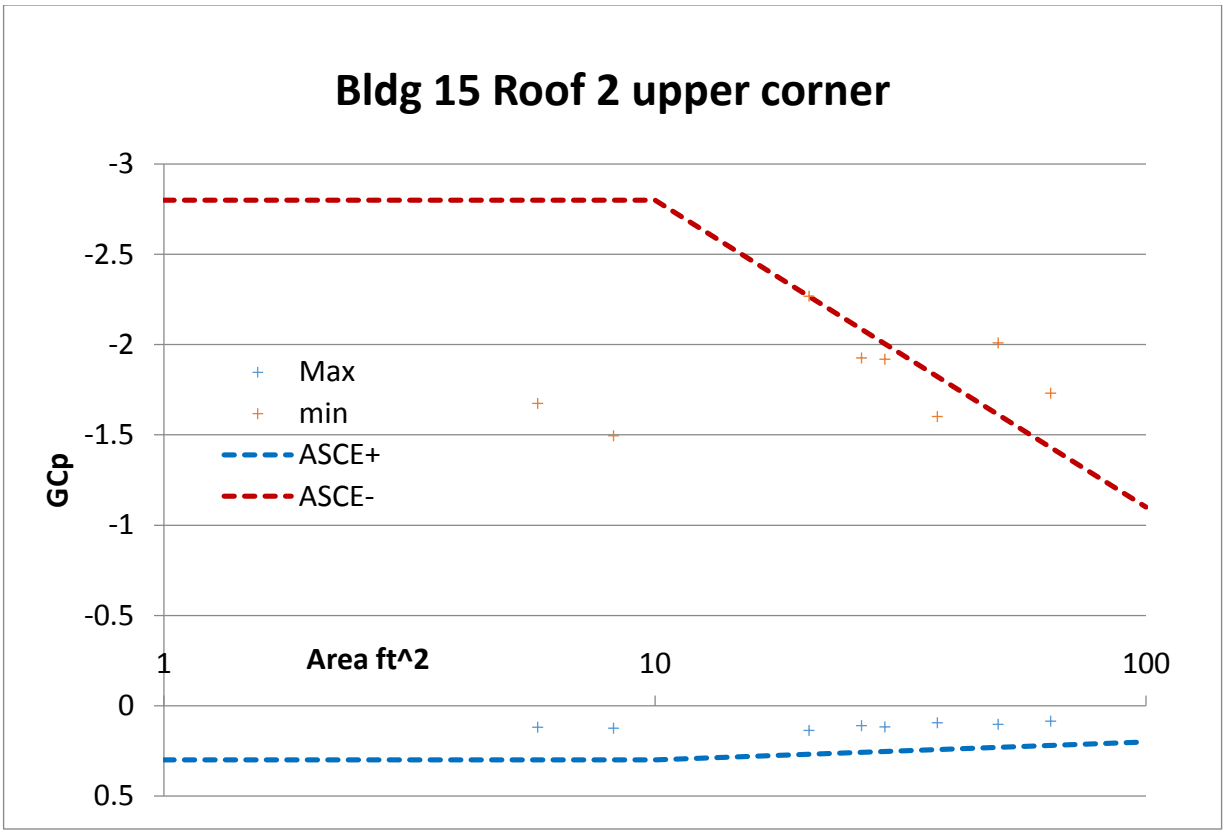

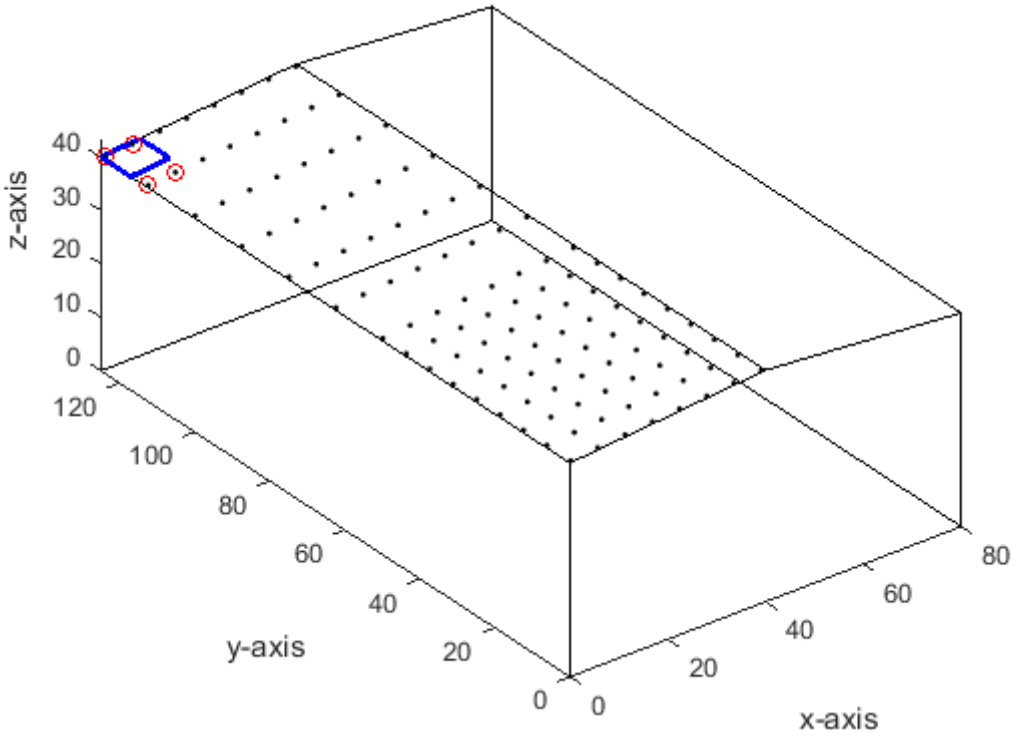

Fig. F6a, b Bldg 15 Roof 2 upper corner (1 ft^2 = 0.0929 m^2)

Appendix G Building 15, Wall 1

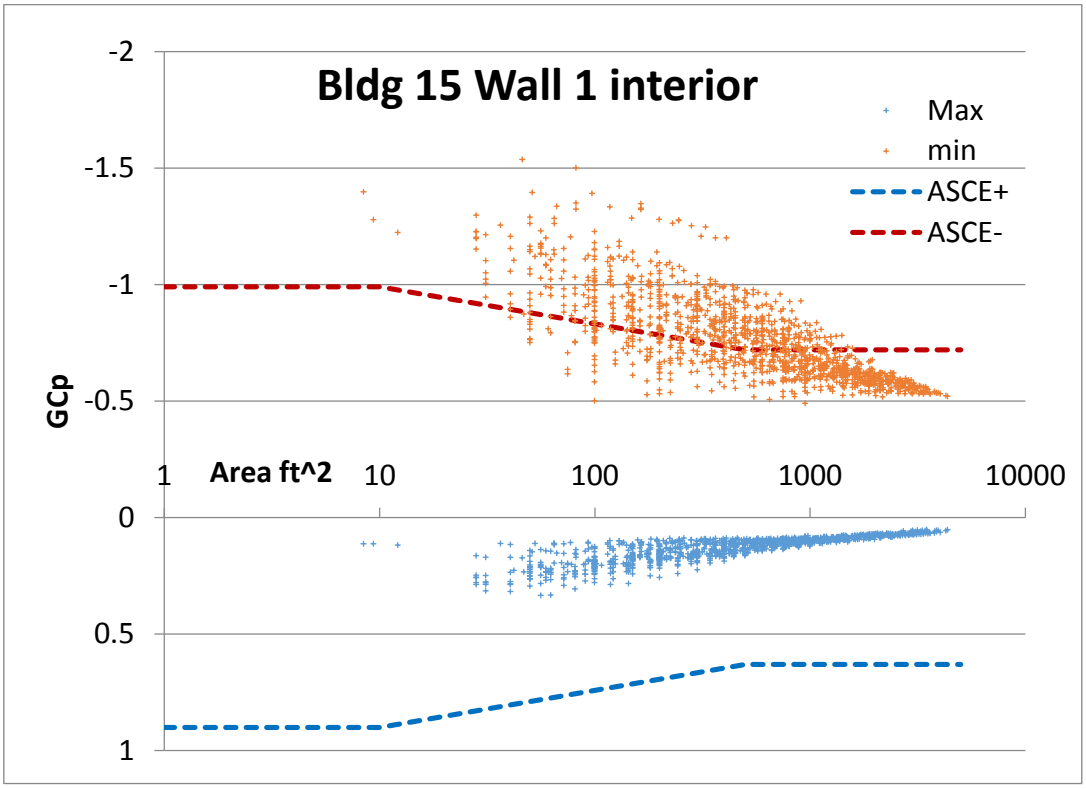

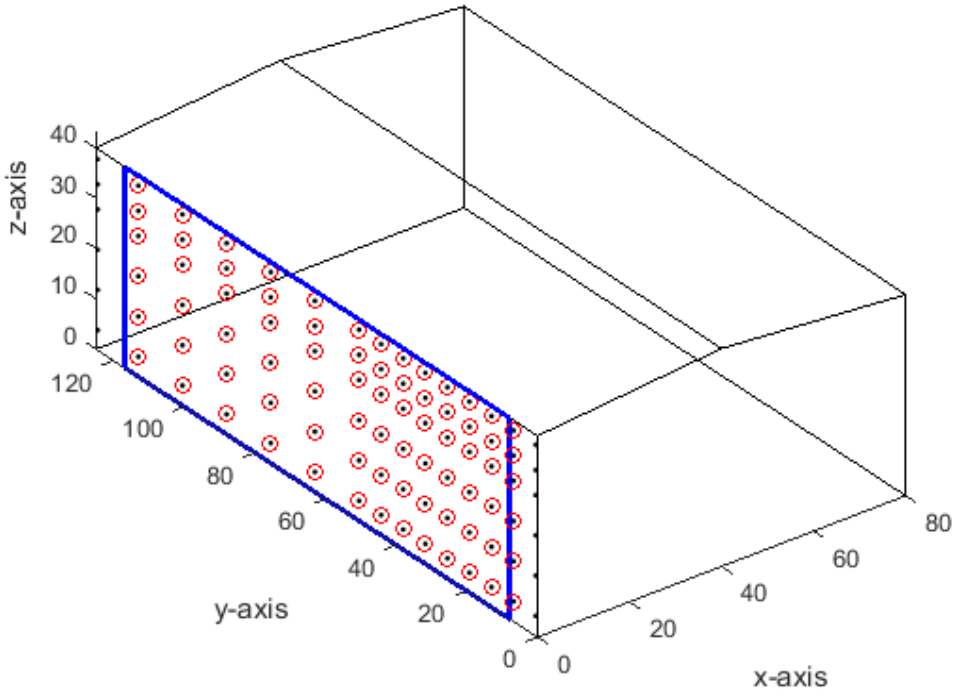

Fig. G1a, b Bldg 15 Wall 1 Interior (1 ft^2 = 0.0929 m^2)

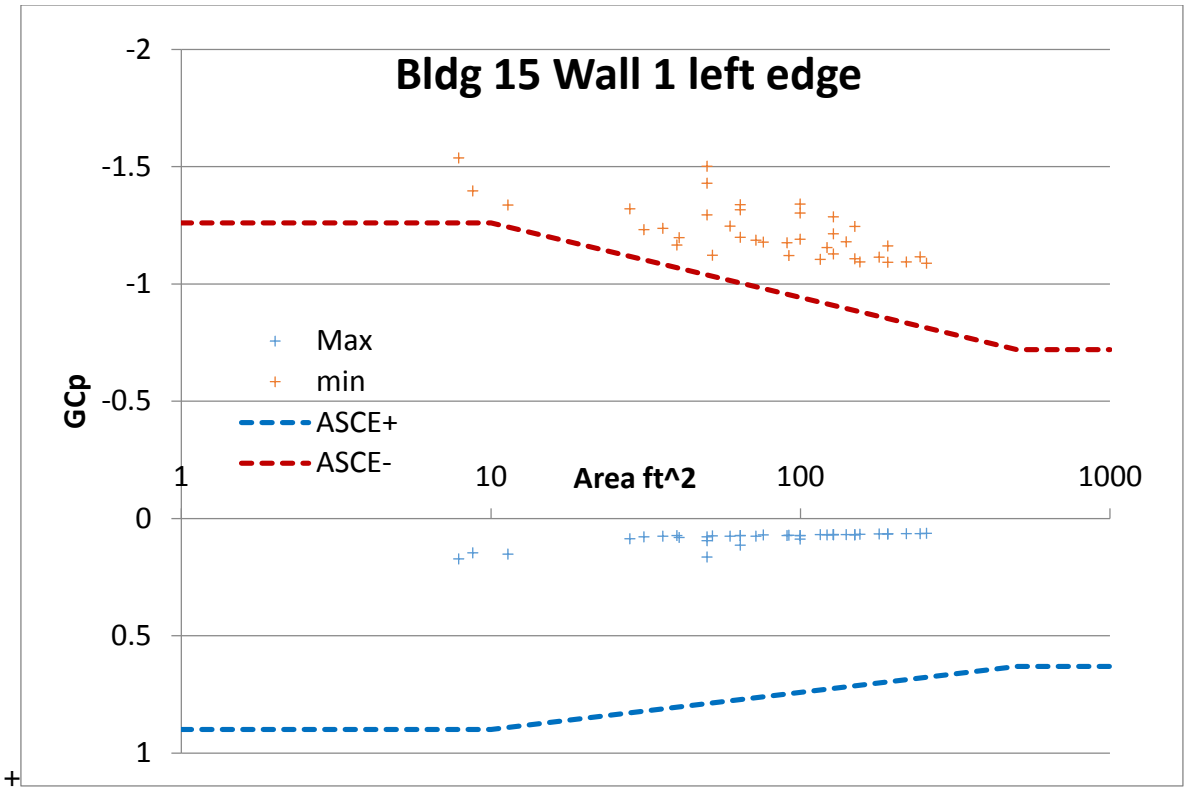

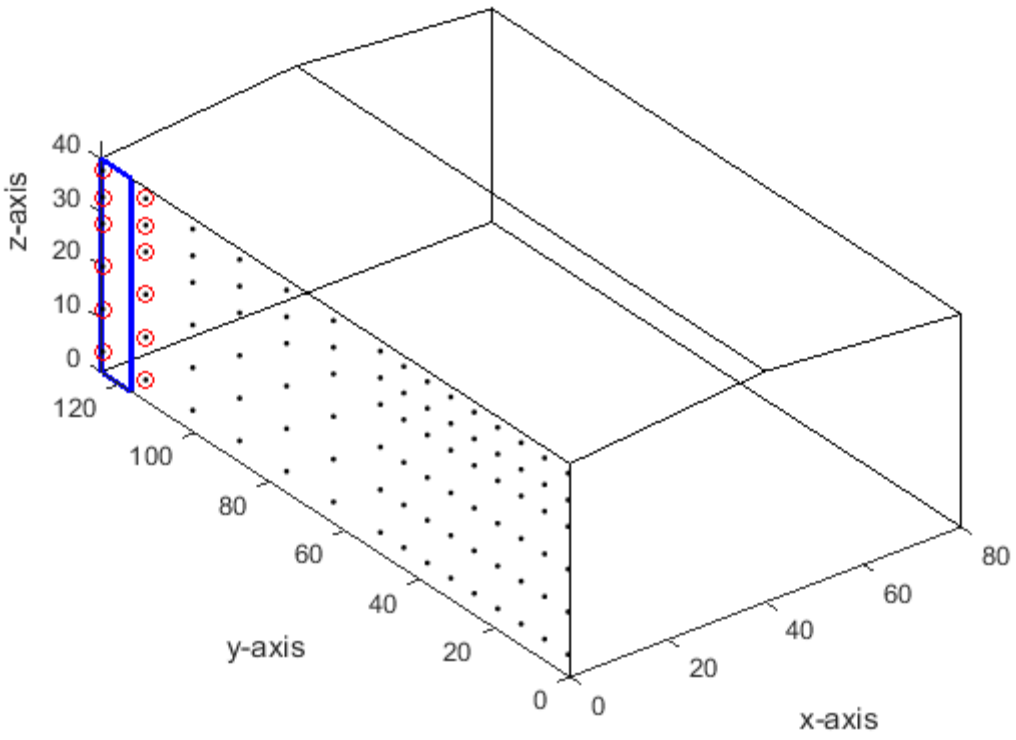

Fig. G2a, b Bldg 15 Wall 1 left edge (1 ft^2 = 0.0929 m^2)

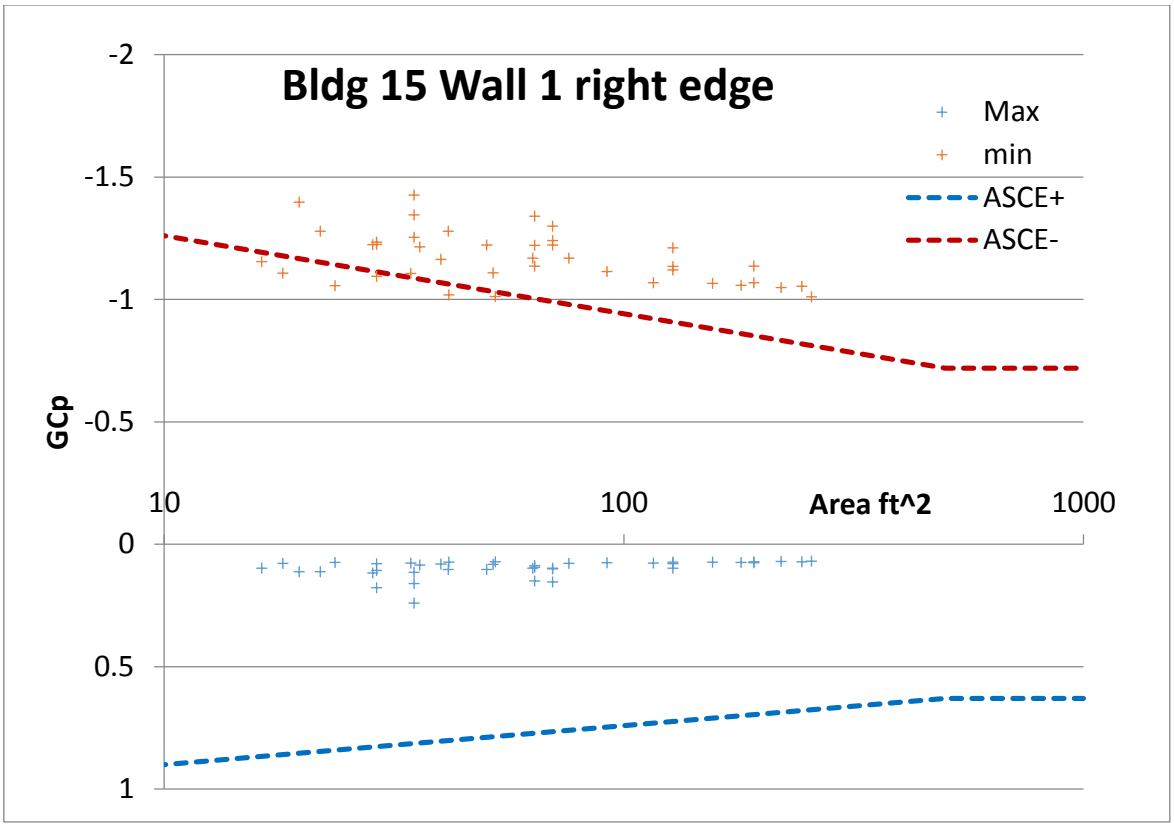

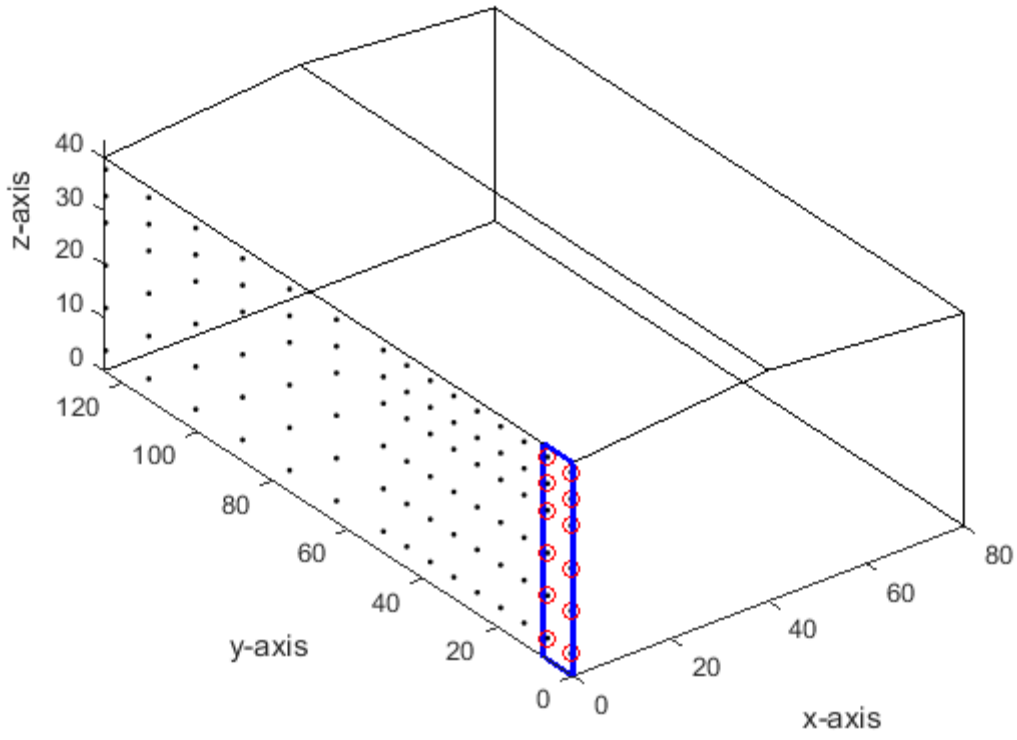

Fig. G3a, b Bldg 15 Wall 1 right edge (1 ft^2 = 0.0929 m^2)

Appendix H Building 15, Wall 4

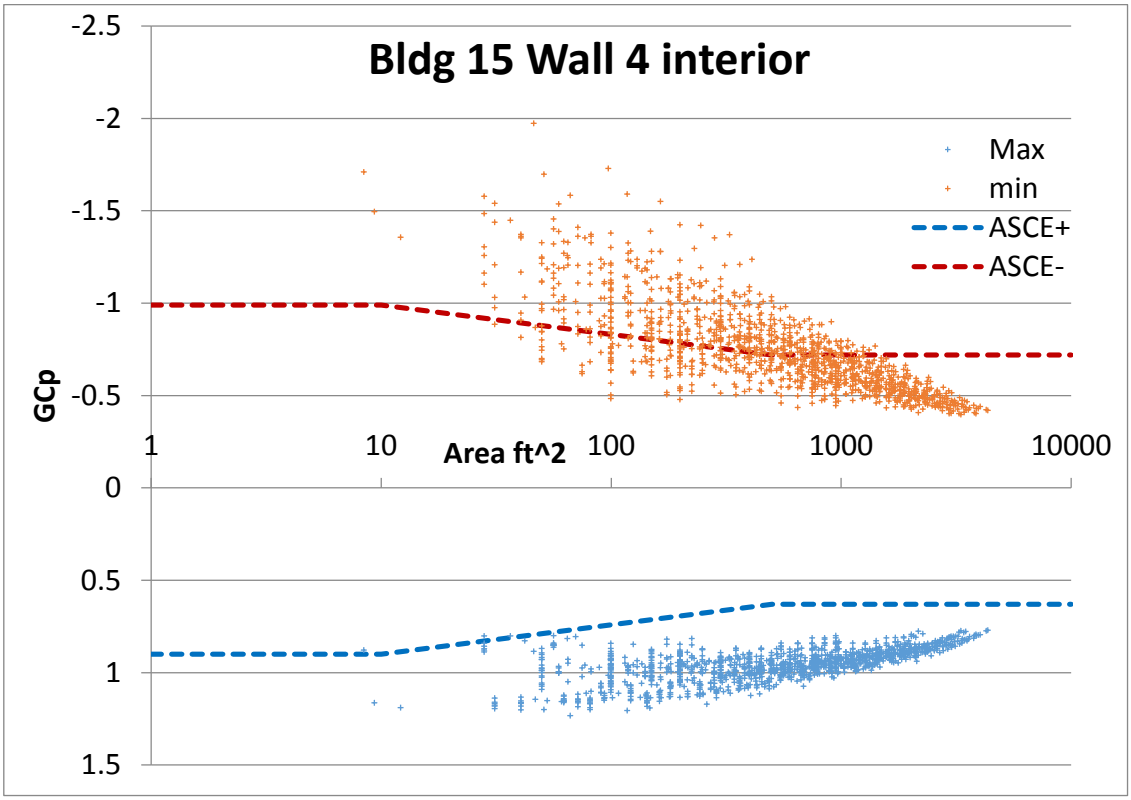

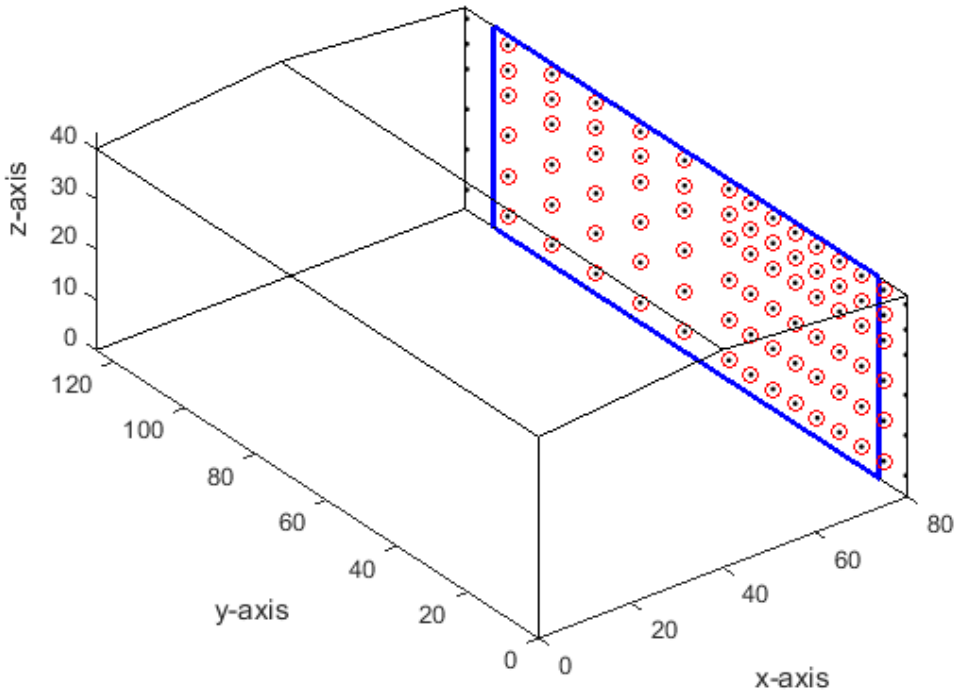

Fig. H1a, b Bldg 15 Wall 4 Interior (1 ft^2 = 0.0929 m^2)

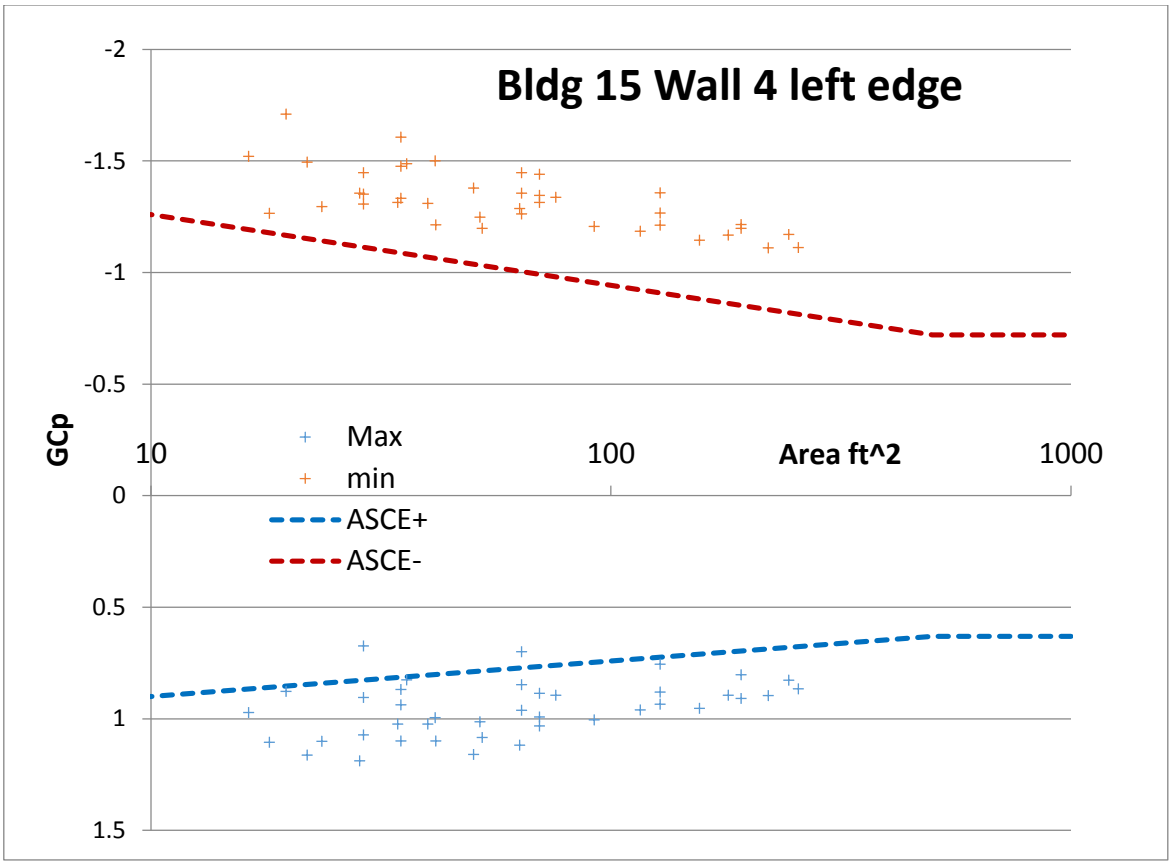

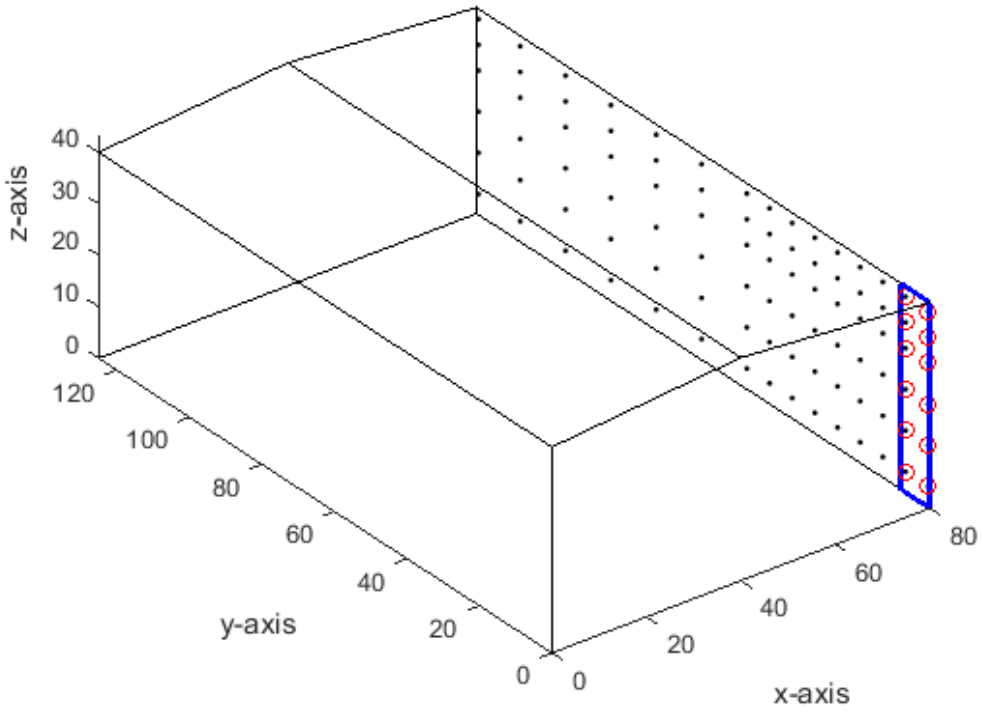

Fig. H2a, b Bldg 15 Wall 4 left edge (1 ft^2 = 0.0929 m^2)

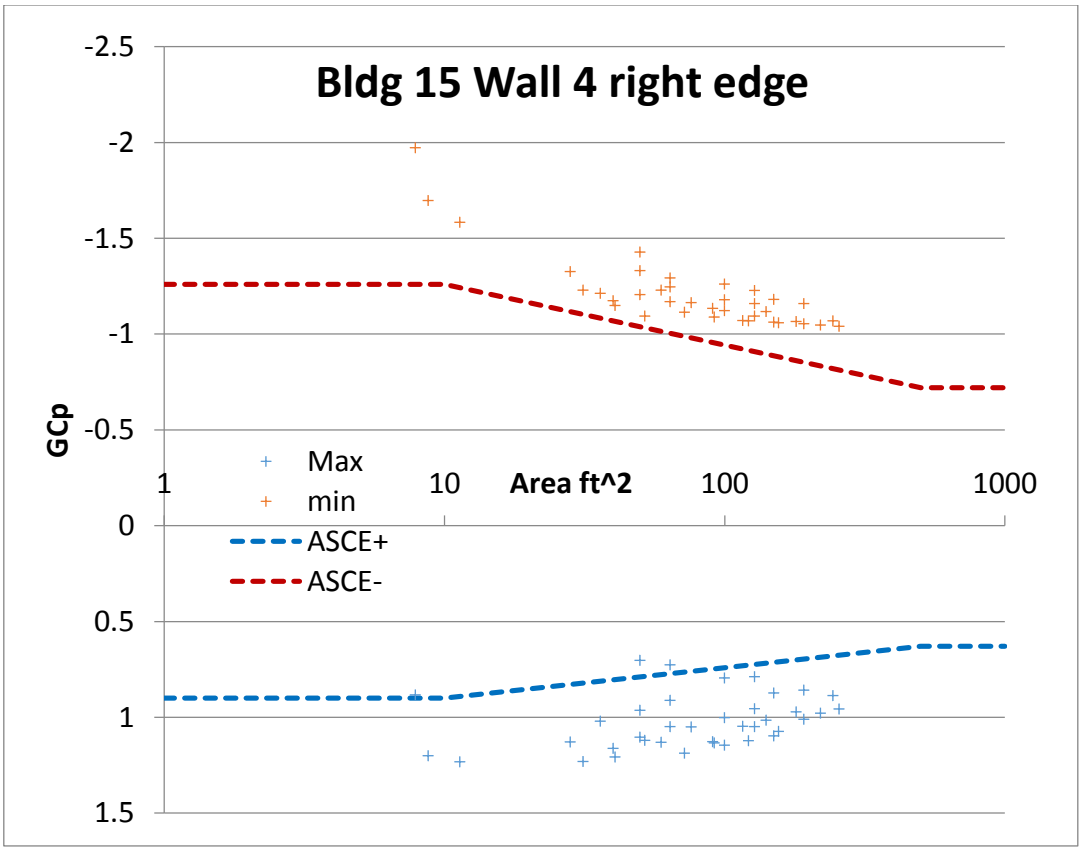

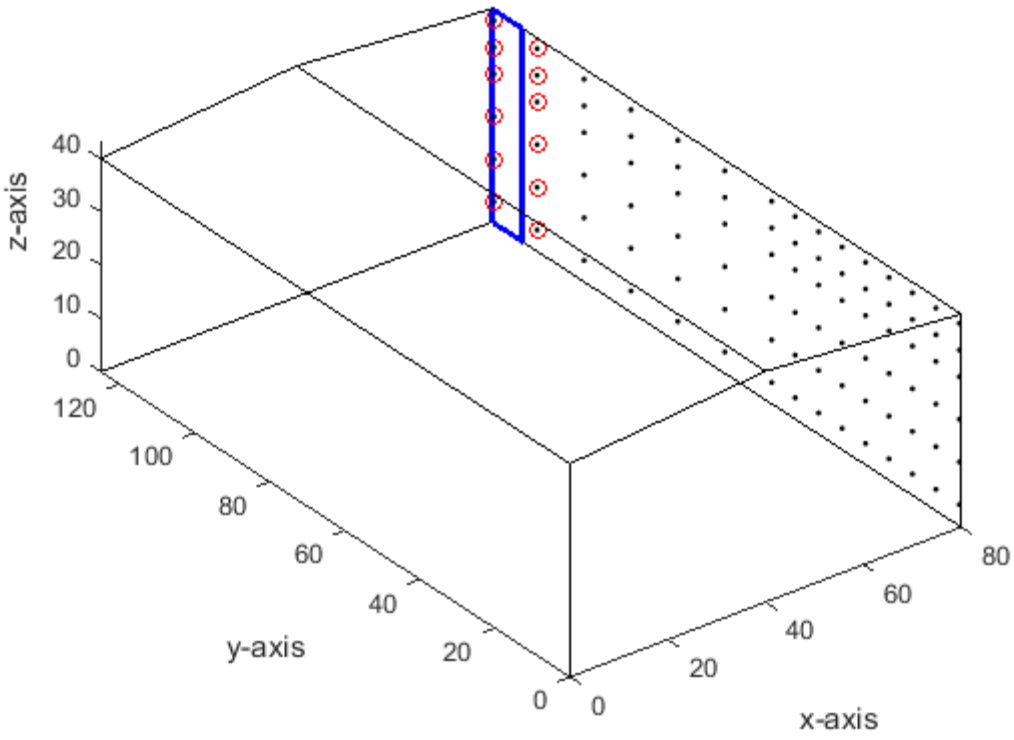

Fig.H3a, b Bldg 15 Wall 4 right edge (1 ft^2 = 0.0929 m^2)